Response to review comments regarding ACPD Janechek et al. "Physical Properties of Secondary Photochemical Aerosol from OH Oxidation of a Cyclic Siloxane"
https://www.atmos-chem-phys-discuss.net/acp-2018-748/

Response to Interactive Comment:

The coauthors thank the two anonymous reviewers for their comments, and the interactive comment from Karl et al. (Emission Fluxes of Siloxanes in the Urban Atmosphere; Thomas Karl, Martin Graus, Marcus Striednig, Stanislav Juran; Institute for Atmospheric and Cryospheric Sciences, University of Innsbruck, Innsbruck, Austria; and Global Change Research Institute, Czech Academy of Sciences, Brno, Czech Republic).

The interactive comment from Karl et al. can be found at https://doi.org/10.5194/acp-2018-748-SC1

> *We appreciate the comment from Karl et al. regarding improved information for direct measurement of cVMS fluxes. We have updated the paper's introduction to mention and cite Karl et al. (2018).*
>
> *Added mention of flux measurements to page 2, line 5-6, and citation to page 2, line 26.*

Response to Anonymous Referee #1:

Reviewer comment:

Janechek et al. describe yields and physical properties of SOA formed from the photooxidation of the D5 volatile siloxane and D5-containing consumer product. Such studies are definitely important because we know very little about the atmospheric fates of these cyclic volatile methylsiloxanes (cVMS) and the study could be useful for an initial step in more accurate modelling which currently is also challenging. A rather shocking discovery from this study is that these volatile silicon-containing organic compounds appear to have much higher yields for secondary organic aerosol (SOA) formation than previously thought which might inspire new questions about how SOA from the large anthropogenic emissions of siloxanes affect human health and climate.

Overall, the paper is well written, and the atmospheric relevance of siloxanes is a timely subject, so it looks like a useful contribution to the literature. However, I have some relatively minor suggestions/comments which hopefully can be successfully addressed during the revision.

> *The co-authors appreciate the supportive comment from reviewer 1.*

1. Why did the authors focus only on D5 experiments? While this is indeed the most common cVMS in consumer care products, other siloxanes are also common in the atmosphere (as the nice community comment emphasizes). I think the authors should consider extending the analysis to other cyclic siloxanes (D3-D7) but if it is not possible

then at least the other compounds should be discussed in terms of how similar or different they might be. I am particularly concerned that your models extrapolate from this study to D4 and D6 so might be completely inaccurate for the mixed siloxane atmospheres (D3-D7).

D_5 was chosen because it is the most common cyclic siloxane in personal care products. It is also often the highest concentration cVMS measured in studies that look at multiple cVMS compounds. Extending the work to D_3, D_4 or D_6 or to linear siloxanes is an excellent idea, but would need to be future work. We added mention in the paper (p. 17, lines 21-24) that extension to other siloxanes is uncertain due to the lack of yield measurements and extension to other species, based on volatility of the precursors (volatility: D_4>D_5>D_6 (Lei et al., 2010).

2. The methodology is very nicely described. However, given the high SOA yields, are you sure that the house air was not introducing any additional precursors or cVMS? Why was the house air used to flow over D5 standard instead of zero air from a catalyst or a zero-air generator? The indoor air may contain very high concentrations of siloxanes and other VOCs (e.g. Tang et al., 2016). It is quite reassuring what is written in P6 L12 "During D5 gas phase measurement and analysis, personal care products that contained cyclic siloxanes were avoided by laboratory personnel." but was the personnel instructed to use no shampoo, soap, creams, or just to avoid antiperspirants? There could potentially be grease or products which could be a strong siloxane source in a lab. I therefore wonder how the authors have convinced themselves there was no significant level of VOCs (e.g. 100 ppb of D4, for instance)? Your assumption of the clean air might be due to the presence of a charcoal filter but was it new and how efficient was it for cVMS? Have you done any measurements of the air before and after the charcoal filter before each yield experiment? I think a zero-air generator would be a much better solution for these type of experiments.

In hindsight, the use of air from the zero air generator would be preferable. However, we checked for SOA formation from the purified air (without addition of D_5). Finding negligible concentrations, we felt confident moving forward with our combination of "zero" air and filtration/purification of the house air. We felt this was sufficient quality assurance that we were correctly attributing yield to the D_5. We do not have a measurement of the siloxane levels before or after the charcoal filter, as we felt our quality assurance was sufficient. After cleaning the chamber (15 hours) background aerosol concentrations were 400 cm^{-3} and 0.001 $\mu g\ m^{-3}$ (with the OFR lights on and RH addition). This additional information has been added to the manuscript on page 4, lines 23-25.

To clarify the avoidance of personal care products, personnel directly handling the sorbent cartridges (and then doing extraction, analysis, handling blanks, etc.) avoided products (all personal care products) with cyclic siloxanes on the product labels. Gloves were used to handle all samples. The supplement contained extensive information on field blanks, method blanks, and duplicate sample. These indicate that precision and accuracy

of our D_5 sampling was acceptable and that procedures to avoid contamination were sufficient.

3. Brass fittings are avoided in VOC sampling. Is there any reason why these were used?

   In hindsight we should have used Teflon fittings rather than brass in conjunction with the Teflon tubing used. While future work should use Teflon fittings, we argue the impact of the brass fittings should be minimal.

   We only quantified D_5 during this work, used high concentrations, long equilibration times, and minimal surface area of metal fittings. Recent research on the interaction of VOCs with tubing have been investigated for a range of compounds and materials but not brass (Pagonis et al., 2018; Pagonis et al., 2017). Metal tubing has shown increased VOC interactions compared to Teflon due to adsorption. However, we believe based on these studies, VOC interaction with metals for the conditions used in this work would be negligible based on several reasons: 1) VOC adsorption has been found to be small even at low concentrations for compounds with volatility comparable to D_5 (saturation concentration of 3 $x10^6$ µg m^{-3} (Lei et al., 2010)), 2) vapor concentrations used in this work were in excess of concentrations that showed quick saturation of tubing adsorption sites, 3) tubing adsorption is reduced in the presence of humidified air greater than 20% RH needed for OFR OH production, and 4) the surface area and contact time between gases and brass was small (Coggon, 2018; Jimenez, 2018).

4. Fig. 3, is one of the points an outlier? Fig S8 informs that these yield extremes occur at the RH of 45%, and are more consistent at RH of 25%. It would be nice to shed more light on understanding the effect of humidity.

   We are not sure if it is an outlier or not. That trial did have a difference from the other trials (see Table 1); it was the only one with 100% power on lights, and high (45%) RH. Since we have no good reason to exclude it, we feel it is best to leave it in the dataset. Our assumption is that readers will see the imprecision in the yield results, and take that as a call for future research to establish more certain and more precise yields – with varying OH concentrations. In other words, we used the OFR primarily as an aerosol generation system to generate the aerosols and subject them to physical tests (such as hygroscopicity). While we were doing that, it was appropriate to also investigate yield. But readers will see (without us having to call extra attention) that the yield results are in need of future studies for confirmation, investigation of chemical mechanism and molecular composition, investigation of artifacts that may be caused by the OFR or other methodological details. Although we already had several caveats in the article, we have added more to stress the yields need replication. We have changed the last sentence of the abstract (p. 1, line 23-24); we have added a caveat about replication into the conclusions (p. 18, lines 10-12). And we have called out the potential outlier in results and discussion (p. 12, lines 20-25).

5. Table 1, water bath temperature only affected the evaporation rate of D5 to the dilution flow. It would be useful to add temperature of the reactor.

We did not measure the internal OFR temperature but rather the incoming air flow which was held constant at room temperature of 22 °C. This is also consistent with reported temperatures from SMPS data files that were measured downstream of the chamber. However the actual OFR temperature was likely slightly warmer due to the lamps. Li et al. (2015) reports that this OFR heating is likely ~2 °C. We have revised the manuscript (p. 4, lines 14-16) to add the estimated reactor temperature and state that no temperature correction has been performed on measurements to account for the reactor being slightly warmer.

6. P7,L32 Should be “Data were”.

   Thanks for the correction. We have fixed the verb.

Anonymous Referee #2:

Janechek et al. provide new laboratory measurements of SOA formed from the OH oxidation of cyclic volatile methyl siloxanes. The authors produce SOA via an OFR and test various aerosol properties, including morphology, composition, volatility, and hygroscopicity. The authors also explore various experimental parameters on SOA yield, and report new yields that are higher than previously measured.

The results from this study are useful for models aimed at understanding organosilicon aerosol properties. I'm particularly interested in the TEM measurements and how these could be useful for identifying organosilicon aerosols in the atmosphere. Overall, I find the methods to test aerosol properties to be good and the conclusions about volatility, hygroscopicity, and composition to be sound. I have some concerns about the aerosol yield conclusions (see below). I would appreciate if the authors addressed these concerns prior to publication.

1. Page 11, lines 1 -15 and Page 11, lines 29-32. I have some concerns with the interpretation of the yield experiments. How certain are the authors that the yield measured at the highest OH exposure is statistically significant? Looking at panels A and C, it seems like this point could be an outlier, but the authors attribute the uptick in yield as an increase in semi- or low-volatility oxidation products.

   This is a very similar comment to reviewer 1, comment 4. We don't have specific information that it is an outlier, and the test conditions are unique. Therefore, the appropriate action (in our opinion) is to report it into the literature and then let it be revisited by future work. As we responded above (reviewer 1, comment 4) we have made the caveats to our yields more consistent throughout the paper.

2. The authors argue that the fate of gas-phase species is condensation to aerosols (line 27), but then note that the experiments were run in particle-free air. I interpret this to mean that the authors are relying on nucleation processes to drive particle formation. If so, this significantly complicates the interpretation of the yield because there is no way of understanding the nucleation rate and its relationship with the vapor condensational sink. Consequently, I believe that the authors are overestimating the aerosol sink and underestimating the aerosol yield. The authors even show this experimentally in the following section (3.2.2). When the authors add 50 nm ammonium sulfate particles, the aerosol mass increases by 44%. Would this not suggest that the maximum yield was not observed for any of the experiments conducted with particle-free air, and that significant condensational losses were to the walls of the chamber?

   In yield experiments, it is crucial that sufficient aerosol be added in order to drive oxidation products away from the walls and to the aerosol phase (Zhang et al. 2014). Consequently, I believe that the seed aerosol experiment described in section 2.2.4 should actually be treated as the yield experiment. If this input of aerosol is significant enough drive most of the oxidation products to the aerosol phase, then I believe the authors can

interpret the effect of OH exposure on aerosol yield; otherwise, I would treat this yield as a lower-limit estimation.

In the paper, the loss to the walls was estimated using a condensational loss model (Palm et al., 2016; Lambe and Jimenez, 2018) which indicated that loss to the walls (and other non-aerosol fates) was minimal, under the assumption that the average of the condensational sink at the entrance (assumed to be zero) and the condensational sink at the exit (measured) was representative of the whole OFR. In other words, the condensational sink assumed was one half that measured at the exit. Although not reported in the paper or the supplement, we have run the condensational loss model for a number of different assumptions for condensational sink. Specifically, we investigated one order of magnitude lower, and three orders of magnitude lower. Only in the case of the condensational sink being 3 orders of magnitude lower did the calculator estimate that condensation to aerosol was not the dominant pathway and even then the dominant pathway was reacting with OH more than 5 times. However, after considering the reviewers comment, Zhang et al. (2014), and the point regarding the yield increase with seed aerosol, we agree that reporting the yields as a lower limit is appropriate. We have changed text in the abstract (p. 1, lines 20-21), results and discussion (p. 13, lines 19-22), and conclusions (p. 18, lines 20-21) sections to reflect this.

3. Section 3.3. I find this section to be quite interesting, though the discussion is very brief. I understand that the primary purpose of this section is to show that the aerosol collected from antiperspirant oxidation exhibits a qualitatively similar TEM spectra as aerosol produced from D5 oxidation. Does this also suggest that D5 was the predominant SOA precursor in the antiperspirant experiment and that other components of the antiperspirant did not contribute to SOA formation?

   That is our working hypothesis but we only have limited proof, from the similarity of the SEM-EDS microscopy done by our collaborator RJ Lee. Morphology, size distribution, and EDS spectra were similar between the two sources.

4. I presume that there were a lot of other components in the antiperspirant that was tested, including fragrances (which were likely a mixture of highly reactive compounds like monoterpenes and terpenoids) and possibly other ingredients, such as glycols. Can the authors provide more details of the ingredient list so that the reader has a sense of what precursors may have been present in the antiperspirant stick? Was D5 listed at the top of this list, which presumably implies that it was a major ingredient?

   Dudzina et al. (2014) reported that the median D_5 mass fraction in antiperspirant was 0.142. This, combined with the elemental spectra of the SOA in EDS (with a prominent Si peak), leads us to believe that a cyclic siloxane (presumably D_5) was the major constituent being oxidized. While we don't know the quantitative breakdown, D_5 was listed as the first inactive ingredient on the product label implying it is a major ingredient. During the Access Review for ACPD, the editor and coauthors agreed that the specific manufacturer and product name would not be released with the article, as the focus on the article was on the general class of personal care products, not specific

products. Thus we are refraining from providing the detailed ingredient list in the open response to review. The ingredient list did include other compounds, such as fragrance, that may form SOA upon oxidation. We have modified the manuscript (p. 14, lines 13-16) to mention that these were complex mixtures that were reacted with other potential SOA precursors.

5. Did the authors also test the composition of the aerosols formed via oxidation of conditioner emissions? I'm curious if the TEM measurements show the same relative elemental composition, or if other peaks (such as carbon) are more abundant. If this spectra is different, then this could point towards the influence of other ingredients on SOA formation.

   Aerosol collection for microscopy was not performed in the case of the conditioner. Therefore, we cannot comment on the relative contribution from Si-containing and other compounds, and we cannot report the morphology or EDS spectrum. During the Access Review for ACPD, the editor and coauthors agreed that the specific manufacturer and product name would not be released with the article, as the focus on the article was on the general class of personal care products, not specific products. Thus we are refraining from providing the detailed ingredient list in the open response to review. It should be noted that cyclomethicone can refer to other cyclic siloxanes and is not specific to D_5. We have modified the manuscript (p. 14, lines 14-15) to state that no microscopy samples were collected for the conditioner source.

6. Ultimately, I think the authors can do a bit more here to put the personal care product experiments into perspective. As written, a reader could interpret these results to suggest that aerosol formed from personal care products containing D5 is exclusively composed of D5 oxidation products! This is unlikely, of course, and not what the authors are intending to show, so some further discussion should be provided. Furthermore, could the TEM technique be useful in understanding organosilicon aerosol in the atmosphere? Presumably, most particles containing silicon in modes < 100 nm would have been derived from secondary processes. Could these TEM measurements be a useful tool in identifying aerosols resulting from organosilicon oxidation?

   Thank you for your suggestions. Our intentions were to not say the generated SOA is exclusively the result of D_5 but merely to show we do get SOA from oxidizing personal care products, and those products (at least for anti-perspirant) have similar SEM EDS spectra as that with pure D_5 SOA. We have revised the manuscript appropriately (p. 14, lines 13-16). We think the SEM-EDS (or TEM-EDS) technique might be a useful method of finding these particles in the environment. But we feel that readers will make that inference on their own, and have not directly stated it.

7. Page 15, lines 3-11. In this section, the authors discuss the relevance of cVMS SOA formation and potential shortcomings of this work. The authors rightfully demonstrate that cVMS will contribute a small fraction to total SOA; however, I believe the authors are overextending when they try to frame these results into the measurements conducted by Bzdek et al. (2014). Specifically, I take issue with the extrapolation of the

organosilicon SOA content. The nano-particle measurements conducted by Bzdek et al. provide a constraint to nucleation processes close to the source, but downwind of major cities like L.A., chemical and meteorological conditions could change and limit the oxidation of organosilicon precursors. Furthermore, an extrapolation to 1.5 ug/m3 seems quite unrealistic. That amount of SOA is comparable to the background SOA in LA believed to come from regional biogenic sources (~2 ug/m3, Hayes et al. 2015).

I recommend that the authors refrain from extrapolating to suggest that there could be unexplained sources of organosilicon precursors. I think it is sufficient to cite Tang et al. (2015) and McDonald et al. (2018) to show that organosilicon SOA precursors are emerging as an important source of VOCs in urban areas, and that incorporating this work into models will help to constrain the VCP impact on urban SOA formation.

While we are personally interested to reconcile that large amount of Si found by Bzdek with the low average atmospheric burden that we anticipate, we are happy to remove that from the paper (p. 16, line 33 – p. 17, line 5), as it is probably too speculative. Thanks.

Other Comments

Page 2, Lines 8 - 10. This sentence seems a bit out of place here, and doesn't necessarily requires its own paragraph. I suggest moving it elsewhere in the introduction (perhaps after the last sentence at line 32?)

Moved to page 2, lines 25-27.

Page 3, Lines 1-20. This material would be better presented as a discussion rather than as an introduction. I would recommend moving this to section 3.1

Moved to Section 3.1, page 10 lines 3-22.

Page 3, Line23-24. This sentence reads as if concentration, size, and morphology were also measured by EDS. Please rephrase.

Revised on page 3, lines 24-25.

Page 4, Line 6. Please add "by photolysis of water" after "in situ"

Done on page 4, line 10.

Page 4, Line 11. It would be clearer to say "temperature-controlled"

Done on page 4, line 17.

Page 4, Line 14. It would be clearer to the reader if you mention that cyclomethicone and cyclopentasiloxane often refer to the same molecule.

Done on page 4, lines 21-22.

Page 5, Line 5. Please note that the "D5 water bath temperature" translates to variations in precursor concentrations.

Combined first and second sentences to make the sentence clearer on page 5, lines 15-16.

Page 5, Lines 11 - 12. From my understanding, it's not crucial that the concentrations be the same; rather, it's important that the OH reactivity be low enough that losses due to OH titration can be ignored. What concentration range of D5 and SO2 was being injected into the OFR?

We included this statement to acknowledge OH suppression caused by external reactants detailed in the PAM chamber chemical kinetics literature (Li et al., 2015; Peng et al., 2016; Peng et al., 2015). In the chamber, OH exposure is dependent on residence time, RH, light intensity, and external OH reactivity (reactant concentration multiplied by the OH rate constant, units of s^{-1}). Higher external OH reactivity leads to lower OH exposure in the chamber, therefore characterizing the OH exposure using higher SO_2 loadings compared to D_5 can result in underestimated D_5 OH exposure. We have revised this statement (p. 5, lines 23-25) to make this clearer and have added discussion of the implications to this in the results and discussion (p. 11, lines 21-27).

It is important to note that we are below the recommended limit of external OH reactivity (30 s^{-1}) for all experiments so that OH concentrations are not suppressed to the extent that other non-OH chemistry is favored.

Incoming SO_2 concentrations were 450 – 1200 ppb [1.1 $x10^{13}$ – 2.9 $x10^{13}$ molec cm^{-3}] (p. 6 line 4)

Incoming D_5 concentrations were 290 – 740 µg m^{-3} [4.7 $x10^{11}$ – 1.2 $x10^{12}$ molec cm^{-3}] (p. 11 line 28)

Accounting for OH rate constants, SO_2 external OH reactivity loadings were 5.4 – 28 times higher than D_5.

D_5: 0.7 – 1.9 s^{-1}
SO_2: 10.1 – 26.3 s^{-1}

Page 5, Line 21. The term "disappearance" suggests that the SO2 was lost by some unknown process. I would recommend replacing with "…measurement of reacted SO2 in the OFR".

Done on page 6, lines 3-4.

Page 5, Line 25. Please add "constant" after "rate".

Done on page 6, line 8.

Page 6, line 2. How well do the OH exposures calculated from Eqns 1 and 2 agree?

The OH exposure calculations are compared on page 11, lines 15-20.

Page 6, Line 26. The semi-colons should be replaced with commas.

We have gone through the manuscript and replaced semicolons with commas where appropriate.

Page 7, Line 12. I would refer to "the DMT" or the "DMT Instrument" as a "CCN counter"

We have gone through the manuscript and replaced "DMT" with "CCN counter" where appropriate.

Page 7, Line 12-13. Consider removing the phrase "The controlled variable in the DMT instrument" and replace with "The thermal gradient was varied from…" for brevity.

Done on page 7, line 26.

Page 7, line 20. By "source", do you mean from the DMA monodisperse outlet?

Yes, rephrased accordingly on page 8, lines 3.

Page 7, line 27 - Page 8, Line 10. The details of data QA are not needed here. I suggest removing, or placing in the supplemental information.

This section has been moved to the supplement under Section S7: Hygroscopicity.

Section 2.5. I'm somewhat confused by the thermal degradation experiments. The authors don't explain in detail why these experiments were performed, or why these might be relevant in the atmosphere. Are there cases in which D5 might be exposed to high temperature that it would decompose and form lower volatility components? Or, is this a check to evaluate potential biases in the volatility experiments? If it is the latter, I would suggest moving this discussion to Section 2.4 and refer to these experiments as controls.

Our motivation was to determine if the chemicals could degrade or be oxidized due to high temperature heating leading to low volatility products. This motivation is referenced in Section 3.6 of the Results and Discussion. An additional statement has been added to page 16, lines 3-5 explaining that these tests also serve as a volatility control test.

Page 10, line 21. What do the authors mean by "reasonable ways?"

As expected. Sentence has been changed on page 11, lines 30-31.

Page 10, line 23. It seems to me that the experiment reached steady state long before 20 hrs! No need to change - I'm just impressed by the length of the experiment.

Page 10, line 24 - 25. This sentence is a bit akward. I might consider rephrasing as “This was followed by a sampling period, during which four gas samples were taken to determine D5 SOA yields.”

Rephrased as suggested on page 12, lines 2-3.

Page 10, line 31. I’m confused why the authors implicate the D5 injection rate as the primary cause for variability. Is it a mixing issue?

We were not sure what was causing the variability, we had some indications that the water level of the water bath containing the heated leg of Teflon (containing liquid D_5) may have been causing variable injection rates. We also suspected that the lights may vary in power in a periodic fashion.

Page 13, line 19. Please add “that” between “shows” and “no”. Also, it is incorrect to write “ka *observed* smaller particles” - please choose a different verb.

Thanks, changed accordingly on page 15, line 8.

Page 13, lines 20-22. Can the authors please clarify the last statement about the higher oxidation state of smaller particles? Is that because the larger particles contain more semivolatile components (e.g. dimers, or second-generation monomers?).

Zhao et al. (2015) and Winkler et al. (2012) report that smaller particles tend to have higher hygroscopicity than larger particles. They suggest smaller particles tend to have more oxidized composition due to lower volatility (Kelvin effect) and also possibly due to higher surface area/volume impacting the incorporation of later generation products or heterogenous oxidation. This section has been revised in the manuscript on page 15, lines 9-13.

Section 3.5, Figure S13. The 10 nm mode is quite noisy. If it is difficult to quantify, why include this mode in the figure? I would find this figure more useful if I could see the zoomed-in traces for 20-110 nm experiments.

Revised figures S13 and S14 in the Supplement excluding 10 nm particles.

Section 3.6. Would thermal degradation be a significant process influencing the lifetime of D5? If so, please provide some justification. If not, I feel like these experiments are better characterized as volatility control experiments - i.e., to ensure that changes in particle concentrations during volatility experiments are not the result of residual gaseous D5 that could degrade and lead to particle formation.

We viewed this not as an issue of lifetime, but as potential indoor source of inhalable materials. If contact of D_5 to hot surfaces (i.e. hairdryer in a bathroom after use of personal care products; cooking elements; heating elements) led to any aerosol formation, then this could be a relevant indoor source. We have changed the section title to Thermal Aerosol Production.

References

Bzdek, B. R., Horan, A. J., Pennington, M. R., Janechek, N. J., Baek, J., Stanier, C. O., and Johnston, M. V.: Silicon is a Frequent Component of Atmospheric Nanoparticles, Environ. Sci. Technol., 48, 11137-11145, doi:10.1021/es5026933, 2014.

Coggon, M.: Personal Communication between Stanier and Jimenez, December, 2018.

Dudzina, T., von Goetz, N., Bogdal, C., Biesterbos, J. W. H., and Hungerbuhler, K.: Concentrations of cyclic volatile methylsiloxanes in European cosmetics and personal care products: Prerequisite for human and environmental exposure assessment, Environ. Int., 62, 86-94, doi:10.1016/j.envint.2013.10.002, 2014.

Hayes, P. L., Carlton, A. G., Baker, K. R., Ahmadov, R., Washenfelder, R. A., Alvarez, S., Rappenglück, B., Gilman, J. B., Kuster, W. C., de Gouw, J. A., Zotter, P., Prévôt, A. S. H., Szidat, S., Kleindienst, T. E., Offenberg, J. H., Ma, P. K., and Jimenez, J. L.: Modeling the formation and aging of secondary organic aerosols in Los Angeles during CalNex 2010, Atmos. Chem. Phys., 15, 5773-5801, doi:10.5194/acp-15-5773-2015, 2015.

Jimenez, J. L.: Personal Communication with Stanier, December 2018.

Karl, T., Striednig, M., Graus, M., Hammerle, A., and Wohlfahrt, G.: Urban flux measurements reveal a large pool of oxygenated volatile organic compound emissions, Proceedings of the National Academy of Sciences, 115, 1186-1191, doi:10.1073/pnas.1714715115, 2018.

Lambe, A., and Jimenez, J. L.: PAM Wiki: Estimation Equations, availabe at: https://sites.google.com/site/pamwiki/hardware/estimation-equations, 2018.

Lei, Y. D., Wania, F., and Mathers, D.: Temperature-Dependent Vapor Pressure of Selected Cyclic and Linear Polydimethylsiloxane Oligomers, J. Chem. Eng. Data, 55, 5868-5873, doi:10.1021/je100835n, 2010.

Li, R., Palm, B. B., Ortega, A. M., Hlywiak, J., Hu, W., Peng, Z., Day, D. A., Knote, C., Brune, W. H., de Gouw, J. A., and Jimenez, J. L.: Modeling the Radical Chemistry in an Oxidation Flow Reactor: Radical Formation and Recycling, Sensitivities, and the OH Exposure Estimation Equation, The Journal of Physical Chemistry A, 119, 4418-4432, doi:10.1021/jp509534k, 2015.

McDonald, B. C., de Gouw, J. A., Gilman, J. B., Jathar, S. H., Akherati, A., Cappa, C. D., Jimenez, J. L., Lee-Taylor, J., Hayes, P. L., McKeen, S. A., Cui, Y. Y., Kim, S.-W., Gentner, D. R., Isaacman-VanWertz, G., Goldstein, A. H., Harley, R. A., Frost, G. J., Roberts, J. M., Ryerson, T. B., and Trainer, M.: Volatile chemical products emerging as largest petrochemical source of urban organic emissions, Science, 359, 760-764, doi:10.1126/science.aaq0524, 2018.

Pagonis, D., Krechmer, J. E., de Gouw, J., Jimenez, J. L., and Ziemann, P. J.: Effects of gas-wall partitioning in Teflon tubing and instrumentation on time-resolved measurements of gas-phase organic compounds, Atmos. Meas. Tech., 10, 4687-4696, doi:10.5194/amt-10-4687-2017, 2017.

Pagonis, D., Deming, B., Liu, X., Talukdar, R., Roberts, J., Krechmer, J., Palm, B., De Gouw, J., Ziemann, P., and Jimenez, J. L.: Effects of Gas-Wall Partitioning in Tubing and Instrumentation on Gas-phase, Aerosol, and Potential Aerosol Measurements, 10th International Aerosol Conference, St. Louis, Missouri, USA, 2018.

Palm, B. B., Campuzano-Jost, P., Ortega, A. M., Day, D. A., Kaser, L., Jud, W., Karl, T., Hansel, A., Hunter, J. F., Cross, E. S., Kroll, J. H., Peng, Z., Brune, W. H., and Jimenez, J. L.: In situ secondary organic aerosol formation from ambient pine forest air using an oxidation flow reactor, Atmos. Chem. Phys., 16, 2943-2970, doi:10.5194/acp-16-2943-2016, 2016.

Peng, Z., Day, D. A., Stark, H., Li, R., Lee-Taylor, J., Palm, B. B., Brune, W. H., and Jimenez, J. L.: HOx radical chemistry in oxidation flow reactors with low-pressure mercury lamps systematically examined by modeling, Atmos. Meas. Tech., 8, 4863-4890, doi:10.5194/amt-8-4863-2015, 2015.

Peng, Z., Day, D. A., Ortega, A. M., Palm, B. B., Hu, W., Stark, H., Li, R., Tsigaridis, K., Brune, W. H., and Jimenez, J. L.: Non-OH chemistry in oxidation flow reactors for the study of atmospheric chemistry systematically examined by modeling, Atmos. Chem. Phys., 16, 4283-4305, doi:10.5194/acp-16-4283-2016, 2016.

Tang, X., Misztal, P. K., Nazaroff, W. W., and Goldstein, A. H.: Siloxanes Are the Most Abundant Volatile Organic Compound Emitted from Engineering Students in a Classroom, Environ. Sci. Technol. Lett., 2, 303-307, doi:10.1021/acs.estlett.5b00256, 2015.

Tang, X., Misztal, P. K., Nazaroff, W. W., and Goldstein, A. H.: Volatile Organic Compound Emissions from Humans Indoors, Environ. Sci. Technol., 50, 12686-12694, doi:10.1021/acs.est.6b04415, 2016.

Winkler, P. M., Ortega, J., Karl, T., Cappellin, L., Friedli, H. R., Barsanti, K., McMurry, P. H., and Smith, J. N.: Identification of the biogenic compounds responsible for size-dependent nanoparticle growth, Geophys. Res. Lett., 39, L20815, doi:10.1029/2012GL053253, 2012.

Zhang, X., Cappa, C. D., Jathar, S. H., McVay, R. C., Ensberg, J. J., Kleeman, M. J., and Seinfeld, J. H.: Influence of vapor wall loss in laboratory chambers on yields of secondary organic aerosol, Proceedings of the National Academy of Sciences, 111, 5802-5807, doi:10.1073/pnas.1404727111, 2014.

Zhao, D. F., Buchholz, A., Kortner, B., Schlag, P., Rubach, F., Kiendler-Scharr, A., Tillmann, R., Wahner, A., Flores, J. M., Rudich, Y., Watne, Å. K., Hallquist, M., Wildt, J., and Mentel, T. F.: Size-dependent hygroscopicity parameter (κ) and chemical composition of secondary organic cloud condensation nuclei, Geophys. Res. Lett., 42, 10,920-910,928, doi:10.1002/2015GL066497, 2015.

Physical Properties of Secondary Photochemical Aerosol from OH Oxidation of a Cyclic Siloxane

Nathan J. Janechek[1,2], Rachel F. Marek[2], Nathan Bryngelson[1,2,*], Ashish Singh[1,2,†], Robert L. Bullard[1,2,‡],William H. Brune[3], Charles O. Stanier[1,2]

[1]Department of Chemical and Biochemical Engineering, University of Iowa, Iowa City, IA, USA
[2]IIHR-Hydroscience and Engineering, University of Iowa, Iowa City, IA, USA
[3]Department of Meteorology and Atmospheric Science, Pennsylvania State University, University Park, PA, USA
[*]Now at Yokogawa Corporation of America - Analytical Process Analyzers
[†]Now at Institute for Advanced Sustainability Studies, Potsdam-14467, Germany
[‡]Now at Lovelace Respiratory Research Institute, Albuquerque, NM, USA

Correspondence to: Charles O. Stanier (charles-stanier@uiowa.edu)

Abstract. Cyclic volatile methyl siloxanes (cVMS) are high production chemicals present in many personal care products. They are volatile, hydrophobic, and relatively long-lived due to slow oxidation kinetics. Evidence from chamber and ambient studies indicates that oxidation products may be found in the condensed aerosol phase. In this work, we use an oxidation flow reactor to produce ~100 μg m^{-3} of organosilicon aerosol from OH oxidation of decamethylcyclopentasiloxane (D_5) with aerosol mass fractions (i.e. yields) of 0.2-0.5. The aerosols were assessed for concentration, size distribution, morphology, sensitivity to seed aerosol, hygroscopicity, volatility and chemical composition through a combination of aerosol size distribution measurement, tandem differential mobility analysis, and electron microscopy. Similar aerosols were produced when vapor from solid antiperspirant ~~or from hair conditioner~~ was used as the reaction precursor. Aerosol yield was sensitive to chamber OH and to seed aerosol, suggesting sensitivity of lower volatility species and recovered yields to oxidation conditions and ~~OFR~~ chamber operation. ~~, indicating an interplay between oxidation conditions and the concentration of lower volatility species.~~ The D_5 oxidation aerosol products were relatively non-hygroscopic, with average hygroscopicity kappa of ~0.01, and nearly non-volatile up to 190°C temperature. ~~Recommended p~~Parameters for exploratory treatment as a semi-volatile organic aerosol in atmospheric models are provided.

1 Introduction

Cyclic volatile methyl siloxanes (cVMS) are high production chemicals (OECD Environment Directorate, 2004) present in many personal care products such as lotions, hair conditioners, and antiperspirants (Horii and Kannan, 2008; Wang et al., 2009; Lu et al., 2011; Dudzina et al., 2014; Capela et al., 2016). Cyclic siloxanes are volatile (Lei et al., 2010), relatively unreactive, and hydrophobic molecules (Varaprath et al., 1996) composed of a Si-O ring backbone with two methyl groups bonded to each Si. The most prevalent cVMS in personal care products is decamethylcyclopentasiloxane (D_5) (Horii and Kannan, 2008; Dudzina et al., 2014; Lu et al., 2011; Wang et al., 2009). Cyclic siloxanes are readily released into the

environment, primarily to the atmosphere (Mackay et al., 2015) by personal care product usage (Tang et al., 2015; Gouin et al., 2013; Montemayor et al., 2013; Coggon et al., 2018). Once in the atmosphere, the primary environmental fate for cVMS is oxidation. The principle sink is reaction with the hydroxyl radical (OH) and the characteristic atmospheric lifetime is ~5-10 days (Atkinson, 1991). Concentration ~~M~~measurements (McLachlan et al., 2010; Genualdi et al., 2011; Yucuis et al., 2013; Ahrens et al., 2014; Companioni-Damas et al., 2014; Tang et al., 2015; Coggon et al., 2018), urban flux measurements (Karl et al., 2018), and ~~and~~ modeling studies (McLachlan et al., 2010; MacLeod et al., 2011; Xu and Wania, 2013; Janechek et al., 2017) show cVMS are ubiquitous. Maximum concentrations occur in indoor spaces and automobile cabin air, up to 380 µg m^{-3} (Coggon et al., 2018) with outdoor urban locations up to 0.65 µg m^{-3} (Buser et al., 2013).

~~Personal care products are increasingly recognized as relevant sources of urban air pollution in developed cities (McDonald et al., 2018; Karl et al., 2018), are likely underrepresented in official inventories, and lead to poorly characterized ozone and secondary organic aerosol production.~~

Cyclic siloxanes have undergone continuing regulatory scrutiny (ECHA, 2018) for environmental impacts such as persistence, bioaccumulation, and toxicity but have entirely focused on the parent (e.g. D_5) compounds, and have not considered oxidation products (Environment Canada and Health Canada, 2008b, a, c; Brooke et al., 2009c, b, a; ECHA, 2015). However, numerous studies have reported particle formation from cVMS oxidation, with a direct link in lab studies or inferred in ambient studies (Bzdek et al., 2014). Chamber studies have shown that a range of non-volatile and semi-volatile oxidation products form upon reaction with OH that can form secondary aerosol (Latimer et al., 1998; Sommerlade et al., 1993; Chandramouli and Kamens, 2001; Wu and Johnston, 2016, 2017). Wu and Johnston (2017) studied the molecular composition and formation pathways of aerosol phase D_5 oxidation products at aerosol loadings of 1-12 µg m^{-3} and identified three main types of species: monomer (substituted D_5), dimer, and ring-opened oxidation products.

Janechek et al. (2017) atmospheric modeling at 36 km resolution provided the first spatial distribution and potential loadings of the oxidation products, of which some fraction likely form aerosol species. Peak oxidized D_5 (o-D_5) occurs downwind of urban areas with a monthly average concentration of 9 ng m^{-3}. Cyclic siloxane oxidation may represent an important source of ambient secondary aerosols with health and climate implications due to potential high loadings and widespread use of the precursor compounds. Personal care products are increasingly recognized as relevant sources of urban air pollution in developed cities (McDonald et al., 2018; Karl et al., 2018), are likely underrepresented in official inventories, and lead to poorly characterized ozone and secondary organic aerosol production.

To improve the community's ability to understand the health and climate impacts of secondary organic silicon particle formation, additional physical and chemical details on the particles are required. In this work, aerosols are produced using an oxidation flow reactor (OFR) which are photochemical flow-through reactors. OFRs are small (liter sized) reactors that use very high oxidation conditions to oxidize reactants in a matter of minutes (Kang et al., 2007; Kang et al., 2011; Lambe et al., 2011a). Advantages of using OFRs include the ability to quickly test a range of aging conditions, reach high oxidant exposures (multi-day exposure) in minutes, and deploy easily for ambient measurements. Additionally, OFRs have been successfully used to generate secondary organic aerosol (SOA) for measurement of hygroscopicity and for the impact

of oxidative aging on cloud condensation nuclei (CCN) activity (Lambe et al., 2011a; Lambe et al., 2011b; Palm et al., 2018).

~~Due to high OH concentrations and higher energy UV light in OFRs, the applicability of generated aerosols under these conditions has been evaluated by comparing aerosol yield (aerosol mass produced / mass of reacted gas precursor) and aerosol composition to well-established environmental chambers. Previous work has generally concluded SOA yield and chemical composition are comparable between OFRs and environmental chambers (Kang et al., 2007; Kang et al., 2011; Lambe et al., 2011a; Lambe et al., 2011b; Lambe et al., 2015; Bruns et al., 2015; Chhabra et al., 2015; Palm et al., 2018). Lambe et al. (2015) reported aerosol composition was independent of the oxidation technique (OFR vs environmental chamber) for similar OH exposures. Slight differences in SOA yield have been reported with OFR yields both higher (Kang et al., 2007) and lower (Lambe et al., 2011a; Bruns et al., 2015; Lambe et al., 2015). Possible differences in yields have been discussed including uncertainty (Bruns et al., 2015), non-identical reactor conditions (Kang et al., 2007; Lambe et al., 2015; Bruns et al., 2015), fragmentation at high oxidant conditions (Kroll et al., 2009; Lambe et al., 2012), and differences in wall losses (Lambe et al., 2011a; Bruns et al., 2015). Wall losses are important to consider for both environmental and OFR chambers when performing yield measurements (Krechmer et al., 2016; Pagonis et al., 2017; Palm et al., 2016).~~

~~OFRs can be erroneously operated under conditions that favor non-OH reactions depending on the chamber conditions. A number of studies have been performed to model the reactor chemistry and develop best operating conditions so that reaction with OH is favored and atmospherically relevant (Li et al., 2015; Peng et al., 2016; Peng et al., 2015). Best operating conditions were recommended based on studying the relative influence of 185 nm and 254 nm photolysis, reaction by ozone (O_3), and $O(^1D)$ and $O(^3P)$ radicals. Additionally, Palm et al. (2016) developed a model to correct for non-aerosol condensation pathways of low-volatility vapor in the chamber. These alternative pathways are condensation to the chamber walls, fragmentation to non-condensable vapors, and residence times not long enough for condensation to occur. If attention is paid to these OFR chamber issues, atmospherically relevant oxidation conditions can be produced.~~

In this work, we generated and characterized secondary aerosol from oxidation of D_5 and personal care product precursors using an OFR. This study characterized the particles for concentration, size, morphology, and energy-dispersive X-ray spectroscopy elemental composition ~~by energy-dispersive X-ray spectroscopy~~. Aerosol mass formation (yield) was quantified and sensitivity of precursor concentration, oxidant exposure, residence time, and seed aerosol was studied. Particle hygroscopicity or cloud seed formation potential was characterized by measurement of the hygroscopicity kappa parameter (κ), which is a measure of the particle water-uptake (Petters and Kreidenweis, 2007). Additionally, particle volatility was assessed by exposing generated aerosols to high temperatures. Finally, aerosol formation by thermal degradation of the parent compound was explored to account for potential aerosol production after contact of D_5 with heated surfaces.

2 Methods

Fifteen experiments were performed (Table S1) which contained five experiments to test aerosol yield sensitivity to system parameters, an experiment to test sensitivity to seed aerosols, two D_5 gas quantification quality control tests, three tests with generation of aerosol from the off-gassing of personal care products, two hygroscopicity measurements, aerosol volatility measurement, and thermal ~~degradation~~ aerosol production of parent D_5. The quality control tests were breakthrough testing of D_5 on the collection cartridge and verification that photo oxidation was the cause of D_5 depletion.

2.1 Aerosol generation and characterization

A 13.3 L Potential Aerosol Mass (PAM) OFR chamber (Kang et al., 2007; Kang et al., 2011; Lambe et al., 2011a) was used to oxidize vapor phase D_5. The OFR was run in the OFR185 mode (Peng et al., 2015) where O_3 and OH are generated in situ by photolysis of oxygen and water. The chamber is designed to operate at very high oxidation conditions yet still maintain atmospherically relevant ratios of OH/O_3 and HO_2/OH (Kang et al., 2007). All characterization and sampling was performed on the centerline exhaust while the 1 or 3 L min^{-1} ring flow (with more exposure to the reactor wall) was discarded as shown in Fig. 1. Compressed air (3.5 or 5 L min^{-1}) was passed through activated carbon and HEPA filters, and humidified to 25-40% relative humidity (RH) (Sigma-Aldrich Optima or Barnstead Nanopure filtered ultrapure reagent grade water). All experiments were performed under ambient conditions of 22 °C but the chamber was likely warmer (~24 °C (Li et al., 2015)) due to the lamps. No temperature correction due to potential OFR heating was employed in this work however. D_5 was introduced into the flow by diffusion from a temperature-controlled ~~heated T~~Teflon tubing leg filled with liquid D_5 (Sigma-Aldrich, purity 97%) controlled using a water bath.

Alternatively, precursor gases were introduced to the system flowing air (5 L min^{-1}, unheated) past personal care products in an Erlenmeyer flask. Results from antiperspirant containing cyclopentasiloxane and leave-in conditioner containing cyclomethicone are reported herein. Cyclopentasiloxane is the industry name for D_5 while cyclomethicone is the general term used for cyclic volatile methyl siloxanes. Prior to introduction to the system, the chamber was cleaned for ~24 h with the lights on and no precursor gas. Chamber and supply air were periodically assessed for cleanliness through checks of aerosol production under humidification and lamp irradiation, and generated concentrations of 400 cm^{-3} (number) and 0.001 µg m^{-3} (mass), well below the levels produced during D_5 oxidation experiments.

To remove organic gases and high concentrations of O_3 from the OFR effluent, two annular denuders using activated carbon (Fisher Scientific~~;~~, 6x14 mesh size) and Carulite 200 (manganese dioxide/copper oxide catalyst~~;~~, Carus Corp.) were used. The activated carbon denuder dimensions were 25 cm outside diameter (OD), 20 cm inside diameter (ID) by 125 cm, while the Carulite denuder had dimensions of 14 cm OD, 1 cm ID by 70 cm. The denuders were packed with material between the OD and ID. Teflon tubing was used upstream of the reactor and copper downstream. Silicon conductive tubing was minimized to limit silicon introduction from sources other than the main reagent.

Aerosols were measured using a TSI 3936L85 SMPS (TSI 3785 CPC, TSI 3080 classifier, TSI 3081 long column DMA, and TSI 3077 Kr-85 2mCi neutralizer). Mass concentration was estimated from the SMPS measured volume concentration assumed for spherical particles using a liquid D_5 density of 0.959 g cm^{-3}. Aerosol sampling covered 9.7 – 422 nm with a sheath flow of 6 L min^{-1} and aerosol flow of 1 L min^{-1}. SMPS measurements were corrected for size specific particle losses from gravitational settling, diffusion, and turbulent inertial deposition caused by tubing, bends, and constrictions (Willeke and Baron, 1993).

Particles were collected on a carbon film nickel transmission electron microcopy (TEM) grids (SPI 200 mesh) for microscopy and elemental analysis using an RJ Lee Group, Inc. Thermophoretic Personal Sampler (TPS100, RJ Lee Group) (Leith et al., 2014). The TPS100 samples was were collected using a hot and cold surface temperature of 110°C and 25°C, respectively, flow rate of 0.005 L min^{-1}, and a 25-min sampling time. The TPS100 samples were analyzed using a field emission scanning electron microscope (FESEM) with scanning transmission electron microscopy (STEM) capabilities (Hitachi S-5500). The FESEM was equipped with an energy dispersive X-ray spectroscopy (EDS) system incorporating a 30 mm^2 silicon drift detector (Bruker Quantax) for collection of elemental composition.

2.2 Yield

Five experiments were run to test the sensitivity of aerosol yield to residence time (flowrate), OH exposure (UV light intensity and RH), and reactant concentration (D_5 water bath temperature). ~~The system settings varied were UV light intensity, flowrate, relative humidity, and D_5 water bath temperature.~~ The influence of seed aerosols was quantified separately using 50 nm ammonium sulfate aerosols.

Experiments included a ~20 h equilibration period followed by an analysis period (~1.7 h) where the D_5 gas concentration was quantified upstream and downstream of the OFR. Gas samples were collected on solid phase extraction (SPE) cartridges. Immediately following D_5 gas collection, the precursor gas was switched to SO_2, allowing calculation of OH exposure. SO_2 with the OFR lights on was measured (Teledyne 100E) for an average of 4.6 h, followed by 3.3 h with the lights off. In this work, SO_2 loadings were 5 – 28 times higher than D_5. We recognize for the best estimate of OH exposure, similar concentrations are desired due to the potential for OH suppression in the chamber (Li et al., 2015; Peng et al., 2016; Peng et al., 2015). ~~.~~The aerosol yield was calculated from the SMPS particle loss-corrected mass concentration and the reacted D_5 gas measurements (aerosol mass / reacted D_5 gas concentration).

2.2.1 OH exposure quantification

OFR OH exposure was quantified using two methods, comparison of SO_2 gas concentrations with and without UV light, and aerosol production from SO_2 oxidation as measured by SMPS. Reference SO_2 gas (5 ppm in N_2) was diluted using mass flow controllers with the volumetric flow verified using a bubble flow meter (Sensidyne Gilian Gilibrator-2). The SO_2 monitor was calibrated following the calibration procedure provided by the manufacturer (slope = 1.400, offset = 41.4 mV). The

monitor calibration was checked using 337 and 981 ppb SO_2 reference gas with the measured monitor concentration within 1.8 and 1.4%, respectively.

The main method of OH exposure quantification used in the analysis was by the measurement ~~of the disappearance of~~ of reacted SO_2 in the OFR (Eq. (1)). The initial SO_2 gas concentration (450 – 1200 ppb) was measured at the OFR exit without UV illumination. The final gas concentration (6 – 190 ppb) was measured similarly, but with UV illumination. All analyzed gas concentrations were the last 20-min average for each respective period after equilibrating for 2-5 h. In Eq. (1) [OH]*t represents the OH exposure (molec s cm^{-3}), $[SO_2]$ and $[SO_2]_0$ the final and initial gas concentrations, respectively, and k_{SO_2} the OH rate constant. The SO_2 oxidation rate constant used was $9x10^{-13}$ cm^3 $molec^{-1}$ s^{-1} (Davis et al., 1979).

$$[OH] * t = \frac{-1}{k_{SO_2}} \ln\left(\frac{[SO_2]}{[SO_2]_0}\right) \quad (1)$$

Alternatively, the OH exposure was also estimated using aerosol production from SO_2 oxidation. This method assumes complete aerosol conversion of SO_2 oxidation. SMPS mass concentrations were calculated using the SMPS size range (9.7 – 422 nm), assuming spherical particles of sulfuric acid density (1.84 g cm^{-3}). OH exposure was calculated using Eq. (2) where [SMPS] represents the measured SO_2 oxidation aerosol mass concentration (1300 – 4200 µg m^{-3}), and $[SO_2]_0$ the SO_2 gas concentration at the OFR inlet. All aerosol measurements were analyzed for the same 20-min period used for the SO_2 gas analysis.

$$[OH] * t = \frac{-1}{k_{SO_2}} \ln\left(1 - \frac{[SMPS]}{[SO_2]_0}\right) \quad (2)$$

2.2.2 D_5 gas measurement

The reacted D_5 concentration was calculated by the difference of upstream and downstream concentration measurements. Duplicate 20-min samples were taken at 0.16 L min^{-1}, with flowrate monitored by a mass flowmeter (TSI 4100) calibrated to a bubble flowmeter (Sensidyne Gilian Gilibrator-2). Samples passed through a particle filter (Millipore Millex-FG 0.20 µm filter, CAT SLFG05010) followed by a SPE cartridge (10 mg isolute ENV+ with 1 mL capacity, Biotage AB) (Kierkegaard and McLachlan, 2010; Yucuis et al., 2013). The upstream and downstream gas sampling lines were constantly sampled at 0.16 L min^{-1} to maintain system flows and pressures, regardless of whether active sampling on sorbent was taking place.

2.2.3 Method for extraction and instrument analysis of D_5 in sample cartridges

During D_5 gas phase measurement and analysis, personal care products that contained cyclic siloxanes were avoided by laboratory personnel. Glassware was combusted overnight at 450°C, and then all supplies including glassware were triple rinsed with methanol, acetone, and hexane immediately prior to use. Solvents were pesticide grade from Fisher Scientific. Cartridges were cleaned by soaking in hexane overnight followed by washing 3 times each with dichloromethane and hexane, respectively. Each cartridge was wrapped in triple-rinsed aluminum foil, sealed in a triple-rinsed amber jar with

PTFE-lined screw cap, and kept in a clean media fridge until deployment. Following deployment each sample was re-wrapped in its aluminum foil, returned to its jar, and transferred to the lab for immediate extraction and analysis.

Sample cartridges were eluted with 1.5 mL hexane into gas chromatography (GC) vials. Sample extracts were spiked with 50 ng PCB 30 (2,4,6-trichlorobiphenyl, Cambridge Isotope Laboratories) immediately prior to instrument analysis as the internal quantification standard. D_5 for the calibration standard was purchased from Moravek Biochemicals. Samples were analyzed using an HP 6890 Series GC with an HP 5973 MSD equipped with an Agilent DB-5 column (30 m x 0.25 mm ID, and 1.0 µm film thickness) in select ion monitoring (SIM) mode. Instrument parameters are in Table S2.

Sufficient elution volume was tested by collecting a second cartridge elution of 1.5 mL for the sample with the highest anticipated concentration, and a cartridge breakthrough test was also performed. Quality Control was assessed through a blank spike test, duplicates, and additional blanks (field, instrument, and method) ~~blanks~~. Values reported herein are not blank corrected. See additional information on these in supplemental information. Non-reactive losses of D_5 in the sampling lines and reactor were examined in an experiment without reactor UV illumination. In duplicate testing the sample mass changed by less than 2% between upstream and downstream sampling points.

2.2.4 Seed aerosol experiment

Seed aerosol influence on yield was quantified using monodisperse 50 nm ammonium sulfate aerosol (~1000 cm^{-3}, 0.2 µg m^{-3}) prepared from atomized and dried ammonium sulfate solution (TSI 3076 atomizer, TSI 3062 dryer) with electrical mobility classification. To maintain system pressures between seed and non-seed conditions, seed aerosol entered through a tube with pressure drop equivalent to a HEPA filter, or was filtered through the HEPA filter. The seed influence was tested at a total chamber flow rate of 3.5 L min^{-1}, 25% RH, and 80% light intensity. Conditions cycled through D_5 only (24-h), D_5 + seed (24-h), D_5 only (12-h), D_5 + seed (12-h), and seed only (12-h).

2.3 Hygroscopicity

Hygroscopicity κ parameters were determined by measuring water supersaturation levels required to grow D_5 SOA into cloud droplets. A Droplet Measurement Technologies ~~(DMT)~~ cloud condensation nuclei (CCN) counter CCN-2 (single column, SN 10/05/0024) was used to generate supersaturation conditions and detect activated (grown) particles (Roberts and Nenes, 2005). A CPC (TSI 3785) sampled a side stream before the CCN counter~~DMT~~ as a measure of the incoming particles. The ~~controlled variable in the DMT instrument was the~~ thermal gradient (ΔT) ~~which~~ was varied from 0.4 to 24 K through up to eleven steps. Thermal gradients were mapped to supersaturations using monodisperse ammonium sulfate as a calibration aerosol with theoretical supersaturations calculated using the AP3 Kohler model (Rose et al., 2008). Additional details are provided in the supplemental information. The ΔT required for activation of any D_5 SOA aerosol was fitted to experimental activation fractions (f, the ratio of ~~DMT~~ CCN and CPC particle counts) using a Gaussian cumulative distribution function.

Eight different monodisperse diameters were tested ranging from 30 to 200 nm. These were produced using a TSI 3080 classifier, TSI long column 3081 DMA, and TSI 3077 neutralizer with sheath air set to 10 L min^{-1}. Tubing lengths were the same from the DMA ~~source~~ to the ~~DMT~~CCN counter, and the ~~source~~ DMA to the CPC, minimizing the effects of differential particle loss. The ~~DMT instrumen~~CCN counter~~t~~ was operated with the recommended total flow of ~0.5 L min^{-1} and a 10:1 sheath to sample flow ratio. Ammonium sulfate (Fisher Scientific, purity ≥99%) calibration aerosols were generated using a solution of 1 g L^{-1} prepared in DI water (TSI 3076 atomizer~~,~~; syringe pump ~15 mL h^{-1}~~,~~; TSI 3062 diffusional dryer) followed by dilution to 2000-3000 cm^{-3}. D_5 SOA was generated using the OFR with a total chamber flow of 5 L min^{-1}, 30% RH, D_5 water bath at 70°C, ring flow at 3 L min^{-1}, and 100% light intensity. The oxidized D_5 aerosol stream was not diluted as concentrations were similar to the diluted ammonium sulfate.

~~Two issues complicated DMT data analysis. First, temperature and flow spikes were observed that were caused by intermittent faults in a sample temperature sensor. This sensor was part of the instrument feedback control loop used to maintain the column thermal gradient, and accordingly these sensor faults upset the column thermal gradient and required some time to settle. Second, for some of the higher ΔT set points, the temperatures were not able to reach the set points but were stable. To correct for these issues, scripts were developed to automatically classify data into stable (used in data analysis) and unstable (excluded) periods. Data were~~as initially binned to 30 s intervals (raw DMT data was at 1 s, CPC data was at 5 s). For each 30 s period, temperature, flow, and pressure stability were calculated and compared to thresholds as described below; periods were then flagged as stable or unstable.

~~Four temperature tests were used: (i) ΔT varied by no more than 0.16 K from the previous 10 s moving average; (ii) T1 (column low temperature) varied by no more than 0.20 K from the previous 10 s moving average; (iii) T3 (column high temperature) varied by no more than 0.20 K from the previous 10 s moving average; and (iv) that the 1 s values of ΔT varied by no more than 0.37 K during the 30 s period. Pressure and flow were checked individually to make sure the relative percent difference between the current value and the 10 s moving average was lower than 4.5%. These data exclusion thresholds were selected by visual inspection of the data, but final data processing was automated. Failure of a single test in any 30 second period led to exclusion from analysis. For periods compliant with these tests (70%), average DMT and CPC concentration were calculated along with the average ΔT.~~

The Gaussian cumulative distribution function in Eq. (3) was used to fit the measured activation fractions to three parameters (a is the activation threshold, b the activation ΔT, and c the sharpness of the inflection point) which represents the average hygroscopicity, κ_a of CCN active particles (Rose et al., 2010). A lower hygroscopicity parameter, κ_t, was determined from a two parameter (b and c~~,~~; a=0.5) fit representing the effective hygroscopicity of both active and inactive CCN particles. The two-parameter method is best used when CCN inactive and active particles are externally mixed and for comparison to H-TDMA data (Rose et al. 2010). If the aerosol is of homogenous composition/CCN activity, internally mixed, and there are no counting efficiency errors or particle losses, κ_a and κ_t should be equal. Deviations in $f \neq 1$ can be used to estimate the fraction of CCN-inactive particles (Rose et al., 2010).

$$f = a\left[1 + erf\left[\frac{(\Delta T - b)}{c\sqrt{2}}\right]\right] \quad (3)$$

The measured diameter and activation supersaturation pairs were used to determine the effective hygroscopicity parameter, κ using Eq. (4), the Kappa-Kohler equation. Here s is the supersaturation ratio, D_{wet} is the wet particle diameter which is unknown, D the dry particle diameter taken as the classifier size selected particle diameter, σ_{sol} is the surface tension assumed for pure water at the column T1 temperature, M_w is the molecular weight of water, and ρ_w is the density of water at T1. Since the surface tension of pure water is assumed rather than the solution properties (due to the lack of physical properties on the D_5 oxidization products) this is the effective hygroscopicity parameter (Rose et al., 2010; Petters and Kreidenweis, 2007). Equation (4) is solved iteratively by guessing an initial κ, finding the D_{wet} that corresponds to the peak supersaturation from the Kohler curve, and using the D_{wet} term found along with the measured supersaturation to solve for a new κ guess which is then substituted into Eq. (4) to find a new D_{wet}. Iteration was stopped when D_{wet} and κ converged to the experimental supersaturation.

$$s = \frac{D_{wet}^3 - D^3}{D_{wet}^3 - D^3(1-\kappa)} exp\left(\frac{4\sigma_{sol}M_w}{RT\rho_w D_{wet}}\right) \quad (4)$$

2.4 Volatility

D_5 SOA was generated as described in 2.3 and then evaporated in a volatility tandem differential mobility analyzer (V-TDMA), previously described in Singh (2015). The V-TDMA featured a 2 s residence time, 1 meter length stainless steel heated and bypass tubes (0.77 cm ID), and a 1 L min^{-1} flowrate. Test aerosols were size selected using electrical classification (TSI 3085) prior to the V-TDMA. Volatility was assessed by comparison of the diameters of unheated and heated aerosols modes, at five temperatures (50, 80, 110, 150, 190°C) and six sizes (10, 20, 30, 50, 80, and 110 nm). These tests were conducted with average aerosol concentrations of 119 – $8x10^4$ cm^{-3} and $1x10^{-4}$ – 18 μg m^{-3} (Table S7). In total, 156 samples were collected over 7 h, or two to four replicates at each diameter/temperature combination. Due to some of the very small size changes observed, a continuous number size distribution mode was fit from the discrete SMPS distribution.

2.5 Thermal aerosol production~~degradation~~

Vapor phase D_5 (estimated mixing ratio of 270 ppm) was generated by bubbling particle free air through liquid D_5 using a gas bubbler at 20°C followed by a HEPA filter to remove droplets. The vapor D_5 was heated up to 550°C using the V-TDMA system or a stainless steel tube placed in a tube furnace. Both tubes had a residence time of 2 s and the resulting effluent was measured by SMPS to determine if particle formation occurred.

3 Results and discussion

3.1 OFR chemistry

Due to high OH concentrations and higher energy UV light in OFRs, the applicability of generated aerosols under these conditions has been evaluated by comparing aerosol yield (aerosol mass produced / mass of reacted gas precursor) and aerosol composition to well-established environmental chambers. Previous work has generally concluded SOA yield and chemical composition are comparable between OFRs and environmental chambers (Kang et al., 2007; Kang et al., 2011; Lambe et al., 2011a; Lambe et al., 2011b; Lambe et al., 2015; Bruns et al., 2015; Chhabra et al., 2015; Palm et al., 2018). Lambe et al. (2015) reported aerosol composition was independent of the oxidation technique (OFR vs environmental chamber) for similar OH exposures. Slight differences in SOA yield have been reported with OFR yields both higher (Kang et al., 2007) and lower (Lambe et al., 2011a; Bruns et al., 2015; Lambe et al., 2015). Possible differences in yields have been discussed including uncertainty (Bruns et al., 2015), non-identical reactor conditions (Kang et al., 2007; Lambe et al., 2015; Bruns et al., 2015), fragmentation at high oxidant conditions (Kroll et al., 2009; Lambe et al., 2012), and differences in wall losses (Lambe et al., 2011a; Bruns et al., 2015). Wall losses are important to consider for both environmental and OFR chambers when performing yield measurements (Krechmer et al., 2016; Pagonis et al., 2017; Palm et al., 2016).

OFRs can be erroneously operated under conditions that favor non-OH reactions depending on the chamber conditions. A number of studies have been performed to model the reactor chemistry and develop best operating conditions so that reaction with OH is favored and atmospherically relevant (Li et al., 2015; Peng et al., 2016; Peng et al., 2015). Best operating conditions were recommended based on studying the relative influence of 185 nm and 254 nm photolysis, reaction by ozone (O_3), and $O(^1D)$ and $O(^3P)$ radicals. Additionally, Palm et al. (2016) developed a model to correct for non-aerosol condensation pathways of low-volatility vapor in the chamber. These alternative pathways are condensation to the chamber walls, fragmentation to non-condensable vapors, and residence times not long enough for condensation to occur. If attention is paid to these OFR chamber issues, atmospherically relevant oxidation conditions can be produced.

The OFR chamber conditions tested in this work were evaluated for non-atmospherically relevant chemistry using the OFR Exposure Estimator (v3.1) tool (Lambe and Jimenez, 2018). The OFR Exposure Estimator tool was developed using a plug-flow kinetic box model to study the importance of 185 and 254 nm photolysis, $O(^1D)$, $O(^3P)$, and O_3 chemistry relative to OH (Li et al., 2015; Peng et al., 2016; Peng et al., 2015). Organic radical species have not been assessed in the tool. HO_2 radicals are an important component in OFR chemistry, as well as in the atmosphere, but generally are negligible for volatile organic compounds (VOC) oxidation due to low reaction rates relative to OH (Peng et al., 2016). In order to ensure the OFR is run under conditions favoring OH reaction, Peng et al. (2016) recommended an external OH reactivity (OHR_{ext}) < 30 s^{-1}, H_2O mixing ratio > 0.8%, and 185 nm UV flux > $1x10^{12}$ photons cm^{-2} s^{-1}. OHR_{ext} refers to the product of the gas concentration and the OH ~~reaction~~ rate constant. All experimental conditions used in our OFR experiments were evaluated using the OFR Exposure Estimator tool and fall in the regime with OH chemistry favored. The regime for the personal care product oxidation (Sect. 3.3) could not be determined due to the lack of an estimate of gas concentration.

However, the personal care concentrations could be up to 20 times greater than the D_5 concentrations used and still fall in the OH-favored regime. Chamber conditions for the 12 scenarios had a water mixing ratio of 0.81 – 1.5% (25-45% RH), OHR_{ext} 0.5 – 26 s^{-1}, and 185 nm photon flux as estimated from Li et al. (2015) 6.5 – 8.6 $x10^{13}$ photons cm^{-2} s^{-1}.

3.2 Yield

SMPS aerosol concentrations were corrected to account for particle losses caused by the denuders and tubing downstream of the OFR. Particle loss correction increased the number concentration 7-11%, mass by 3-5%, and decreased the number distribution mode slightly. Upstream and downstream SO_2 gas concentrations matched within 9% without OFR illumination, indicating SO_2 was not lost to surfaces or leaks. Calculated OH exposure based on SO_2 oxidation varied from 1.60 to 5.12 $x10^{12}$ molec s cm^{-3}, which is equivalent to 12 to 40 days of atmospheric aging assuming an OH concentration of $1.5x10^6$ molec cm^{-3} (Palm et al., 2016). Measured OH exposures were 4 – 5 times lower than OH exposure predicted from the OFR Exposure Estimator tool in Sect. 3.1. A likely source of uncertainty in the predicted OH exposure is UV light intensity which was estimated from the intensity output from a similar OFR reported in Li et al. (2015). Despite using the same lamp model, light intensity likely varies due to age-related reduction or production differences. Previous evaluation of the predicted OH exposures found values to be within a factor of 3 for 90% of SO_2 derived OH estimates (Li et al., 2015).

The SO_2 gas phase derived OH exposures were evaluated compared to the estimate derived from SO_2 oxidation aerosol measurements. Generally, there was good agreement between the two methods. The aerosol derived estimate of OH exposure, agreed within a factor of 3.6 for experiment 1, and a factor of 1.0-1.8 for the remaining experiments which used higher SO_2 concentrations due to low unreacted SO_2 concentrations in the first trial.~~for the SO_2 monitor.~~ Generally, the aerosol derived OH estimates were lower than the estimates from SO_2 gas reactive consumption. One explanation for lower SO_2 derived OH exposure is the potential for loss of sulfate aerosol in the OFR (Lambe et al., 2011a).

It should be noted however, that extending the OH exposure estimates measured from SO_2 oxidization and applying to the D_5 conditions, one must be careful to consider the external OH reactivity differences due to OH suppression (Peng et al., 2016; Peng et al., 2015; Li et al., 2015). Under the given experimental conditions, SO_2 external OH reactivity loadings were 5-28 times higher than D_5 loadings and therefore OH exposure conditions would be anticipated to be higher for D_5 experiments. The OFR Exposure Estimator tool predicts that under the given experimental conditions, D_5 OH exposure may be 1.5-2 times higher than those reported from SO_2 measurements. While this does not change the conclusions drawn from this work, the uncertainty in OH exposure should be acknowledged.

D_5 gas concentrations (Fig. S4) upstream of the chamber ranged from 290 – 740 µg m^{-3}, and downstream from 9 – 24 µg m^{-3}. This suggests the reactor consumed nearly all of the precursor gas. Gas measurements had good reproducibility between duplicate samples, and between replicate conditions (trials 2 and 4). Additionally, gas concentrations varied as expected ~~in reasonable ways~~ with respect to dilution flows and to the water bath temperature that was driving D_5 evaporation into the system.

A typical yield experiment is shown in Fig. 2. Experiments included a ~20 h settling period for the system to attain a steady state. This was followed by a ~2 h sampling period, ~~yield determination period,~~ during which ~~the~~ four gas samples were taken to determine ~~-~~D_5 SOA yields. ~~gas concentrations were measured (2 upstream and 2 downstream) and these were used for determination of reactive organic gas (ΔROG) and associated yield calculation.~~ Similar to Kang et al. (2007), the settling period often had an initial maxima in mass and number during the first few hours. After the yield determination period, SO_2 was used to determine OH exposure. Aerosol fluctuations tended to be more stable for the 3.5 L min^{-1} tests than 5 L min^{-1}. During the analysis period, aerosol concentrations were reasonably stable in time, with temporal variability (expressed as relative percent difference at 3.5 L min^{-1}) of 9 – 11% and 9 – 13% for number and mass concentrations, respectively. At the higher 5 L min^{-1} flow, variability increased to 18 – 26% (number) and 8 – 32% (mass). We suspect variability in the D_5 injection rate as a primary cause of variability in the SMPS-detected aerosols from the OFR. Table 1 contains aerosol statistics for the analysis periods.

Yields varied between 0.22 – 0.50 corresponding to aerosol concentrations of 68 – 220 µg m^{-3}. Yield was generally invariant of reacted D_5, increased monotonically with OH exposure, and generally increased with aerosol mass (Fig. 3). Reactive organic gas (ΔROG) did not increase with OH exposure since OH was in excess and D_5 was limiting. OH exposure had a strong effect on yield, which is consistent with chemical changes to the products with greater OH exposure. Increasing aerosol yield with higher OH exposure has been observed in OFR studies with other reactants but yield typically reaches a maximum above which fragmentation reactions likely decrease yield (Lambe et al., 2011a; Lambe et al., 2012; Lambe et al., 2015). No yield maximum with respect to OH exposure was observed. Wu and Johnston (2017) reported aerosol yields of 0.08 – 0.16 at aerosol loadings of 1.2 – 12 µg m^{-3} (at constant OH) with yields increasing with reacted D_5 and aerosol loadings. Wu and Johnston (2017) caution that their yields are based on estimated rather than measured D_5 consumption. Our data point for trial 4 (yield of 0.5) is higher than the others, which were in the 0.22-0.3 range. While the experimental conditions of trial 4 were unique (high RH, high light intensity, low flow, and long residence time) and consistent with a potentially high yield, we note that we did not perform additional experiments which would replicate or invalidate this finding; we further note that variability (in time) of mass was approximately ~~was~~ up to 13% (by mass) as low flow and 32% (by mass) at high flow.

Wu and Johnston (2017) suggest the aerosol composition is highly dependent on aerosol mass loading with less volatile ring-opened species at low loadings and as particles grow, composition shifts to dimer formation and semi-volatile monomer species. This implies that at the high loadings observed in this work, aerosol composition is likely dominated by semi-volatile monomer species and non-volatile dimer species. In context of available knowledge of aerosol formation for cVMS, Wu and Johnston (2017) observed aerosol size affected aerosol composition, and this work shows the extent of oxidation may also contribute to aerosol chemistry.

3.2.1 Fate of condensable products in the OFR

Condensable vapor (i.e. semi-volatile reaction products) in the OFR can form aerosol, or condense to chamber walls, or undergo fragmentation to non-~~volatile~~ condensable compounds through multiple OH oxidation, or exit the chamber as a uncondensed semi-volatile gas (Palm et al., 2016). Experiment-specific fates of condensable vapor for the OFR conditions used in this work were assessed using a condensational loss model (Palm et al., 2016; Lambe and Jimenez, 2018). The model compares the relative timescales of competing fates for low volatility organic compounds (LVOC). We modified the LVOC fate model to our chamber conditions for the five yield experiments, and assumed an LVOC diffusion coefficient for the single OH substituted D_5 molecule, 4.64×10^{-6} m^2 s^{-1} (Janechek et al., 2017). Recommendations for gas diffusion sticking coefficient, OFR volume, eddy diffusion coefficient, number of reactions with OH required to render non-~~volatile~~ condensable through ~~fractionation~~fragmentation, and surface/volume ratio were from Palm et al. (2016). For the condensational sink calculations (Table S5), the average of the SMPS measurement of the entrance (particle free) and exit was used. For the five yield experiments, the predominant calculated fate is condensation to aerosols (>97%) and aerosol concentrations were not corrected for non-aerosol condensation losses.

Chamber experiments were typically run with particle free incoming air so nucleation must play an important role in aerosol formation within the chamber owing to the high yields and mass loadings observed. If initial particle growth is fast enough to serve as sufficient condensation sinks for condensable vapors, then the non-aerosol fates are negligible due to the high aerosol concentrations. Alternatively, if the condensational sink is low, the dominant fate is expected to be multi-generational OH oxidation that could lead to fragmentation. For the range of OH conditions tested in this work, no evidence of fragmentation was observed due to increasing yield with OH exposure. Although the predominant fate of condensation to aerosols remained above 87% in the fate model even for reductions in the condensational sink by ~~2~~an order~~s~~ of magnitude, our yields may be biased low due to the neglecting of loss to the chamber walls. This is possibly supported by the increase in yields described in 3.2.2.

3.2.2 Seed aerosol effect

The seed aerosol influence on aerosol yield was quantified by averaging the final 2 h of SMPS measurements for each of the periods described in Sect. 2.2.4. Here 50 nm ammonium sulfate seed aerosol was added upstream of the reactor to serve as a condensational sink for aerosol formation. The addition of seed aerosols resulted in an increase in number concentration of 2.6%, and mass concentration of 44%. Wu and Johnston (2017) similarly observed positive yield sensitivity to ammonium sulfate seed aerosols.

3.3 Personal care product as reactant

Replacing liquid D_5 with personal care products as the source of reactive gases similarly generated aerosols when oxidized using the OFR. Using a 10 mg solid flake of antiperspirant as the vapor source led to immediate production of over 2000 µg

m^{-3} in the OFR with decay to 600 µg m^{-3} within 1 h, and 60 µg m^{-3} after 4 h. The addition of fresh antiperspirant returned the aerosol concentrations to the initial level. The source of the aerosols was verified to be photooxidation of volatilized components of ~~a~~ the personal care product since the cleaned chamber concentrations prior to introduction was 0.03 µg m^{-3}, and removing the personal care product or turning off the chamber lights resulted in rapid concentration decrease. The use of 25 mg of conditioner as the vapor source was qualitatively similar but resulted in much lower aerosol loadings of around 40 µg m^{-3}, possibly due to lower cVMS content (Wang et al., 2009; Dudzina et al., 2014).

Particle morphology and elemental composition of D_5 and antiperspirant generated aerosols were analyzed using electron microscopy. The antiperspirant sample was collected 2 h after the initial flake was added to the system with average SMPS concentrations of $2x10^6$ cm^{-3}, 370 µg m^{-3}, and mode of 50 nm. Similar morphology and elemental composition was observed compared to the generated particles using pure D_5 (Fig. 4). Particles generated from both sources had spherical morphology with some aggregates. Elemental composition was consistent from a siloxane source with Si and O elemental peaks observed relative to the background. Background peaks of nickel and carbon were observed consistent with the TEM grid. The techniques employed herein can confirm the presence of Si in the SOA formed from the antiperspirant, but cannot attribute the fraction of the SOA formed to the various ingredients in the antiperspirant. Samples from the SOA formed from conditioner were not collected for microscopy. In both cases, the personal care products are known to contain other SOA precursors, such as fragrances that may contain monoterpenes and terpenoids.

3.4 Hygroscopicity

The CCN measurements up to 1.9% supersaturation were used to calculate the effective hygroscopicity parameter κ for the oxidized D_5 aerosols. As described in the methods section, first the ~~DMT~~ CCN counter temperature differential ΔT was correlated to the supersaturation (S) using theoretical calculations of ammonium sulfate activation supersaturation and measured ammonium sulfate activation ΔT. The result was $S = 0.08449 * \Delta T - 0.1323$ (R^2 of 0.994). The linear fit was used to correlate the cVMS 3-parameter and 2-parameter activation ΔT to critical supersaturation needed for κ calculation.

The cVMS measurements (Fig. 5) were corrected for size dependent particle losses and counting efficiencies by dividing by the maximum activation fraction from the ammonium sulfate uncorrected 3-parameter fit. The size dependent maximum activation fractions used were 0.78, 0.87, 0.91, 0.92, 0.94, 0.96, 0.97, and 1.00 for 30, 50, 70, 90, 110, 140, 170, and 200 nm particles, respectively. The remaining deviations from $f_{max} \neq 1$ for cVMS sizes 70-200 nm was attributed to non-homogeneous aerosol composition. Oxidized D_5 particles at 30 and 50 nm were too small to exhibit enough activation behavior for calculations (at supersaturations of 1.9%); therefore, κ calculations for oxidized D_5 started at 70 nm.

The average D_5 oxidation aerosol κ_a and κ_t were 0.011 and 0.0065, respectively. Figure 6 (Table S6) show the D_5 oxidation and ammonium sulfate aerosol size dependent effective hygroscopicity parameters as determined by the 3-parameter and 2-parameter fits, labeled κ_a and κ_t, respectively. Typical κ values range from 0 for insoluble materials such as soot (Rose et al., 2010) to 1.28 for NaCl (Petters and Kreidenweis, 2007). A large κ value corresponds to a species that more easily serve as CCN than a species with a small κ value. Zhao et al. (2015) reported examples of secondary organic aerosol κ

ranging from 0.01 – 0.2, while Lambe et al. (2011b) reported $8x10^{-4}$ – 0.28. The κ for oxidized D_5 aerosol are on the low end of previously reported SOA. Some literature-reported organic compounds with κ below 0.03 include adipic acid and suberic acid (Cerully et al., 2014) and SOA from OFR oxidation of hydrophobic precursors such as C-17 alkane, bis(2-ethylhexyl) sebacate (BES), and engine lubricating oil (Lambe et al., 2011b). The average ammonium sulfate kappa value was calculated using the same algorithm, and a value of 0.79 was obtained. However, there was considerable error for the linear fit correlating ~~DMT~~ CCN counter ΔT to supersaturation at low supersaturations for ammonium sulfate particle sizes of 140 – 200 nm (percent error of 30%). This was also observed in Rose et al. (2008) for their low supersaturations.

Figure 6 shows that no clear size dependence was observed for κ_t, while κ_a ~~observed~~ resulted in smaller particles exhibiting larger kappa values. This suggests the cVMS oxidation aerosol composition was size dependent in our experiments with smaller particles likely more oxidized. For SOA, higher hygroscopicity for smaller particles likely arises from more oxidized composition with possible explanations thought to be the Kelvin effect and greater surface area/volume ratios impacting heterogenous oxidation or increased incorporation of later generation products ~~The observed decreasing trend of κ with increasing particle size has been observed before in SOA~~ (Zhao et al., 2015; Winkler et al., 2012). ~~and attributed to smaller particles being more highly oxidized.~~

3.5 Volatility

Particle diameter shift (Fig. S13) between heated and non-heated aerosols indicated the D_5 oxidation aerosols produced from the OFR were nearly non-volatile. Particle shrinkage increased with increasing temperature and for smaller sizes which have increased vapor pressure due to particle curvature (Kelvin effect). However, no particles other than 10 nm experienced greater than 4% shrinkage. Particles with 10 nm diameters experienced shrinkage up to 27% but low particle numbers (100-1700 cm^{-3}) and temporal variability complicated the interpretation. Number concentrations (Fig. S14) largely stayed unchanged within ± 15% between heated and unheated cases for particles of size 20 – 110 nm.

3.6 Thermal ~~degradation~~aerosol production

Since indoor air with high concentrations of cVMS will periodically be contacted against hot surfaces (heating elements of cooking, heating, hobby, and personal care devices), we assessed whether air with D_5, heated up to 550°C would result in any aerosol formation. Siloxane and silicone polymer (polydimethylsiloxane, ~~;~~ PDMS) are reported as thermally stable (Hall and Patel, 2006; Clarson and Semlyen, 1986), while Erhart et al. (2016) report polymerization of liquid siloxanes at 300° and decomposition at 400°C. We could find no reports in the literature on a thermal degradation temperature for D_5 in air, or whether thermal degradation products might tend to condense onto preexisting aerosols or to homogeneously nucleate. Octamethylcyclotetrasiloxane (D_4) has been reported to catalytically polymerize through interaction with a borosilicate container wall when heated to 420°C under vacuum (Clarson and Semlyen, 1986).

No particle formation was observed for any of the tested temperatures (100, 150, 200, 250, and 550°C). With the experimental configuration, condensable decomposition products could occur but elude detection by condensing onto the

tubing walls. Therefore, D_5 vapor was heated to 550°C and after heating, 80 nm ammonium sulfate seed particles were introduced to provide a condensational sink for the cooling condensable gases. No growth in the seed aerosols was observed.

These experiments also serve as a control to the volatility experiments. Residual D_5 in the vapor phase, heated along with the SOA aerosols, would not be expected to generate any condensable product that could complicate interpretation of the results in Section 3.5.

3.7 Relevance and unanswered questions

In Janechek et al. (2017), the propensity for SOA generation from D_4, D_5, and D_6 across North America was modeled by tracking the OH oxidation products in the gas phase in the CMAQ photochemical grid air quality model. The Janechek et al. (2017) results can therefore be interpreted as the ambient aerosol concentration under the assumption of 100% aerosol mass fraction (yield). Averaged over the North American modeling domain, the oxidized D_5 concentration peaked in summer at ~0.8 ng m^{-3}, and the peak monthly averaged concentration occurred downwind of population centers, and was ~10 ng m^{-3}. Adjusting these downward using the yields found in this work (0.2-0.5) or to the lower yield measured by Wu and Johnston (2017) (0.08 – 0.16), one would infer~~argue~~ that secondary organosilicon aerosols from personal care products should be a very minor mass contributor to outdoor aerosol. However, they should be ubiquitous – present as a widespread and diffuse background anthropogenic secondary organosilicon aerosol. A possible estimate of the strength of this "signal" is ~0.1 ng m^{-3}, based on a reduction of the levels from Janechek et al. (2017) according to the yield experiments of this work.

However, a number of questions remain about this. The assessment done by Janechek et al. (2017) looked only at (a) well-mixed outdoor air (mixed at a spatial scale of 36 km), and (b) D_4, D_5 and D_6 from estimated personal care product use. Other sources of volatile Si were not considered. McDonald et al. (2018) estimated volatile chemical products (VCPs) represent half the petrochemical derived VOC emissions and the major contributor to potential SOA.

Future questions about secondary organosilicon aerosols include: (a) how relevant are the harsh oxidation (high OH) conditions used in available experimental work for the real atmosphere, (b) what are silicon oxidation product concentrations (gas and particle) in indoor environments and microenvironments such as cars where up to 25 ppb D_5 have been observed (Coggon et al., 2018), (c) how well do personal care products with D_4-D_6 represent all SOA-producing organosilicon gases, and (d) how do Si-containing and non-silicon containing SOA precursors interact, since both are clearly present from VCPs. While Tang et al. (2015) showed that 31% of molecules offgassed in an indoor environment were cVMS, and McDonald et al. (2018) showed that a large ambient contribution to anthropogenic SOA is from VCPs – the situation of a substantial anthropogenic organosilicon SOA contribution from Si-containing VCPs cannot yet be ruled out. Reaction of VCPs in the atmosphere can also contribute to O_3 formation.

The only probable ambient detection of photochemical organosilicon SOA in the literature is that of Bzdek et al. (2014), who measured a 1-h averaged peak of 5.5 ng m^{-3} of Si using Nano-Aerosol Mass Spectrometer (NAMS) in Pasadena, California ~~which measures only~~ in the 20-25 nm range. Other detections by the same instrument occurred in coastal Delaware on the US East Coast. ~~Using the fact that cVMS oxidation products are only 38% Si, and that the 20-25 nm range~~

~~typically represents ~1% of the condensational sink (Bullard et al., 2017), we can extrapolate organosilicon SOA of 1.5 μg m^{-3} from Bzdek et al. (2014). At over 1000 times the expected organosilicon SOA for that location from Janechek et al. (2017), the result raises questions whether the difference is due solely to the reduction in concentration in the model due to spatial and temporal averaging, or whether there are more fundamental gaps in our understanding of the sources and chemistry of silicon-containing ultrafine and secondary aerosols~~.

If our understanding of the chemistry, physics, and sources is complete, then issues of spatio-temporal variability can be addressed through finer scale models and comparison to enhanced measurements. For large-scale models that aim to produce a regional, continental, or hemispheric organosilicon signature from cVMS personal care products, the best available information on yield is shown in Fig. 7, which combines experimental data from this work and Wu and Johnston (2017). Fitting the data to Eq. (5), an Odum two parameter semi-volatile model, results in parameters with yields (α) of 0.14, and 0.82, respectively for saturation concentrations (c*) of 0.95 μg m^{-3} and 484 μg m^{-3}. The variable α is the mass based stoichiometric yield, K_{om} the particle phase partitioning coefficient (m^3 μg^{-1}) which is equivalent to 1/c* (μg m^{-3}), M_o the aerosol mass concentration (μg m^{-3}), and Y the aerosol yield (aerosol mass fraction). Accordingly, ambient modeling of cVMS SOA could be performed with these parameters, or with a one product model using the lower volatility species (α of 0.14 at c* of 0.95 μg m^{-3}), or a non-volatile product with yield of ~0.1. Information about the temperature dependence of these values is currently unknown.

$$Y = M_o\left(\frac{\alpha_1 K_{om,1}}{1 + K_{om,1}M_o} + \frac{\alpha_2 K_{om,2}}{1 + K_{om,2}M_o}\right) \quad (5)$$

These estimates are subject to the obvious caveats of the high concentration experiments done to date, the uncertainties of applying OFR results to the ambient atmosphere, and the possibility of alternate oxidants or undiscovered aqueous or heterogeneous pathways. It is also important to point out that the application of the D_5 yield measurements to other siloxanes (e.g. D_4 or D_6) is uncertain due to the lack of yield measurements for these compounds. D_4 SOA has been confirmed in chamber work (Wu and Johnston, 2016) but yields were not quantified. One would anticipate based on decreasing volatility with ring size of the precursors (Lei et al., 2010), yields would increase for larger siloxanes. Regardless, ~~But they~~this work should be sufficient as a guide for future laboratory, modeling, and field experiments on the subject of organosilicon aerosols.

4 Conclusions

This study adds to the short list of laboratory confirmations where aerosol formation from OH oxidation of D_5 has been observed and provides one of the first assessments of particle morphology. In this work, a further confirmation of atmospheric relevance was conducted by verifying that similar aerosols were produced when vapor from solid antiperspirant ~~or from hair conditioner~~ was used as the reactant. A number of important physical properties of these aerosols have now

been established, including morphology via electron microscopy, chemical composition (EDS analysis microscopy), sensitivity to seed aerosol, volatility (V-TDMA), and hygroscopicity (CCN activation). We can conclude that in our OFR experiments D_5 with OH produces non-volatile, nearly insoluble aerosols at high yields. Electron microscopy and EDS analysis indicated fractal chain agglomerates were formed in the OFR, with substantial Si and O in the elemental EDS spectra. Using gases emitted from personal care products as the OFR reactant, generated particles with similar morphology and chemical composition compared to the D_5 experiments. Yield dependence on OH exposure and size dependence of hygroscopicity suggest that multiple condensable products make up these aerosols. This is consistent with the proposed mechanism and molecular product assignments of Wu and Johnston (2017).

~~In a companion paper, aerosols were assessed for acute toxicity in lung tissue during in vitro testing, as well as for propensity to induce biomarkers of inflammation (King et al., 2018).~~ I~~An i~~mportant caveats of our work are~~is~~ the high concentrations under which these experiments were conducted, and the limited number of trials for yield, with only one at each condition.

Through integration of this work with other experiments (Wu and Johnston, 2017) and modeling (Janechek et al., 2017), we have proposed aerosol yield parameterization suitable for atmospheric modeling, and can now estimate the SOA yield from personal care product ~~D_4, D_5, and D_6~~ cVMS. The SOA from silicon containing personal care products is likely present downwind of many populated areas, and thus may be an additional marker of anthropogenic aerosols. Field confirmation of these values, determination of spatial-temporal patterns, and reconciling of the limited modeling and observational studies are needed.

Additionally, this work provides much needed physical property data and yield parameterization to describe aerosol formation. With the caveats of the low number of replicates, high concentrations, and uncertainty due to sensitivity to seed aerosol, we provide ~~A~~ a recommendations for modelers~~ is to use one of the following, depending on the modeling framework and goals~~: (a) two parameter semi-volatile model with yield parameters of 0.14, and 0.82, respectively for saturation concentrations (c*) of 0.95 μg $m^{-3}$and 484 μg m^{-3}; (b) one product model using the lower volatility species (α of 0.14 at c* of 0.95 μg m^{-3}); (c) a non-volatile product with yield of ~0.1.

Competing interests

The authors declare that they have no conflict of interest.

Acknowledgements

This research was funded by the National Institute of Environmental Health Sciences through the University of Iowa Environmental Health Sciences Research Center (NIEHS/NIH P30ES005605), the Iowa Superfund Research Program, National Institute of Environmental Health Sciences (grant P42ES013661), and the National Science Foundation (grant

ATM-0748602). We thank RJ Lee Group for providing the TPS100 sampler and for performing the microscopy and elemental analysis. We also thank Keri Hornbuckle for use of her analytical environmental chemistry lab and for discussions about the research.

References

Ahrens, L., Harner, T., and Shoeib, M.: Temporal variations of cyclic and linear volatile methylsiloxanes in the atmosphere using passive samplers and high-volume air samplers, Environ. Sci. Technol., 48, 9374-9381, doi:10.1021/es502081j, 2014.

Atkinson, R.: Kinetics of the Gas-Phase Reactions of a Series of Organosilicon Compounds with OH and NO3 Radicals and O3 at 297 +/- 2 K, Environ. Sci. Technol., 25, 863-866, doi:10.1021/es00017a005, 1991.

Brooke, D., Crookes, M., Gray, D., and Robertson, S.: Environmental Risk Assessment Report: Decamethylcyclopentasiloxane, Environment Agency of England and Wales, Bristol, UK, 2009a.

Brooke, D., Crookes, M., Gray, D., and Robertson, S.: Environmental Risk Assessment Report: Dodecamethylcyclohexasiloxane, Environment Agency of England and Wales, Bristol, UK, 2009b.

Brooke, D., Crookes, M., Gray, D., and Robertson, S.: Environmental Risk Assessment Report: Octamethylcyclotetrasiloxane, Environment Agency of England and Wales, Bristol, UK, 2009c.

Bruns, E. A., El Haddad, I., Keller, A., Klein, F., Kumar, N. K., Pieber, S. M., Corbin, J. C., Slowik, J. G., Brune, W. H., Baltensperger, U., and Prévôt, A. S. H.: Inter-comparison of laboratory smog chamber and flow reactor systems on organic aerosol yield and composition, Atmos. Meas. Tech., 8, 2315-2332, doi:10.5194/amt-8-2315-2015, 2015.

Bullard, R. L., Singh, A., Anderson, S. M., Lehmann, C. M. B., and Stanier, C. O.: 10-Month characterization of the aerosol number size distribution and related air quality and meteorology at the Bondville, IL Midwestern background site, Atmos. Environ., 154, 348-361, doi:10.1016/j.atmosenv.2016.12.055, 2017.

Buser, A. M., Kierkegaard, A., Bogdal, C., MacLeod, M., Scheringer, M., and Hungerbuhler, K.: Concentrations in Ambient Air and Emissions of Cyclic Volatile Methylsiloxanes in Zurich, Switzerland, Environ. Sci. Technol., 47, 7045-7051, doi:10.1021/es3046586, 2013.

Bzdek, B. R., Horan, A. J., Pennington, M. R., Janechek, N. J., Baek, J., Stanier, C. O., and Johnston, M. V.: Silicon is a Frequent Component of Atmospheric Nanoparticles, Environ. Sci. Technol., 48, 11137-11145, doi:10.1021/es5026933, 2014.

Capela, D., Alves, A., Homem, V., and Santos, L.: From the shop to the drain - Volatile methylsiloxanes in cosmetics and personal care products, Environ. Int., 92-93, 50-62, doi:10.1016/j.envint2016.03.016, 2016.

Cerully, K. M., Hite, J. R., McLaughlin, M., and Nenes, A.: Toward the Determination of Joint Volatility-Hygroscopicity Distributions: Development and Response Characterization for Single-Component Aerosol, Aerosol Science and Technology, 48, 296-312, doi:10.1080/02786826.2013.870326, 2014.

Chandramouli, B., and Kamens, R. M.: The photochemical formation and gas-particle partitioning of oxidation products of decamethyl cyclopentasiloxane and decamethyl tetrasiloxane in the atmosphere, Atmos. Environ., 35, 87-95, doi:10.1016/s1352-2310(00)00289-2, 2001.

Chhabra, P. S., Lambe, A. T., Canagaratna, M. R., Stark, H., Jayne, J. T., Onasch, T. B., Davidovits, P., Kimmel, J. R., and Worsnop, D. R.: Application of high-resolution time-of-flight chemical ionization mass spectrometry measurements to estimate volatility distributions of α-pinene and naphthalene oxidation products, Atmos. Meas. Tech., 8, 1-18, doi:10.5194/amt-8-1-2015, 2015.

Clarson, S. J., and Semlyen, J. A.: STUDIES OF CYCLIC AND LINEAR POLY(DIMETHYLSILOXANES) .21. HIGH-TEMPERATURE THERMAL-BEHAVIOR, Polymer, 27, 91-95, doi:10.1016/0032-3861(86)90360-5, 1986.

Coggon, M. M., McDonald, B. C., Vlasenko, A., Veres, P. R., Bernard, F., Koss, A. R., Yuan, B., Gilman, J. B., Peischl, J., Aikin, K. C., DuRant, J., Warneke, C., Li, S.-M., and de Gouw, J. A.: Diurnal Variability and Emission Pattern of Decamethylcyclopentasiloxane (D5) from the Application of Personal Care Products in Two North American Cities, Environ. Sci. Technol., 52, 5610-5618, doi:10.1021/acs.est.8b00506, 2018.

Companioni-Damas, E. Y., Santos, F. J., and Galceran, M. T.: Linear and cyclic methylsiloxanes in air by concurrent solvent recondensation-large volume injection-gas chromatography-mass spectrometry, Talanta, 118, 245-252, doi:10.1016/j.talanta.2013.10.020, 2014.

Davis, D. D., Ravishankara, A. R., and Fischer, S.: SO2 OXIDATION VIA THE HYDROXYL RADICAL - ATMOSPHERIC FATE OF HSOx RADICALS, Geophys. Res. Lett., 6, 113-116, doi:10.1029/GL006i002p00113, 1979.

Dudzina, T., von Goetz, N., Bogdal, C., Biesterbos, J. W. H., and Hungerbuhler, K.: Concentrations of cyclic volatile methylsiloxanes in European cosmetics and personal care products: Prerequisite for human and environmental exposure assessment, Environ. Int., 62, 86-94, doi:10.1016/j.envint.2013.10.002, 2014.

ECHA: Annex XV Restriction Report Proposal for a Restriction (D4 and D5), Health & Safety Executive, Bootle, UK, 2015.
ECHA: 10 new substances added to the Candidate List: https://echa.europa.eu/-/ten-new-substances-added-to-the-candidate-list, access: June 2018, 2018.
Environment Canada and Health Canada: Screening Assessment for the Challenge Octamethylcyclotetrasiloxane (D4), 2008a.
Environment Canada and Health Canada: Screening Assessment for the Challenge Decamethylcyclopentasiloxane (D5), 2008b.
Environment Canada and Health Canada: Screening Assessment for the Challenge Dodecamethylcyclohexasiloxane (D6), 2008c.
Erhart, T. G., Golz, J., Eicker, U., and van den Broek, M.: Working Fluid Stability in Large-Scale Organic Rankine Cycle-Units Using Siloxanes-Long-Term Experiences and Fluid Recycling, Energies, 9, 16, doi:10.3390/en9060422, 2016.
Genualdi, S., Harner, T., Cheng, Y., MacLeod, M., Hansen, K. M., van Egmond, R., Shoeib, M., and Lee, S. C.: Global Distribution of Linear and Cyclic Volatile Methyl Siloxanes in Air, Environ. Sci. Technol., 45, 3349-3354, doi:10.1021/es200301j, 2011.
Gouin, T., van Egmond, R., Sparham, C., Hastie, C., and Chowdhury, N.: Simulated use and wash-off release of decamethylcyclopentasiloxane used in anti-perspirants, Chemosphere, 93, 726-734, doi:10.1016/j.chemosphere.2012.10.042, 2013.
Hall, A. D., and Patel, M.: Thermal stability of foamed polysiloxane rubbers: Headspace analysis using solid phase microextraction and analysis of solvent extractable material using conventional GC–MS, Polym. Degrad. Stab., 91, 2532-2539, doi:10.1016/j.polymdegradstab.2005.12.017, 2006.
Horii, Y., and Kannan, K.: Survey of organosilicone compounds, including cyclic and linear siloxanes, in personal-care and household products, Arch. Environ. Con. Tox., 55, 701-710, doi:10.1007/s00244-008-9172-z, 2008.
Janechek, N. J., Hansen, K. M., and Stanier, C. O.: Comprehensive atmospheric modeling of reactive cyclic siloxanes and their oxidation products, Atmos. Chem. Phys., 17, 8357-8370, doi:10.5194/acp-17-8357-2017, 2017.
Kang, E., Root, M. J., Toohey, D. W., and Brune, W. H.: Introducing the concept of Potential Aerosol Mass (PAM), Atmos. Chem. Phys., 7, 5727-5744, doi:10.5194/acp-7-5727-2007, 2007.
Kang, E., Toohey, D. W., and Brune, W. H.: Dependence of SOA oxidation on organic aerosol mass concentration and OH exposure: experimental PAM chamber studies, Atmos. Chem. Phys., 11, 1837-1852, doi:10.5194/acp-11-1837-2011, 2011.
Karl, T., Striednig, M., Graus, M., Hammerle, A., and Wohlfahrt, G.: Urban flux measurements reveal a large pool of oxygenated volatile organic compound emissions, Proceedings of the National Academy of Sciences, 115, 1186-1191, doi:10.1073/pnas.1714715115, 2018.
Kierkegaard, A., and McLachlan, M. S.: Determination of decamethylcyclopentasiloxane in air using commercial solid phase extraction cartridges, J. Chromatogr. A, 1217, 3557-3560, doi:10.1016/j.chroma.2010.03.045, 2010.
King, B. M., Janechek, N. J., Bryngelson, N., Adamcakova-Dodd, A., Lersch, T., Bunker, K., Casuccio, G., Thorne, P. S., Stanier, C. O., and Fiegel, J.: Cell Responses to Secondary Photochemical Aerosols Generated from OH Oxidation of Cyclic Siloxanes, In Preparation, 2018.
Krechmer, J. E., Pagonis, D., Ziemann, P. J., and Jimenez, J. L.: Quantification of Gas-Wall Partitioning in Teflon Environmental Chambers Using Rapid Bursts of Low-Volatility Oxidized Species Generated in Situ, Environ. Sci. Technol., 50, 5757-5765, doi:10.1021/acs.est.6b00606, 2016.
Kroll, J. H., Smith, J. D., Che, D. L., Kessler, S. H., Worsnop, D. R., and Wilson, K. R.: Measurement of fragmentation and functionalization pathways in the heterogeneous oxidation of oxidized organic aerosol, PCCP, 11, 8005-8014, doi:10.1039/B905289E, 2009.
Lambe, A., and Jimenez, J. L.: PAM Wiki: Estimation Equations, availabe at: https://sites.google.com/site/pamwiki/hardware/estimation-equations, 2018.
Lambe, A. T., Ahern, A. T., Williams, L. R., Slowik, J. G., Wong, J. P. S., Abbatt, J. P. D., Brune, W. H., Ng, N. L., Wright, J. P., Croasdale, D. R., Worsnop, D. R., Davidovits, P., and Onasch, T. B.: Characterization of aerosol photooxidation flow reactors: heterogeneous oxidation, secondary organic aerosol formation and cloud condensation nuclei activity measurements, Atmos. Meas. Tech., 4, 445-461, doi:10.5194/amt-4-445-2011, 2011a.
Lambe, A. T., Onasch, T. B., Massoli, P., Croasdale, D. R., Wright, J. P., Ahern, A. T., Williams, L. R., Worsnop, D. R., Brune, W. H., and Davidovits, P.: Laboratory studies of the chemical composition and cloud condensation nuclei (CCN) activity of secondary organic aerosol (SOA) and oxidized primary organic aerosol (OPOA), Atmos. Chem. Phys., 11, 8913-8928, doi:10.5194/acp-11-8913-2011, 2011b.
Lambe, A. T., Onasch, T. B., Croasdale, D. R., Wright, J. P., Martin, A. T., Franklin, J. P., Massoli, P., Kroll, J. H., Canagaratna, M. R., Brune, W. H., Worsnop, D. R., and Davidovits, P.: Transitions from Functionalization to Fragmentation Reactions of Laboratory Secondary Organic Aerosol (SOA) Generated from the OH Oxidation of Alkane Precursors, Environ. Sci. Technol., 46, 5430-5437, doi:10.1021/es300274t, 2012.
Lambe, A. T., Chhabra, P. S., Onasch, T. B., Brune, W. H., Hunter, J. F., Kroll, J. H., Cummings, M. J., Brogan, J. F., Parmar, Y., Worsnop, D. R., Kolb, C. E., and Davidovits, P.: Effect of oxidant concentration, exposure time, and seed particles on secondary organic aerosol chemical composition and yield, Atmos. Chem. Phys., 15, 3063-3075, doi:10.5194/acp-15-3063-2015, 2015.

Latimer, H. K., Kamens, R. M., and Chandra, G.: The Atmospheric Partitioning of Decamethylcylcopentasiloxane (D5) and 1-Hydroxynonomethylcyclopentasiloxane (D4TOH) on Different Types of Atmospheric Particles, Chemosphere, 36, 2401-2414, doi:10.1016/S0045-6535(97)10209-0, 1998.

Lei, Y. D., Wania, F., and Mathers, D.: Temperature-Dependent Vapor Pressure of Selected Cyclic and Linear Polydimethylsiloxane Oligomers, J. Chem. Eng. Data, 55, 5868-5873, doi:10.1021/je100835n, 2010.

Leith, D., Miller-Lionberg, D., Casuccio, G., Lersch, T., Lentz, H., Marchese, A., and Volckens, J.: Development of a Transfer Function for a Personal, Thermophoretic Nanoparticle Sampler, Aerosol Sci. Technol., 48, 81-89, doi:10.1080/02786826.2013.861593, 2014.

Li, R., Palm, B. B., Ortega, A. M., Hlywiak, J., Hu, W., Peng, Z., Day, D. A., Knote, C., Brune, W. H., de Gouw, J. A., and Jimenez, J. L.: Modeling the Radical Chemistry in an Oxidation Flow Reactor: Radical Formation and Recycling, Sensitivities, and the OH Exposure Estimation Equation, The Journal of Physical Chemistry A, 119, 4418-4432, doi:10.1021/jp509534k, 2015.

Lu, Y., Yuan, T., Wang, W., and Kannan, K.: Concentrations and assessment of exposure to siloxanes and synthetic musks in personal care products from China, Environ. Pollut., 159, 3522-3528, doi:10.1016/j.envpol.2011.08.015, 2011.

Mackay, D., Cowan-Ellsberry, C. E., Powell, D. E., Woodburn, K. B., Xu, S., Kozerski, G. E., and Kim, J.: Decamethylcyclopentasiloxane (D5) environmental sources, fate, transport, and routes of exposure, Environ. Toxicol. Chem., 34, 2689-2702, doi:10.1002/etc.2941, 2015.

MacLeod, M., von Waldow, H., Tay, P., Armitage, J. M., Wohrnschimmel, H., Riley, W. J., McKone, T. E., and Hungerbuhler, K.: BETR global - A geographically-explicit global-scale multimedia contaminant fate model, Environ. Pollut., 159, 1442-1445, doi:10.1016/j.envpol.2011.01.038, 2011.

McDonald, B. C., de Gouw, J. A., Gilman, J. B., Jathar, S. H., Akherati, A., Cappa, C. D., Jimenez, J. L., Lee-Taylor, J., Hayes, P. L., McKeen, S. A., Cui, Y. Y., Kim, S.-W., Gentner, D. R., Isaacman-VanWertz, G., Goldstein, A. H., Harley, R. A., Frost, G. J., Roberts, J. M., Ryerson, T. B., and Trainer, M.: Volatile chemical products emerging as largest petrochemical source of urban organic emissions, Science, 359, 760-764, doi:10.1126/science.aaq0524, 2018.

McLachlan, M. S., Kierkegaard, A., Hansen, K. M., van Egmond, R., Christensen, J. H., and Skjoth, C. A.: Concentrations and Fate of Decamethylcyclopentasiloxane (D-5) in the Atmosphere, Environ. Sci. Technol., 44, 5365-5370, doi:10.1021/es100411w, 2010.

Montemayor, B. P., Price, B. B., and van Egmond, R. A.: Accounting for intended use application in characterizing the contributions of cyclopentasiloxane (D5) to aquatic loadings following personal care product use: antiperspirants, skin care products and hair care products, Chemosphere, 93, 735-740, doi:10.1016/j.chemosphere.2012.10.043, 2013.

OECD Environment Directorate: The 2004 OECD List of High Production Volume Chemicals, 2004.

Pagonis, D., Krechmer, J. E., de Gouw, J., Jimenez, J. L., and Ziemann, P. J.: Effects of gas-wall partitioning in Teflon tubing and instrumentation on time-resolved measurements of gas-phase organic compounds, Atmos. Meas. Tech., 10, 4687-4696, doi:10.5194/amt-10-4687-2017, 2017.

Palm, B. B., Campuzano-Jost, P., Ortega, A. M., Day, D. A., Kaser, L., Jud, W., Karl, T., Hansel, A., Hunter, J. F., Cross, E. S., Kroll, J. H., Peng, Z., Brune, W. H., and Jimenez, J. L.: In situ secondary organic aerosol formation from ambient pine forest air using an oxidation flow reactor, Atmos. Chem. Phys., 16, 2943-2970, doi:10.5194/acp-16-2943-2016, 2016.

Palm, B. B., de Sá, S. S., Day, D. A., Campuzano-Jost, P., Hu, W., Seco, R., Sjostedt, S. J., Park, J. H., Guenther, A. B., Kim, S., Brito, J., Wurm, F., Artaxo, P., Thalman, R., Wang, J., Yee, L. D., Wernis, R., Isaacman-VanWertz, G., Goldstein, A. H., Liu, Y., Springston, S. R., Souza, R., Newburn, M. K., Alexander, M. L., Martin, S. T., and Jimenez, J. L.: Secondary organic aerosol formation from ambient air in an oxidation flow reactor in central Amazonia, Atmos. Chem. Phys., 18, 467-493, doi:10.5194/acp-18-467-2018, 2018.

Peng, Z., Day, D. A., Stark, H., Li, R., Lee-Taylor, J., Palm, B. B., Brune, W. H., and Jimenez, J. L.: HOx radical chemistry in oxidation flow reactors with low-pressure mercury lamps systematically examined by modeling, Atmos. Meas. Tech., 8, 4863-4890, doi:10.5194/amt-8-4863-2015, 2015.

Peng, Z., Day, D. A., Ortega, A. M., Palm, B. B., Hu, W., Stark, H., Li, R., Tsigaridis, K., Brune, W. H., and Jimenez, J. L.: Non-OH chemistry in oxidation flow reactors for the study of atmospheric chemistry systematically examined by modeling, Atmos. Chem. Phys., 16, 4283-4305, doi:10.5194/acp-16-4283-2016, 2016.

Petters, M. D., and Kreidenweis, S. M.: A single parameter representation of hygroscopic growth and cloud condensation nucleus activity, Atmos. Chem. Phys., 7, 1961-1971, doi:10.5194/acp-7-1961-2007, 2007.

Roberts, G. C., and Nenes, A.: A continuous-flow streamwise thermal-gradient CCN chamber for atmospheric measurements, Aerosol Sci. Technol., 39, 206-221, doi:10.1080/027868290913988, 2005.

Rose, D., Gunthe, S. S., Mikhailov, E., Frank, G. P., Dusek, U., Andreae, M. O., and Pöschl, U.: Calibration and measurement uncertainties of a continuous-flow cloud condensation nuclei counter (DMT-CCNC): CCN activation of ammonium sulfate and sodium chloride aerosol particles in theory and experiment, Atmos. Chem. Phys., 8, 1153-1179, doi:10.5194/acp-8-1153-2008, 2008.

Rose, D., Nowak, A., Achtert, P., Wiedensohler, A., Hu, M., Shao, M., Zhang, Y., Andreae, M. O., and Poeschl, U.: Cloud condensation nuclei in polluted air and biomass burning smoke near the mega-city Guangzhou, China - Part 1: Size-resolved measurements and implications for the modeling of aerosol particle hygroscopicity and CCN activity, Atmos. Chem. Phys., 10, 3365-3383, doi:10.5194/acp-10-3365-2010, 2010.

Singh, A.: Measurement of the physical properties of ultrafine particles in the rural continental U.S., The University of Iowa, 2015.

Sommerlade, R., Parlar, H., Wrobel, D., and Kochs, P.: Product Analysis and Kinetics of the Gas-Phase Reactions of Selected Organosilicon Compounds with OH Radicals Using a Smog Chamber - Mass Spectrometer System, Environ. Sci. Technol., 27, 2435-2440, doi:10.1021/es00048a019, 1993.

Tang, X., Misztal, P. K., Nazaroff, W. W., and Goldstein, A. H.: Siloxanes Are the Most Abundant Volatile Organic Compound Emitted from Engineering Students in a Classroom, Environ. Sci. Technol. Lett., 2, 303-307, doi:10.1021/acs.estlett.5b00256, 2015.

Varaprath, S., Frye, C. L., and Hamelink, J.: Aqueous solubility of permethylsiloxanes (silicones), Environ. Toxicol. Chem., 15, 1263-1265, doi:10.1002/etc.5620150803, 1996.

Wang, R., Moody, R. P., Koniecki, D., and Zhu, J.: Low molecular weight cyclic volatile methylsiloxanes in cosmetic products sold in Canada: implication for dermal exposure, Environ. Int., 35, 900-904, doi:10.1016/j.envint.2009.03.009, 2009.

Willeke, K., and Baron, P. A.: Aerosol Measurement Principles, Techniques, and Applications, Van Nostrand Reinhold, New York, 1993.

Winkler, P. M., Ortega, J., Karl, T., Cappellin, L., Friedli, H. R., Barsanti, K., McMurry, P. H., and Smith, J. N.: Identification of the biogenic compounds responsible for size-dependent nanoparticle growth, Geophys. Res. Lett., 39, L20815, doi:10.1029/2012GL053253, 2012.

Wu, Y., and Johnston, M. V.: Molecular Characterization of Secondary Aerosol from Oxidation of Cyclic Methylsiloxanes, J. Am. Soc. Mass. Spectr., 27, 402-409, doi:10.1007/s13361-015-1300-1, 2016.

Wu, Y., and Johnston, M. V.: Aerosol Formation from OH Oxidation of the Volatile Cyclic Methyl Siloxane (cVMS) Decamethylcyclopentasiloxane, Environ. Sci. Technol., 51, 4445-4451, doi:10.1021/acs.est.7b00655, 2017.

Xu, S., and Wania, F.: Chemical fate, latitudinal distribution and long-range transport of cyclic volatile methylsiloxanes in the global environment: a modeling assessment, Chemosphere, 93, 835-843, doi:10.1016/j.chemosphere.2012.10.056, 2013.

Yucuis, R. A., Stanier, C. O., and Hornbuckle, K. C.: Cyclic siloxanes in air, including identification of high levels in Chicago and distinct diurnal variation, Chemosphere, 92, 905-910, doi:10.1016/j.chemosphere.2013.02.051, 2013.

Zhao, D. F., Buchholz, A., Kortner, B., Schlag, P., Rubach, F., Kiendler-Scharr, A., Tillmann, R., Wahner, A., Flores, J. M., Rudich, Y., Watne, Å. K., Hallquist, M., Wildt, J., and Mentel, T. F.: Size-dependent hygroscopicity parameter (κ) and chemical composition of secondary organic cloud condensation nuclei, Geophys. Res. Lett., 42, 10,920-910,928, doi:10.1002/2015GL066497, 2015.

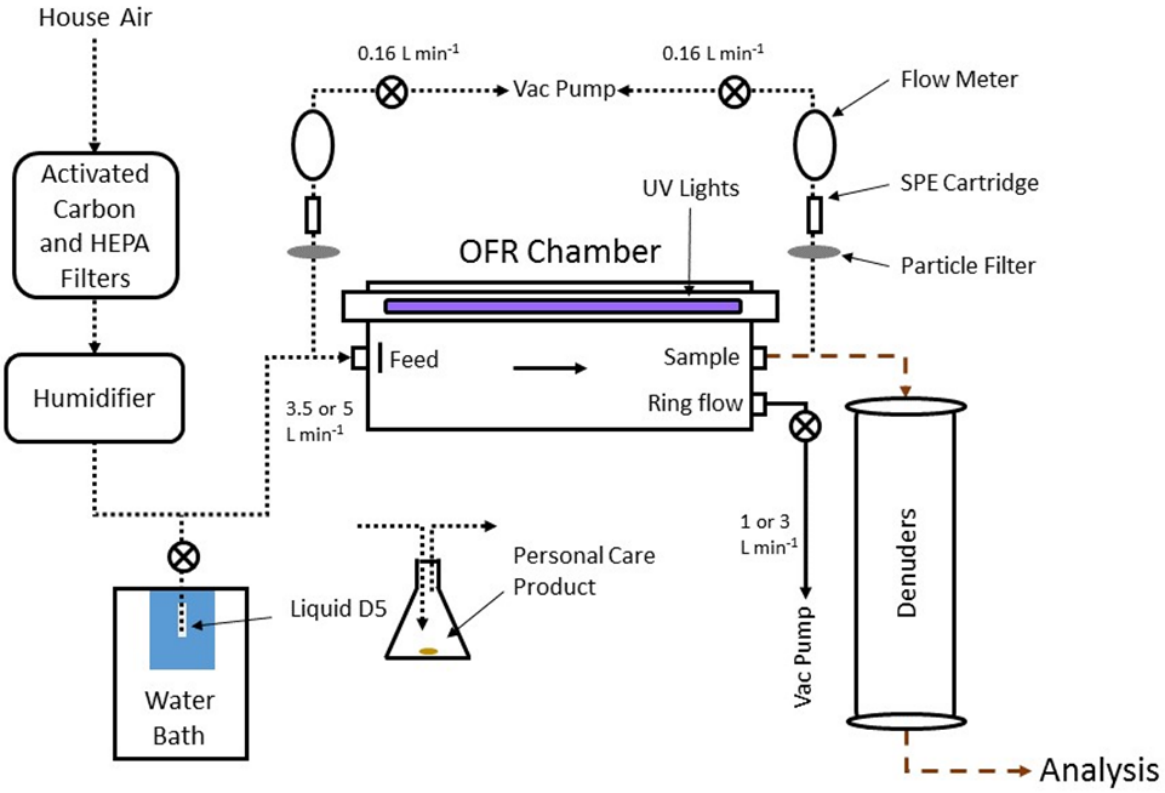

Figure 1: Flow diagram for generation of aerosols in the OFR. Aerosols were analyzed by SMPS, TPS100, V-TDMA, and DMT-CCN instruments. Delivery of the precursor gas was either by diffusion of liquid D_5 controlled by a water bath or flowing air past a personal care product placed in an Erlenmeyer flask. Short dashed lines in the diagram indicate Teflon tubing, long dashed represent copper tubing, and solid lines represent conductive silicon tubing.

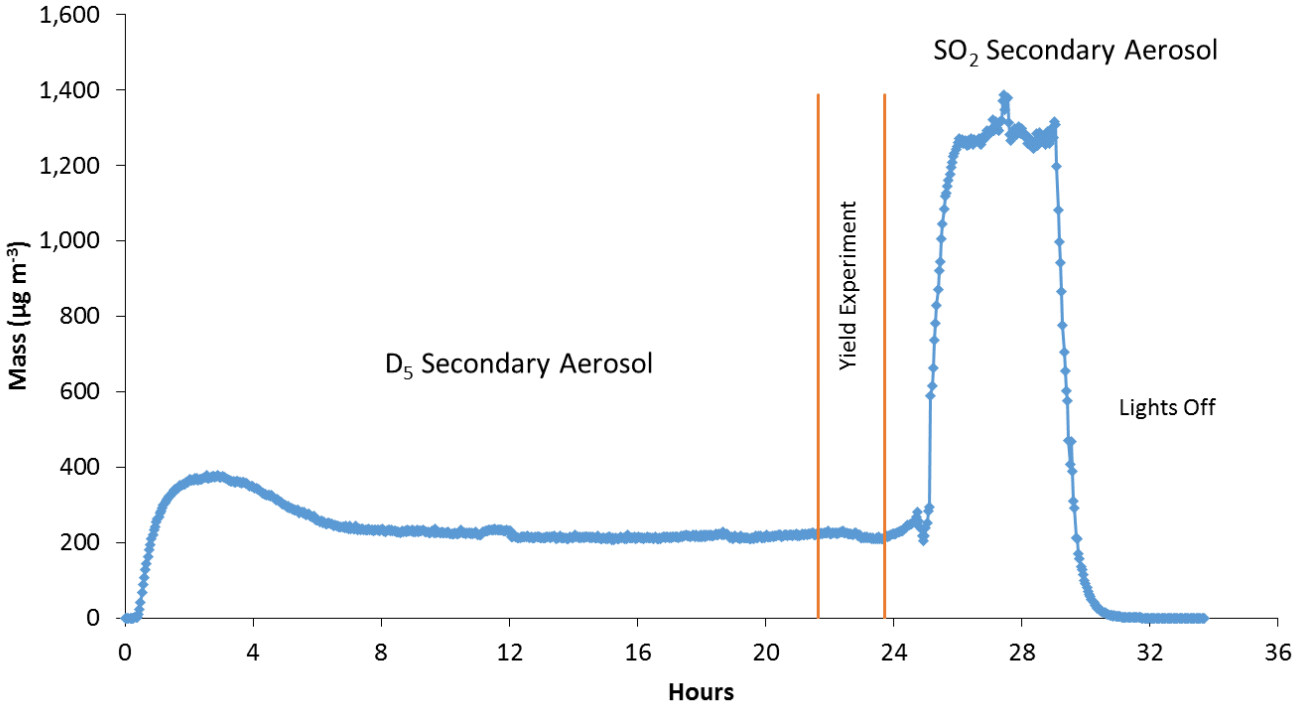

Figure 2: SMPS time series of a typical yield experiment. An equilibration period was run for ~20 h prior to measuring the D_5 gas concentration upstream and downstream of the OFR (yield experiment period~~;~~ ~1.7 h). Aerosol measurements used for yield analysis were from the yield experiment period. After the yield experiment period, the precursor gas was switched to SO_2 for OH quantification. An SO_2 monitor was used to measure SO_2 downstream of the chamber with and without the OFR lights on.

Table 1: Summary of the yield trials. D_5 reacted gas concentration represents the average of the upstream minus the average of the downstream measurements. Number, mass, and mode represent the average SMPS aerosol values for the yield experiment period. Equivalent age represents the atmospheric aging assuming an OH concentration of $1.5x10^6$ molec cm^{-3}.

Trial	Flow (L min^{-1})	RH (%)	Water Bath (°C)	Lights (%)	D_5 Reacted (µg m^{-3})	Number (cm^{-3})	Mass (µg m^{-3})	Mode (nm)	OH Exposure (molec s cm^{-3})	Eq. Age (days)	Yield
1	3.5	45	70	80	725	3.47E+05	219.7	83.2	4.8E+12	37.1	0.30
2	3.5	25	60	80	356	2.57E+05	84.0	59.4	2.3E+12	17.4	0.24
3	5	25	70	80	480	3.58E+05	107.1	69.6	1.6E+12	12.4	0.22
4	3.5	45	60	100	358	3.07E+05	180.7	79.8	5.1E+12	39.5	0.50
5	5	25	60	100	280	3.31E+05	68.4	57.0	2.7E+12	20.8	0.24

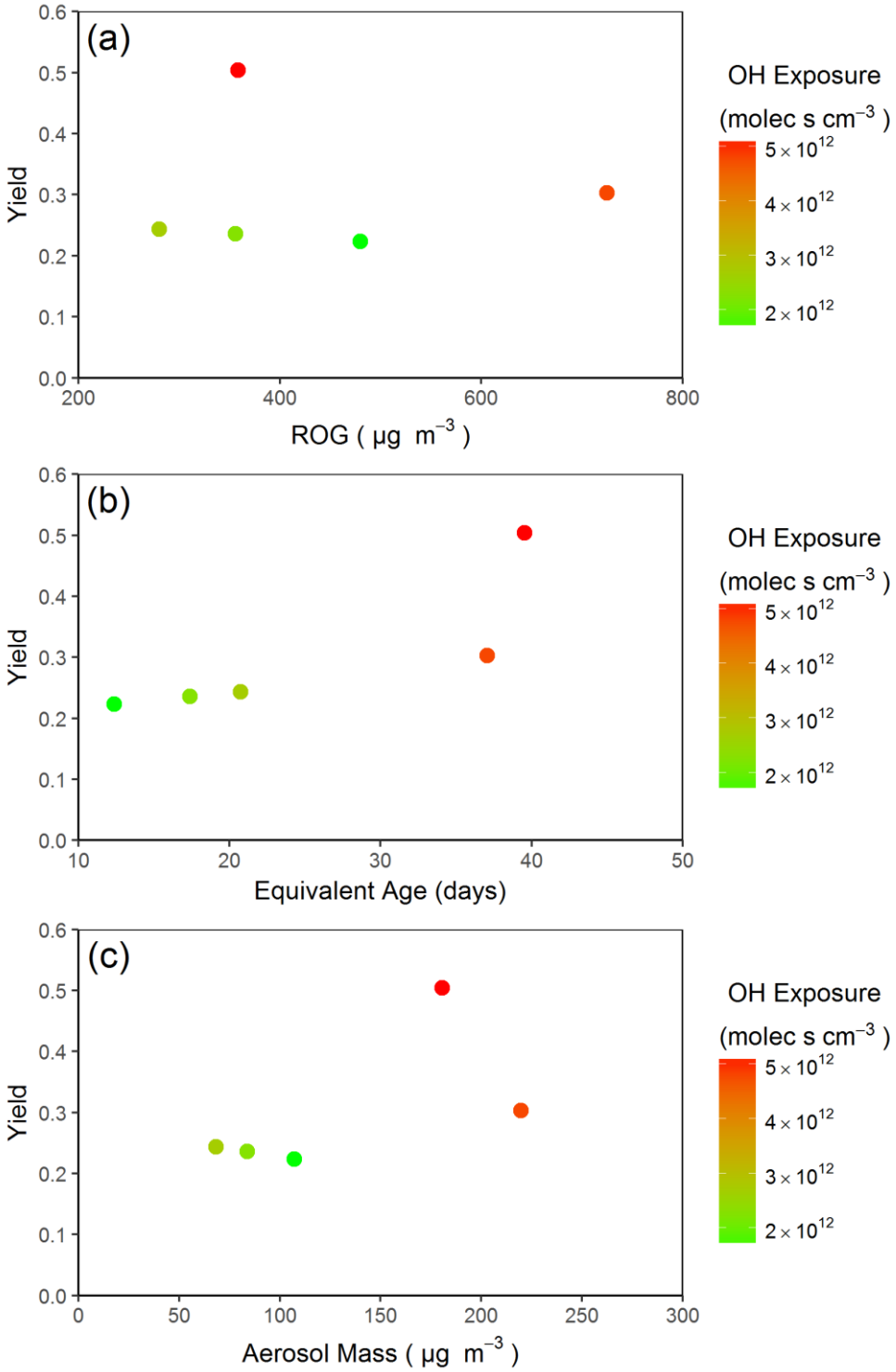

Figure 3: Measured D_5 oxidation aerosol yield as a function of (a) ROG (reacted D_5), (b) equivalent age assuming an OH concentration of 1.5x10^6 molec cm^{-3}, and (c) aerosol mass. Data points are color coded according to OH exposure.

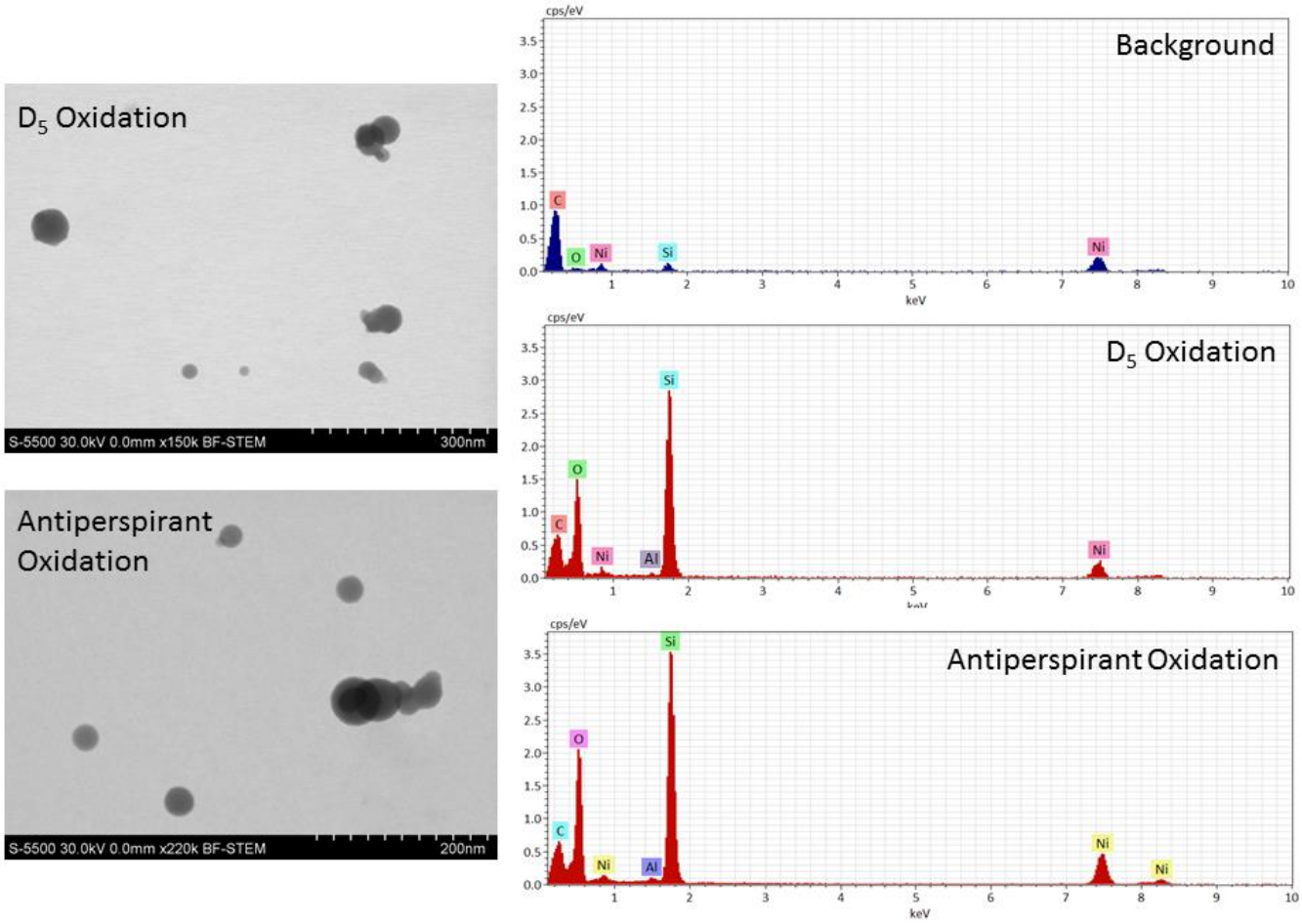

Figure 4: STEM-EDS analysis of D_5 oxidation aerosols and antiperspirant oxidation aerosols obtained from analysis of TPS100 samples.

5

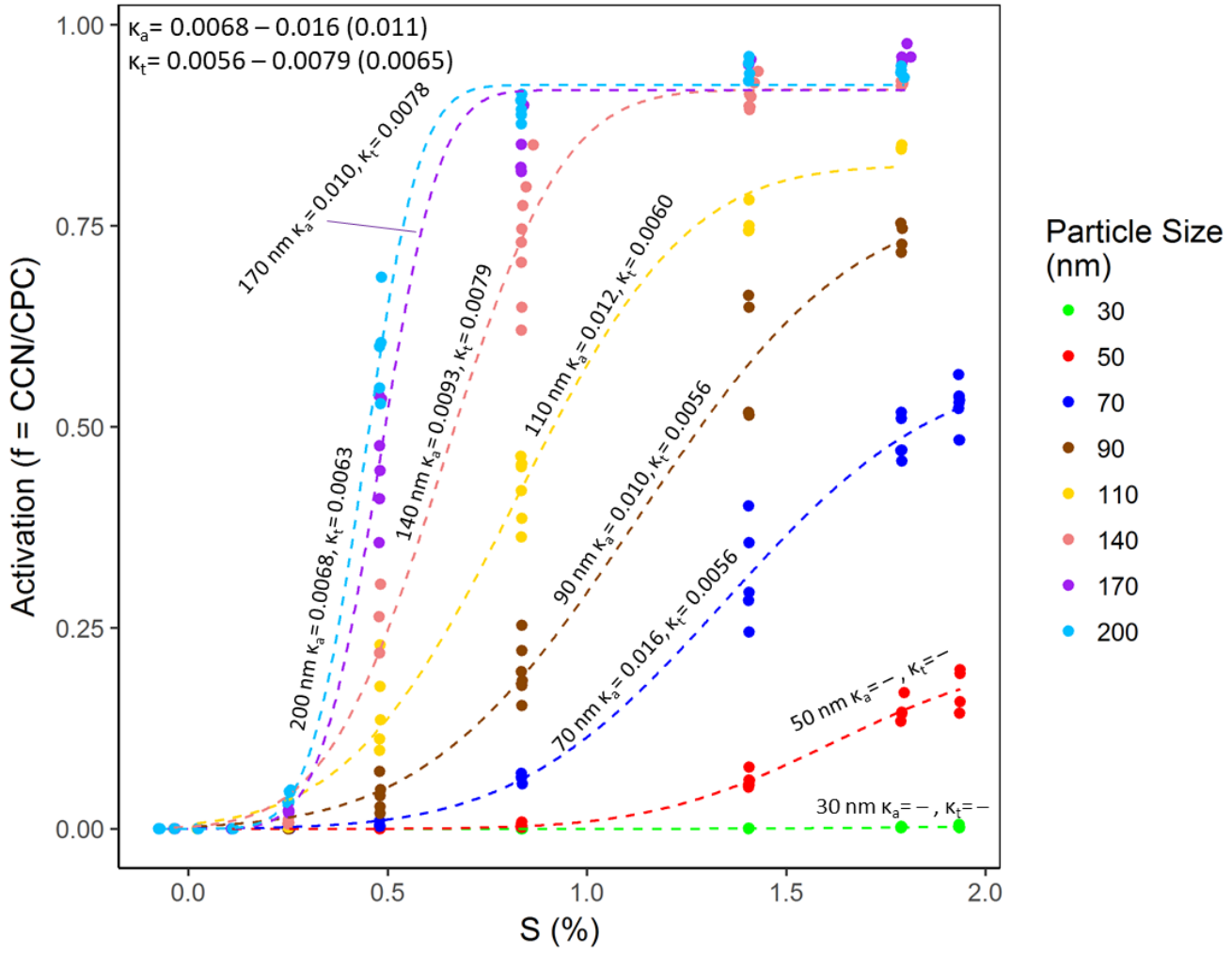

Figure 5: D_5 oxidation aerosol CCN activation curve. Size specific κ_a and κ_t are tabulated for particles 70 – 200 nm. The calculated kappa parameter range and average (in parenthesis) is tabulated in the upper left. Each point represents an average 30 s ~~DMT~~CCN/CPC measurement.

5

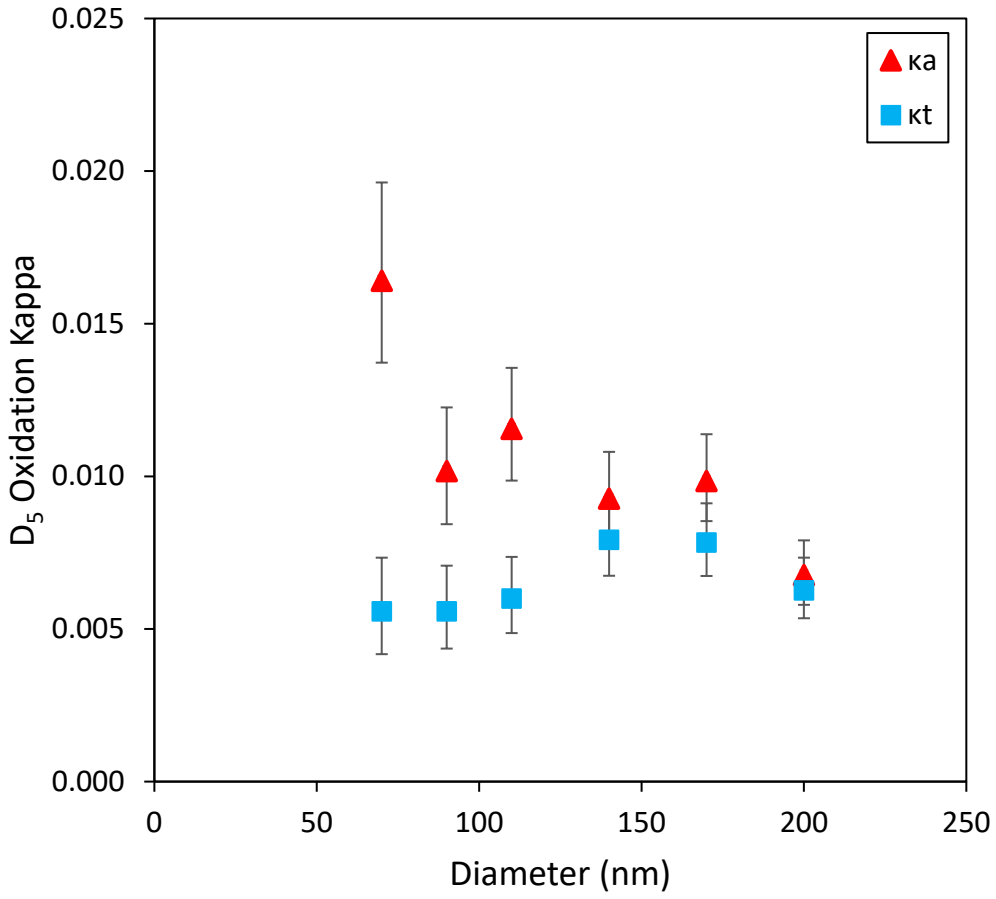

Figure 6: Size resolved kappa parameters for D_5 oxidation aerosols. Error bars represent the 95% confidence interval.

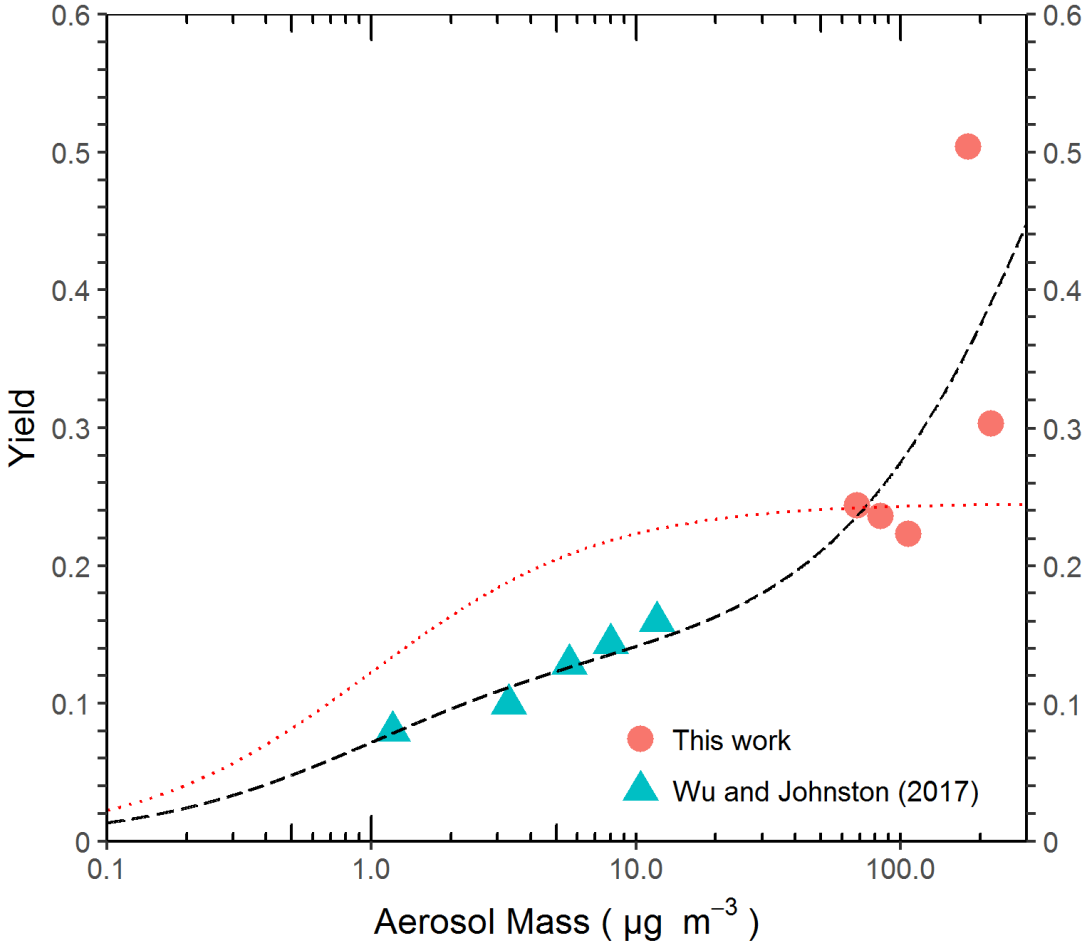

Figure 7: Two product model fit (black long dash) and one product model fit with saturation concentration (c*) of 1 µg m^{-3} (red short dash) overlaid with chamber data from this work and D_5 oxidation experiments of Wu and Johnston (2017). Parameters for the two product model fit are yields of 0.14, and 0.82, respectively for c* of 0.95 µg m^{-3} and 484 µg m^{-3}. Parameters for the one product model are a c* of 1 µg m^{-3} and yield of 0.25.

Supplemental Material

Physical Properties of Secondary Photochemical Aerosol from OH Oxidation of a Cyclic Siloxane

By Nathan J. Janechek[1,2], Rachel F. Marek[2], Nathan Bryngelson[1,2,*], Ashish Singh[1,2,†], Robert L. Bullard[1,2,‡],William H. Brune[3], Charles O. Stanier[1,2]

[1]Department of Chemical and Biochemical Engineering, University of Iowa, Iowa City, IA, USA

[2]IIHR-Hydroscience and Engineering, University of Iowa, Iowa City, IA, USA

[3]Department of Meteorology and Atmospheric Science, Pennsylvania State University, University Park, PA, USA

[*]Now at Yokogawa Corporation of America - Analytical Process Analyzers

[†]Now at Institute for Advanced Sustainability Studies, Potsdam-14467, Germany

[‡]Now at Lovelace Respiratory Research Institute, Albuquerque, NM, USA

*Corresponding author. Address correspondence to charles-stanier@uiowa.edu

Table of Contents

Section S1: General information

Table S1: Experiments performed, chamber settings, and analysis methods for the generation and characterization of cVMS secondary aerosol.

Flow (LPM)	Ring Flow (LPM)	RH (%)	Water Bath (°C)	Lights (%)	Purpose	Analysis	Notes
3.5	1	45	70	80	Yield 1	SMPS, D_5 gas, SO_2 gas	SMPS far
3.5	1	25	60	80	Yield 2	SMPS, D_5 gas, SO_2 gas	SMPS near
5	3	25	70	80	Yield 3	SMPS, D_5 gas, SO_2 gas	SMPS far
3.5	1	45	60	100	Yield 4	SMPS, D_5 gas, SO_2 gas	SMPS far
5	3	25	60	100	Yield 5	SMPS, D_5 gas, SO_2 gas	SMPS near
3.5	1	25	50	80	Seed test	SMPS	
3.5	1	25	60	off	QC test - D_5 chamber test to verify photochemical reaction the source of D_5 loss	SMPS, D_5 gas	
3.5	1	25	70	off	QC test - SPE cartridge breakthrough	D_5 gas	Tested upstream only
-	-	-	-	-	Ammonium sulfate CCN calibration	DMT-CCN, CPC	
5	3	30	70	100	cVMS CCN measurement	DMT-CCN, CPC	
5	3	30	-	100	Antiperspirant oxidation test 1	SMPS	
5	3	30	-	100	Antiperspirant oxidation test 2	SMPS, TPS100	
5	3	30	-	100	Hair conditioner oxidation test 1	SMPS	
5	3	30	70	100	Volatility measurement	SMPS, V-TDMA	
-	-	-	-	-	Heating of D_5 vapor to 100 - 250°C	SMPS	
-	-	-	-	-	Heating of D_5 vapor to 550°C	SMPS	
-	-	-	-	-	Heating of D_5 vapor to 550°C and 80 nm ammonium sulfate seed aerosols	SMPS	

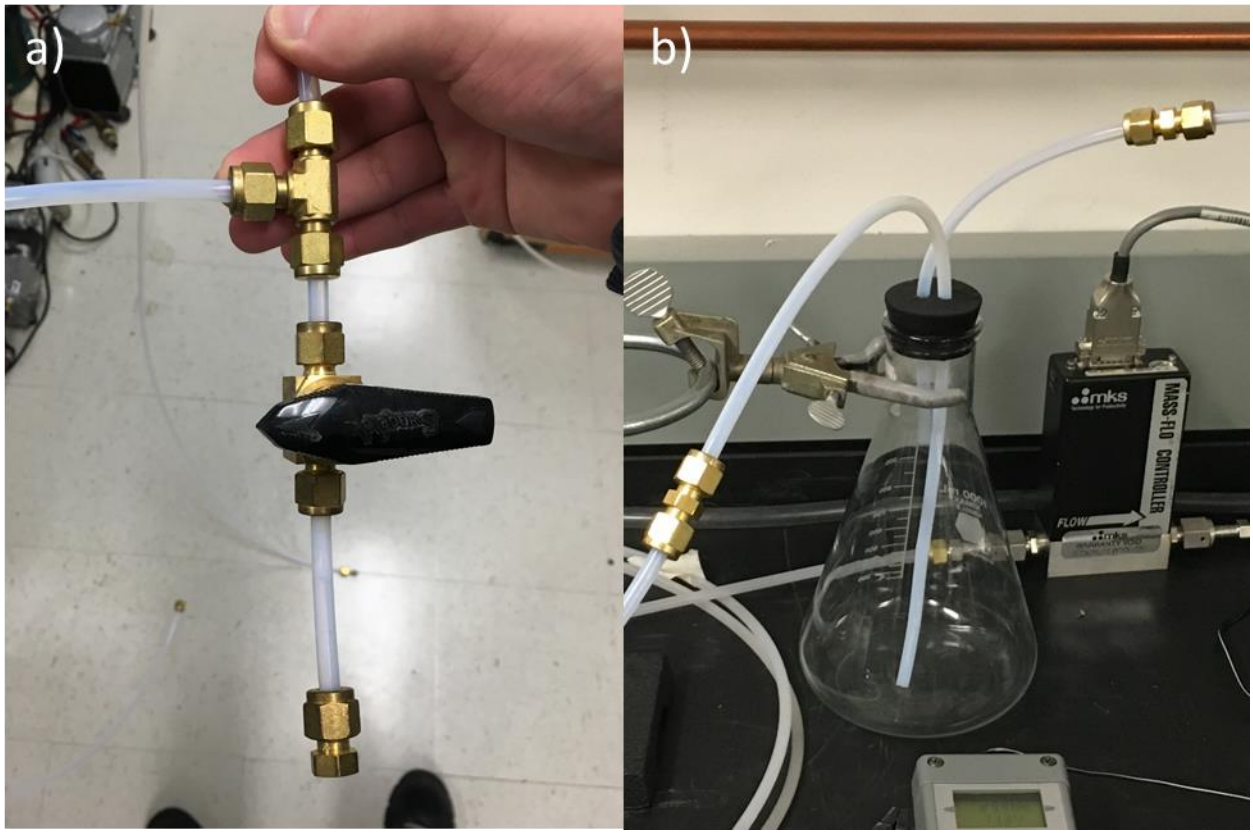

Figure S1: Cyclic siloxane delivery for a) liquid D_5 diffusion and b) flowing air past personal care product.

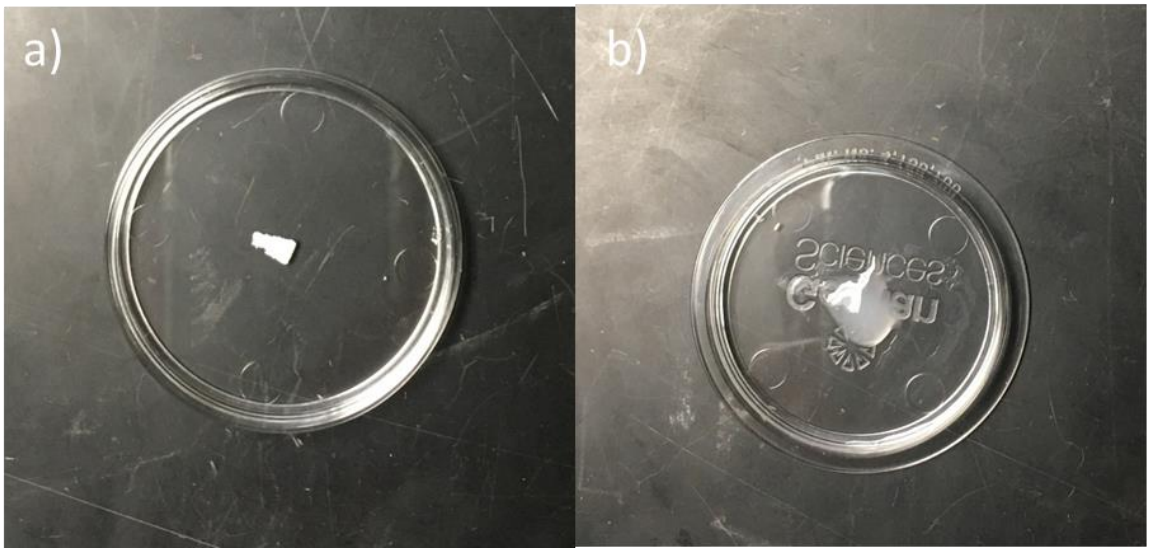

Figure S2: Representative amounts of personal care product placed in flask for cyclic siloxane delivery. Panel a) ~10 mg antiperspirant, and b) ~25 mg hair conditioner. Air was passed through the flask and fed into the OFR.

Section S2: D_5 gas sampling quality control results

Sufficient elution volume was tested by collecting a second cartridge elution of 1.5 mL for the sample with the highest anticipated concentration. Mass in the second elution was negligible compared to the primary elution (2.5% and 1.9% in duplicate testing). A cartridge breakthrough test was performed under the highest anticipated concentration sampling conditions, where a backup cartridge was connected behind the primary cartridge in the sampling setup. The backup cartridge was eluted into a separate GC vial and analyzed. Mass on the backup cartridge was negligible compared to the primary cartridge (0.6% in both duplicates).

Quality Control was assessed through a blank spike test; duplicates; and field, instrument, and method blanks. In the blank spike test, cleaned sample cartridges were spiked with D_5 and eluted with hexane to determine D_5 recovery from cartridges. Recoveries were 96% and 97% in duplicate testing. Duplicate samples and blanks were collected and analyzed. Relative percent difference ranged from 1 to 7% in the method blank duplicates, 1 to 13% in the field blank duplicates, 1 to 3% for the upstream sample duplicates, and 1 to 21% for the downstream sample duplicates. Contamination during sample deployment and handling in the field was monitored by analyzing field blanks. Mass on the field blanks ranged from 9 to 56 ng per blank. Contamination from glassware, cartridges, and solvents was monitored by analyzing method blanks which consisted of cleaned sample cartridges stored in a clean media fridge until analysis. Two method blanks per yield test were run through the extraction process in parallel with the samples. Mass on the method blanks ranged from 10 to 67 ng. Samples were not blank corrected.

Section S3: D_5 gas sampling details

Table S2: GC and MS parameters for D_5 gas concentration quantification.

GC parameters	Injector	3 washes in DCM, 3 washes in hexane pre- and post-injection
		3 sample pumps
		Fast plunger speed
		Injection volume 2 µL with a 10 µL syringe
	Oven Program	Initial temperature 60 ^{o}C, hold 2 min
		Rate 20 ^{o}C/min to final temp 250 ^{o}C, hold 5 min
		Total run time 16.5 min
		Flow 0.8 mL/min
	Inlet	Helium carrier gas
		Splitless mode
		Temperature 200 ^{o}C
		Pressure 5.3 psi
		Purge flow 50 mL/min, purge time 1 min, flow 53.6 mL/min
		Gas saver 20 mL/min, saver time 2 min
		3 min solvent delay
	Transfer line	Temperature 280 ^{o}C
	Post run	5 min at 60 ^{o}C
MS parameters	temperatures	MS source 250 ^{o}C, MS quad 150 ^{o}C
SIM mode	Ions monitored	355 (D_5) and 258 (PCB 30)

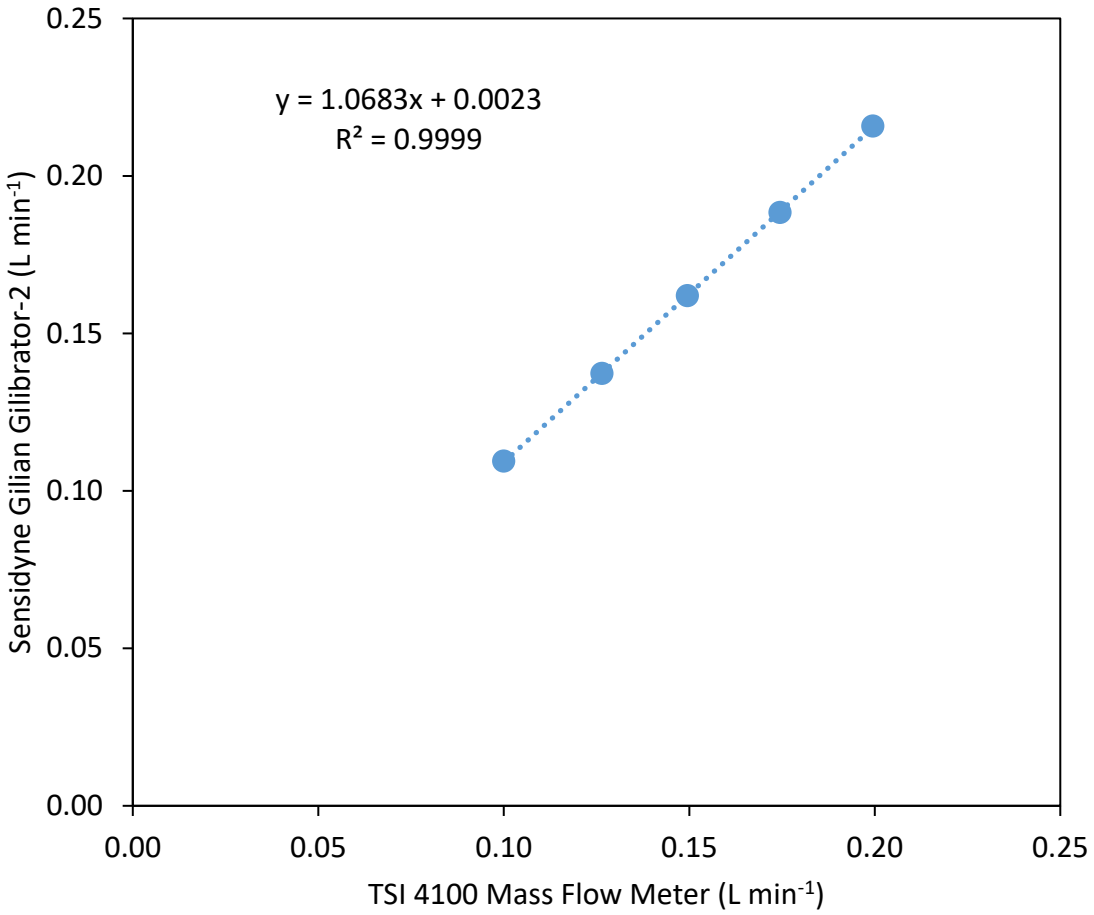

Figure S3: Calibration fit used to convert measured mass flow (TSI 4100) to volumetric flow for D_5 gas sampling. The volumetric flow was determined using a Sensidyne Gillian Gilibrator-2.

Table S3: D_5 gas sampling details. Samples with D_5 measured upstream of the OFR chamber are labeled "US", concentrations measured downstream of the reactor are labeled "DS". The label "P" and "B" refer to primary and backup cartridges, respectively. The reported flowrates are the calibrated volumetric flow rates.

Test	Sample	Sampling Time (min)	Average Flowrate (L min^{-1})	Total Volume (L)	Measured D_5 (ng)	D_5 Concentration (µg m^{-3})
Breakthrough	US1P	20.2	0.161	3.24	2619.3	808.2
Breakthrough	US2P	20.6	0.159	3.27	2645.3	809.3
Breakthrough	US1B	20.2	0.161	3.24	15.3	4.7
Breakthrough	US2B	20.6	0.159	3.27	14.8	4.5
Chamber Test	US1	20.0	0.162	3.24	1421.3	439.1
Chamber Test	US2	20.0	0.162	3.23	1387.5	429.3
Chamber Test	DS1	20.0	0.163	3.25	1400.7	430.4
Chamber Test	DS2	20.0	0.163	3.25	1387.0	426.4
Yield 1	US1	20.0	0.162	3.25	2399.5	739.2
Yield 1	US2	20.0	0.163	3.26	2413.4	740.7
Yield 1	DS1	20.0	0.167	3.33	54.9	16.5
Yield 1	DS2	20.0	0.166	3.32	44.4	13.4
Yield 2	US1	20.0	0.164	3.28	1210.2	369.5
Yield 2	US2	20.0	0.164	3.28	1243.7	378.8
Yield 2	DS1	20.0	0.164	3.28	59.3	18.1
Yield 2	DS2	20.0	0.164	3.28	58.7	17.9
Yield 3	US1	20.0	0.165	3.30	1628.4	493.8
Yield 3	US2	20.0	0.164	3.28	1679.4	511.3
Yield 3	DS1	20.0	0.162	3.24	68.0	21.0
Yield 3	DS2	20.0	0.161	3.23	78.2	24.2
Yield 4	US1	20.2	0.163	3.29	1246.3	378.9
Yield 4	US2	20.2	0.161	3.26	1207.6	370.8
Yield 4	DS1	20.2	0.159	3.21	55.9	17.4
Yield 4	DS2	20.1	0.158	3.16	48.6	15.4
Yield 5	US1	20.0	0.162	3.25	929.1	286.1
Yield 5	US2	20.0	0.162	3.25	954.9	294.1
Yield 5	DS1	20.0	0.166	3.31	32.5	9.8
Yield 5	DS2	20.0	0.164	3.28	30.7	9.4

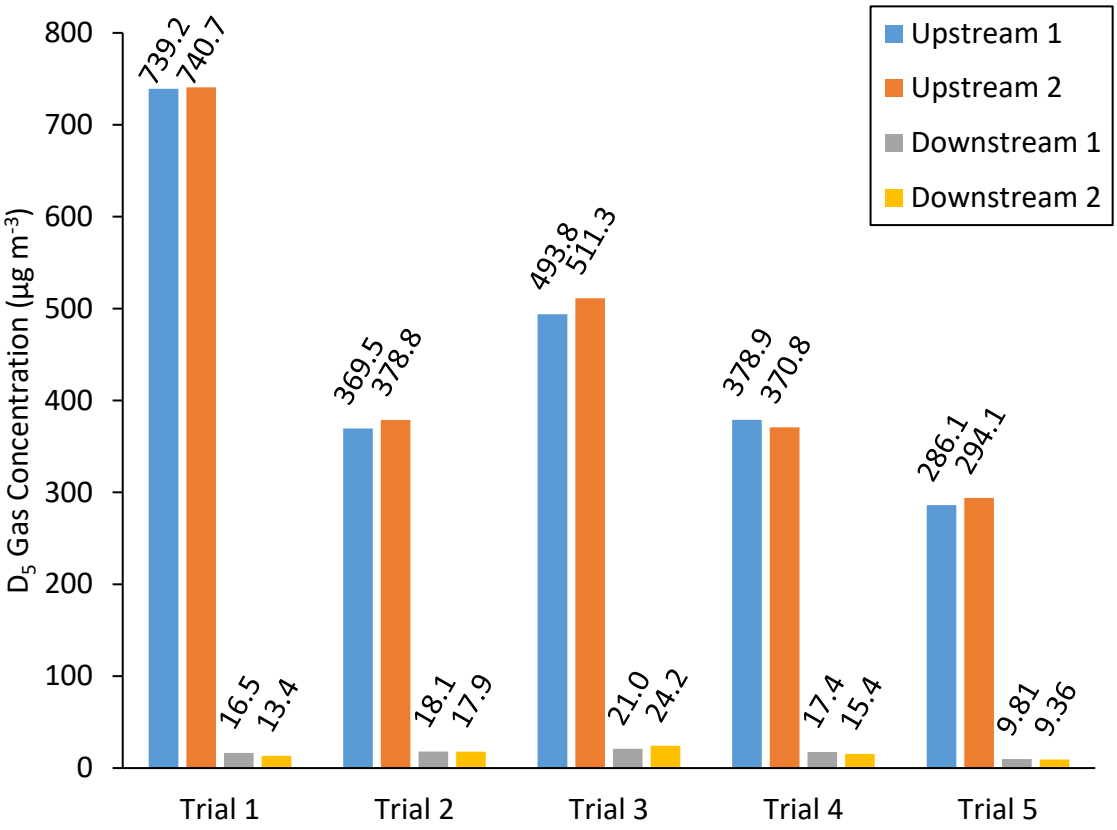

Figure S4: D_5 gas concentrations (µg m^{-3}) were quantified upstream and downstream of the OFR using SPE cartridges. Upstream 1 and 2, and downstream 1 and 2 refer to the duplicate trials.

Section S4: Particle loss correction

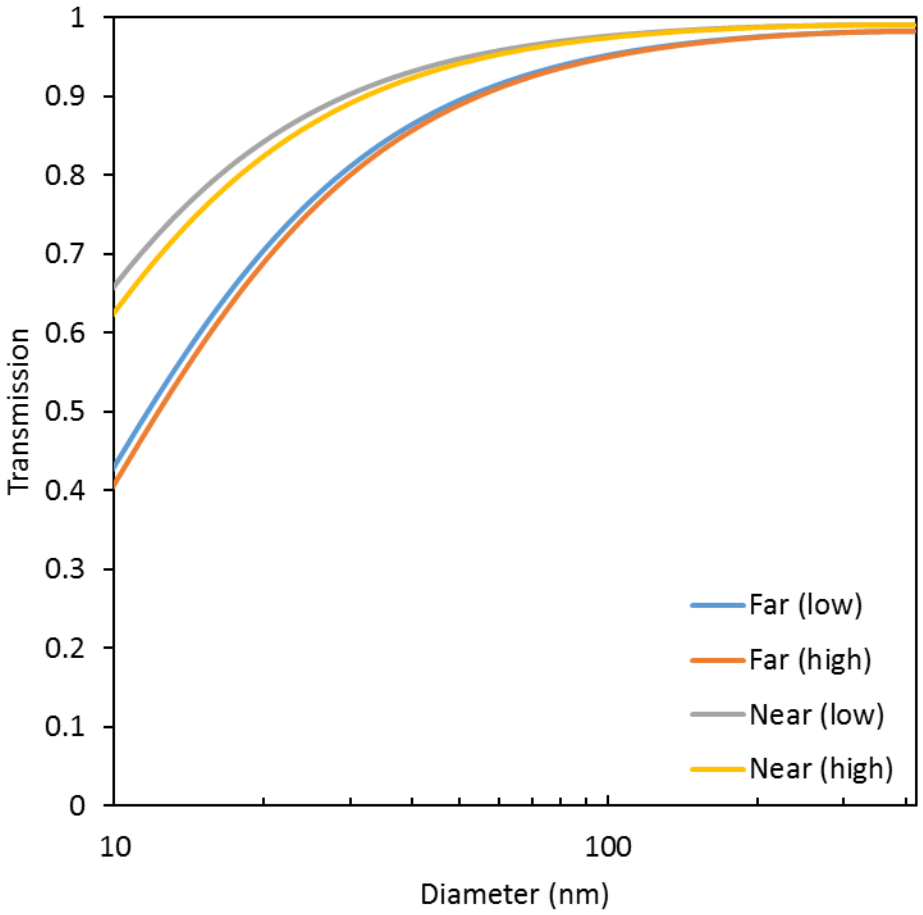

Figure S5: Modeled particle transmission for configurations with D_5 gas sampling. Far and near refer to SMPS placement relative to the OFR. Low and high refers to the incoming total flow of 3.5 L min^{-1} or 5 L min^{-1}, respectively.

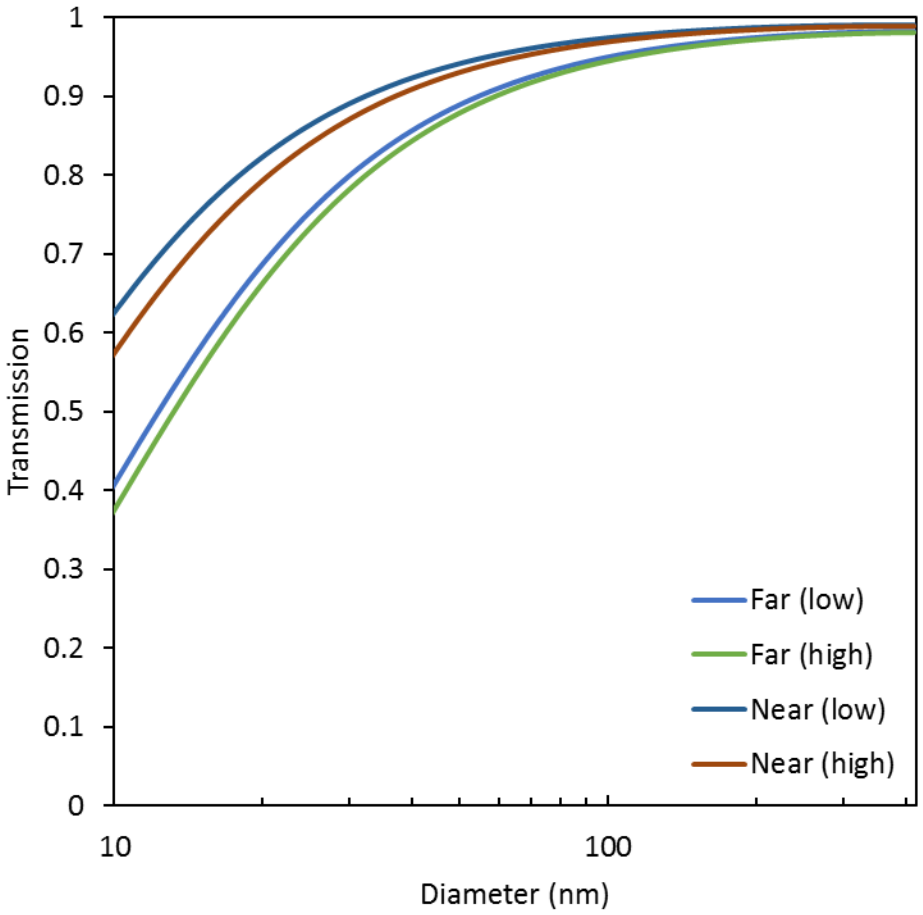

Figure S6: Modeled particle transmission for configurations with SO_2 gas sampling. Far and near refer to SMPS placement relative to the OFR. Low and high refers to the incoming total flow of 3.5 L min^{-1} or 5 L min^{-1}, respectively.

Table S4: List of corresponding SMPS placement and flow conditions for particle transmission correction.

Yield Test	SMPS Placement	Flow
1	Far	Low
2	Near	Low
3	Far	High
4	Far	Low
5	Near	High

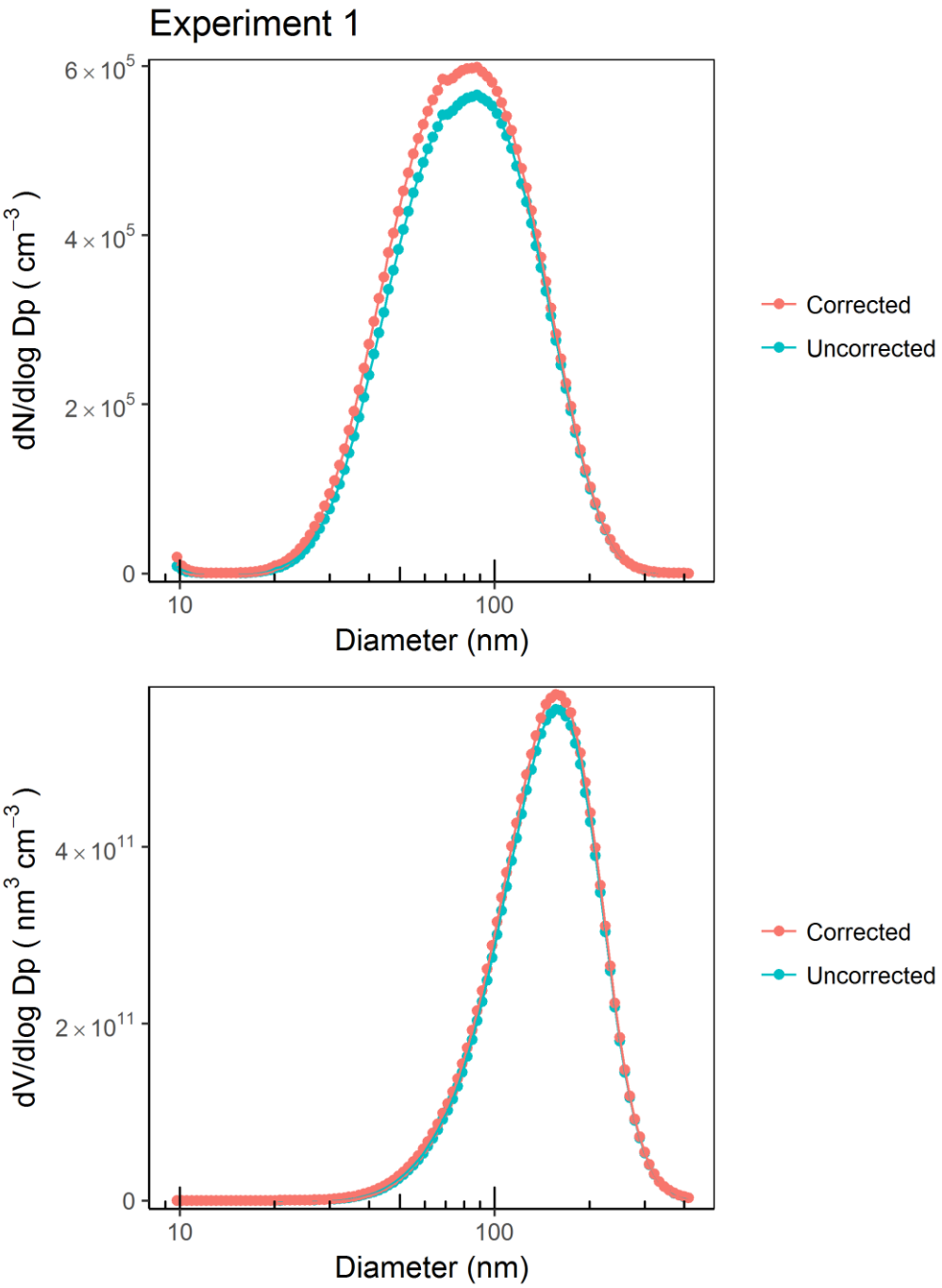

Figure S7: SMPS measured average number and volume D_5 oxidation aerosol size distributions for the yield experiment period. Corrected distributions are corrected for modeled particle losses in the denuders and tubing.

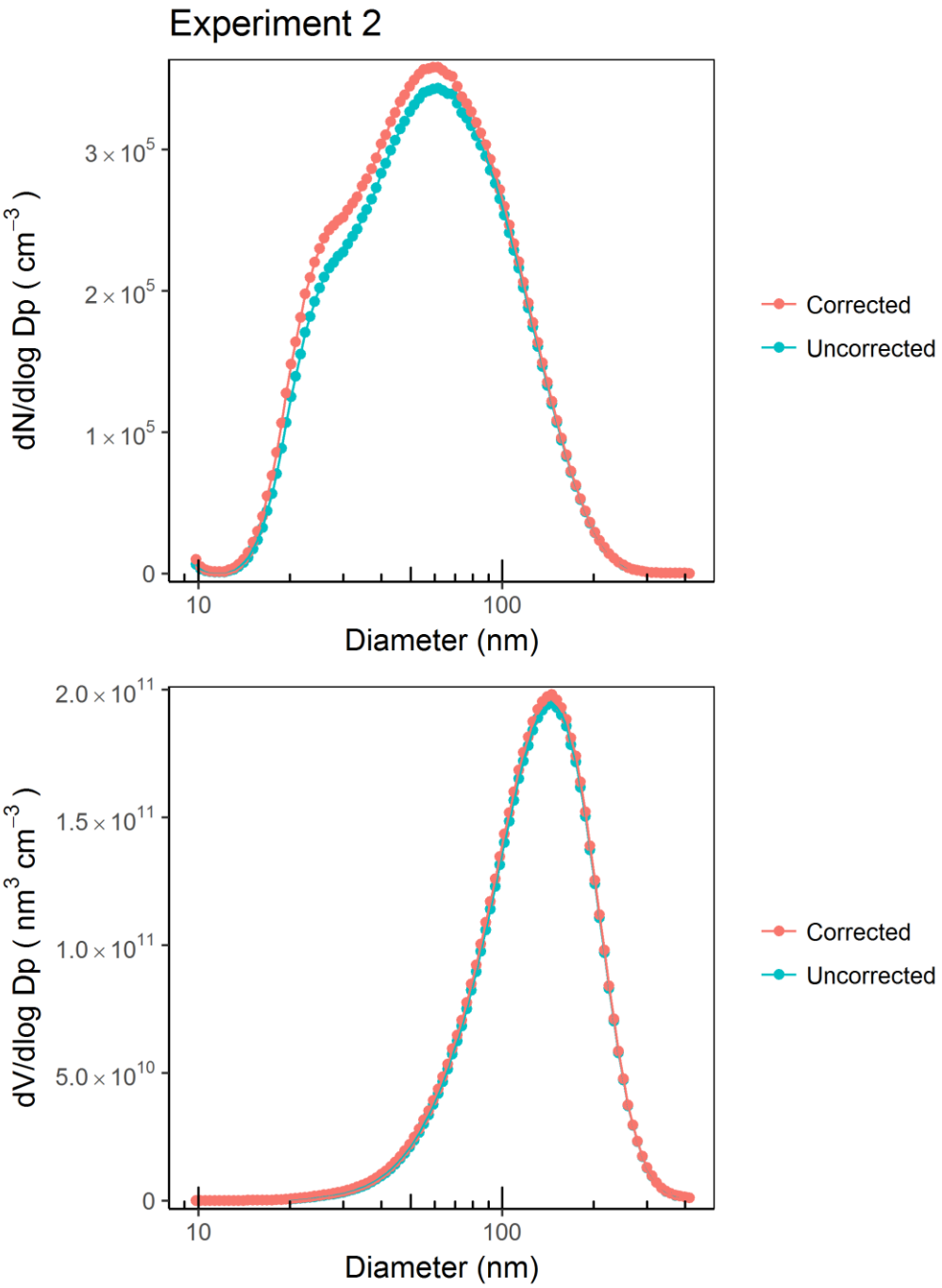

Figure S7: Continued

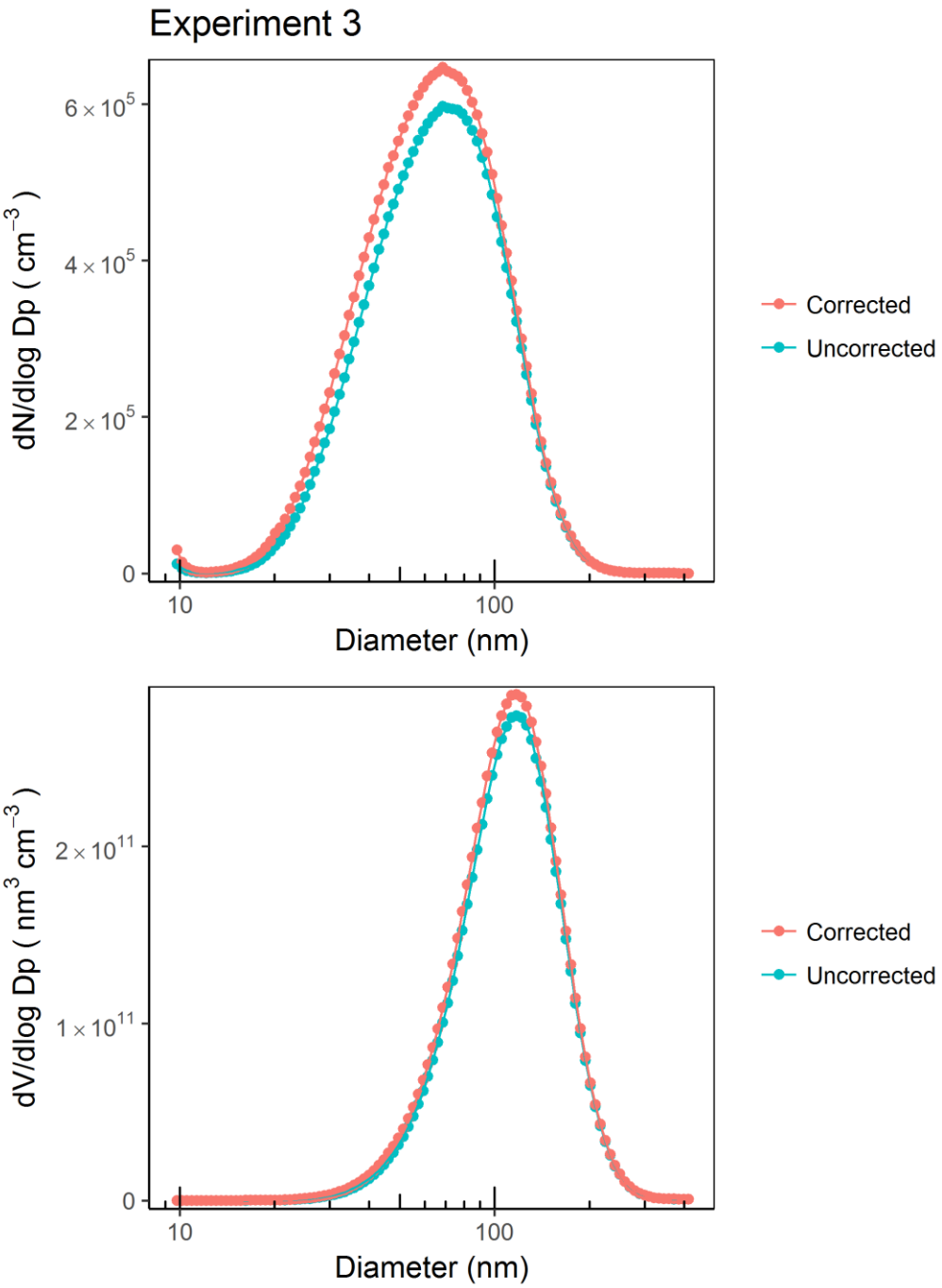

Figure S7: Continued

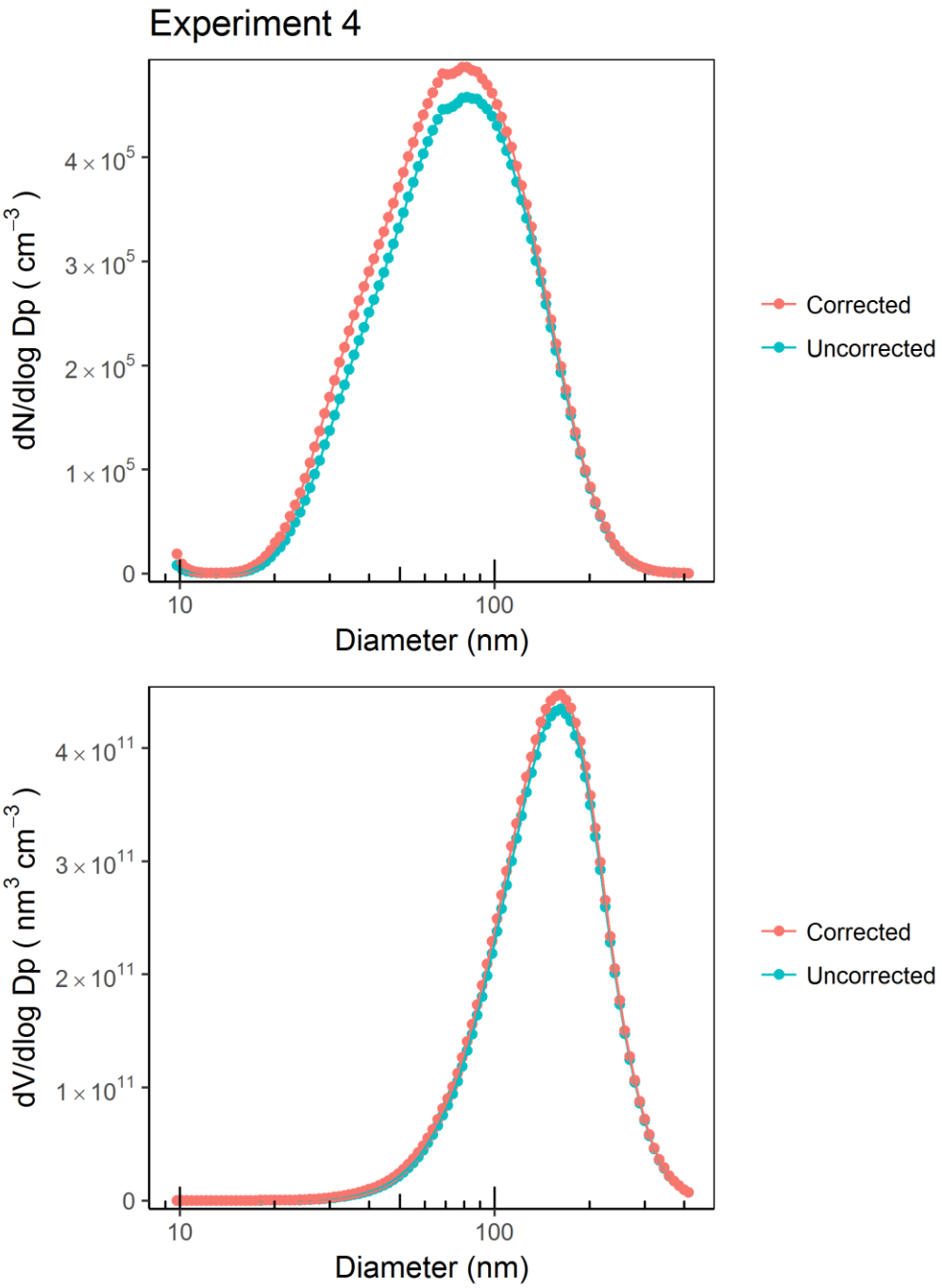

Figure S7: Continued

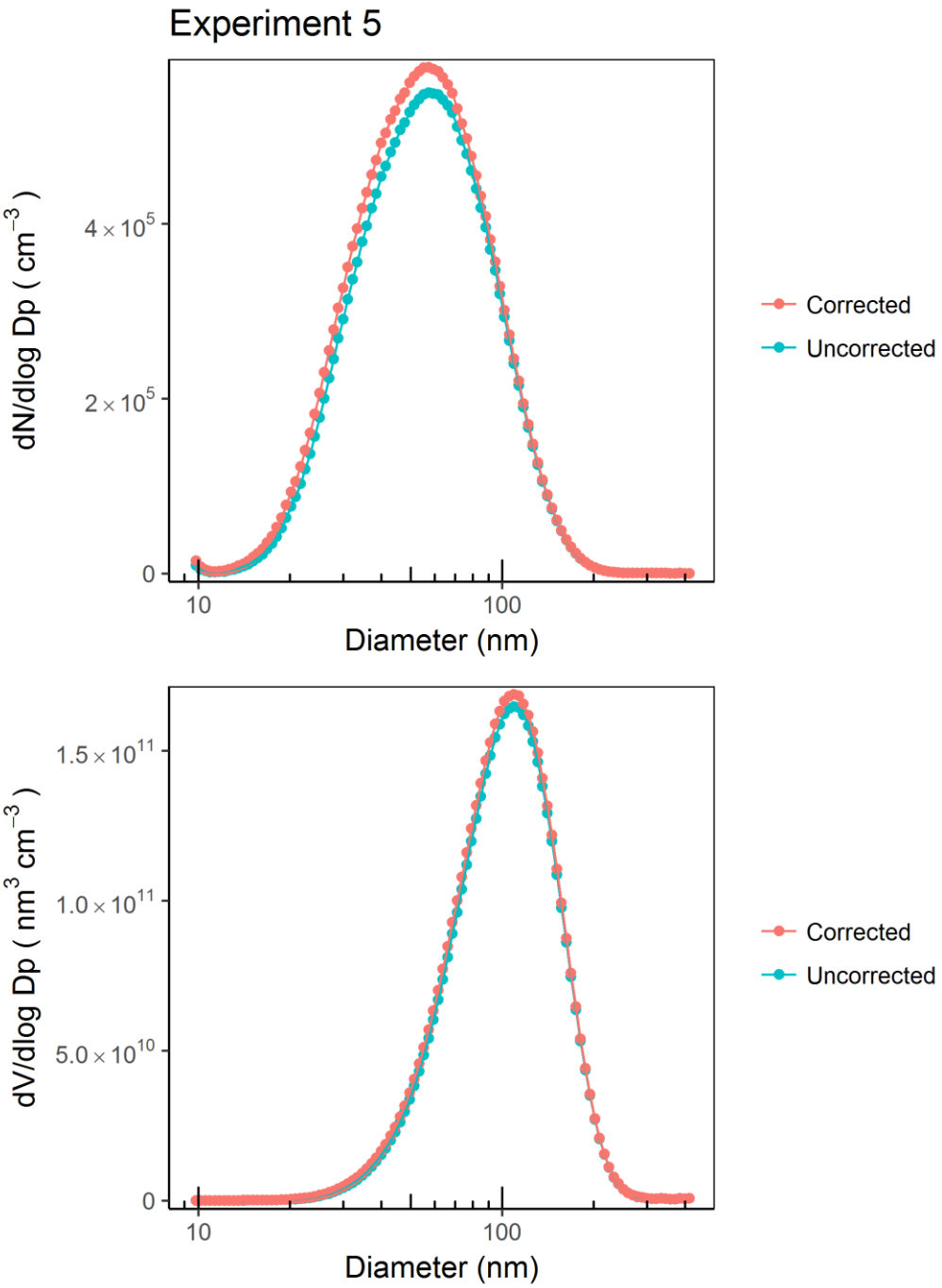

Figure S7: Continued

Section S5: Yield sensitivity

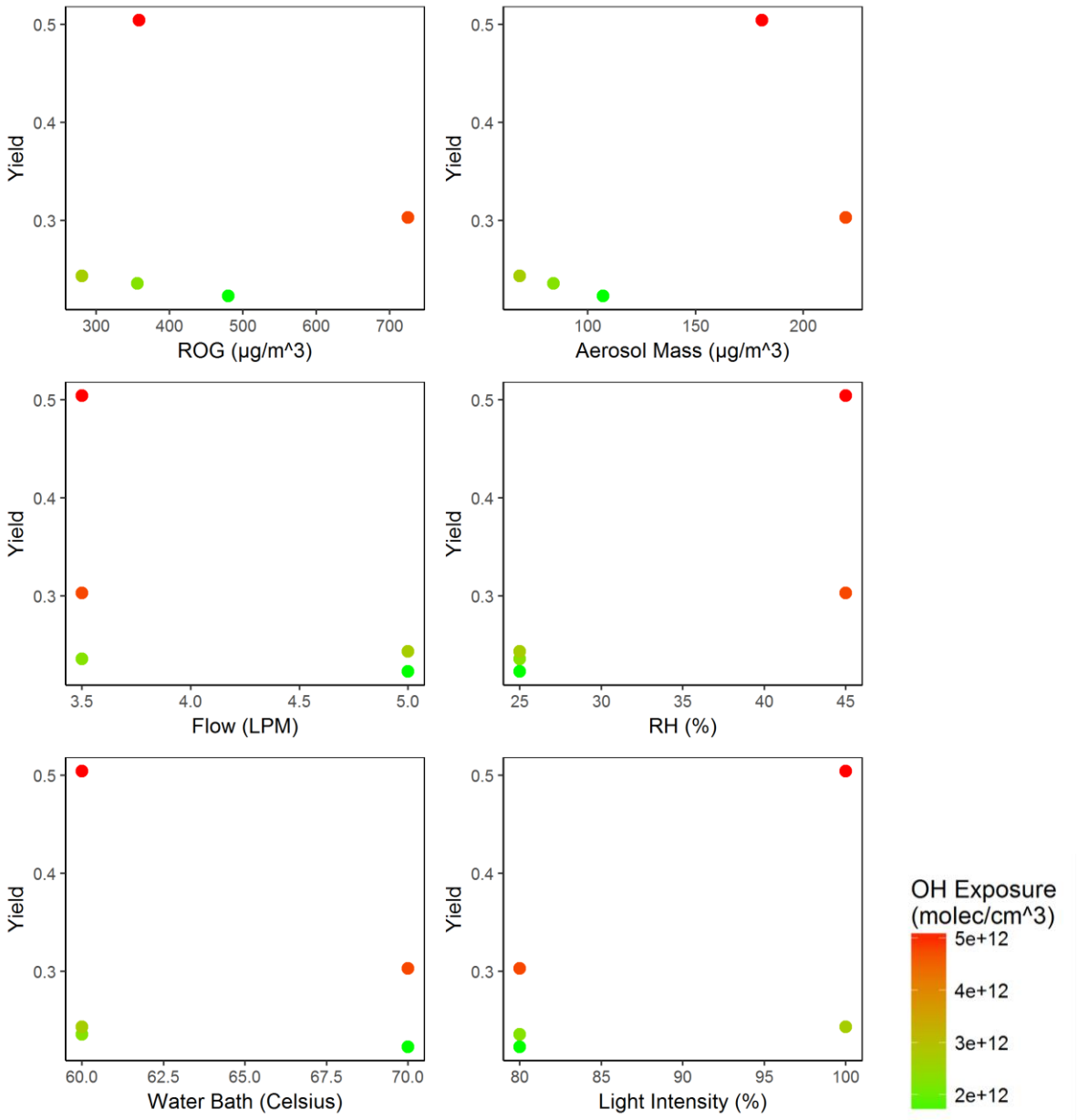

Figure S8: Measured D_5 oxidation aerosol yield as a function of system parameters. Data points are color coded according to OH exposure.

Section S6: Condensational sink input

Table S5: Calculated condensational sink (CS) calculations used for LVOC modeling (Sect. 3.2.1). CS was calculated according to Palm et al. (2016) which recommends the average of the incoming and output OFR CS. For the yield experiments, the output D_5 oxidation aerosol number concentration was averaged with 0 particle incoming air.

Experiment	Incoming Aerosol (cm^{-3})	Output Aerosol (cm^{-3})	CS (m^{-2})	CS rate (s^{-1})
Yield 1	0	3.47E+05	6619	0.3860
Yield 2	0	2.57E+05	3427	0.1998
Yield 3	0	3.58E+05	5173	0.3017
Yield 4	0	3.07E+05	5471	0.3190
Yield 5	0	3.31E+05	4035	0.2353

Section S7: Hygroscopicity

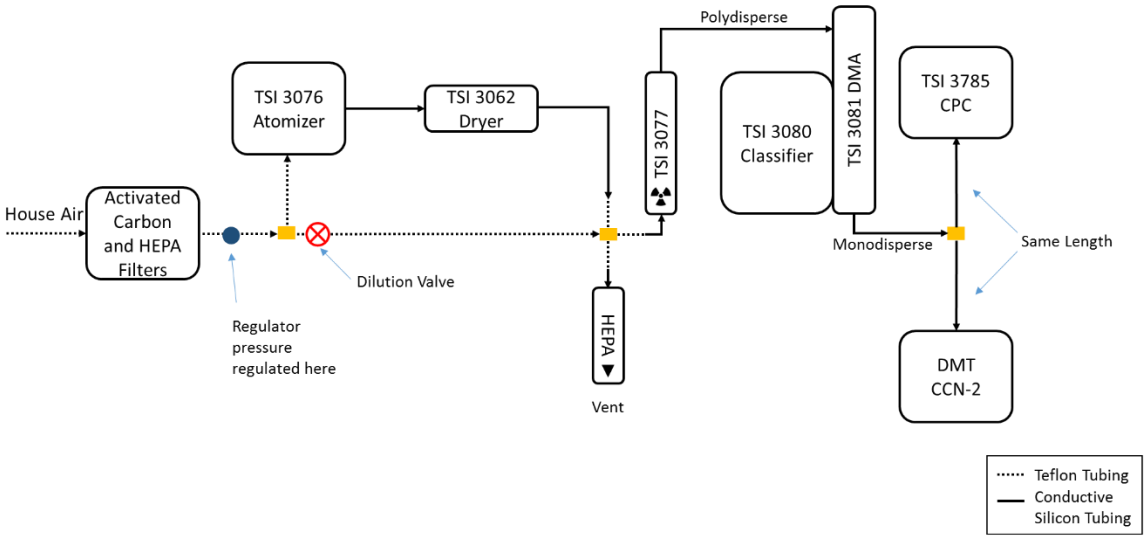

Figure S9: Ammoniums sulfate aerosol CCN testing flow diagram.

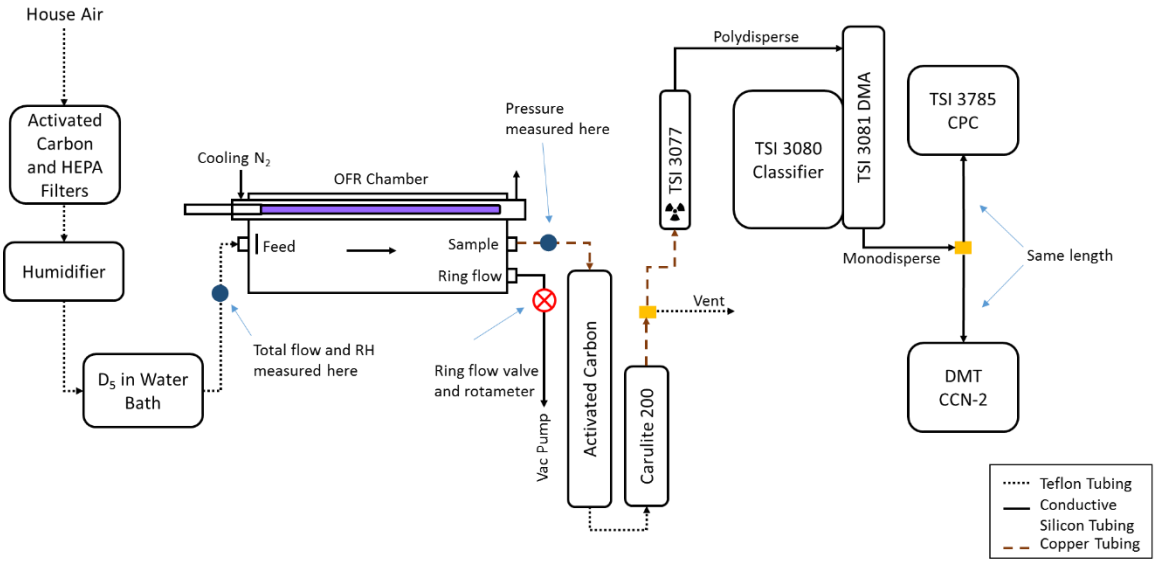

Figure S10: D_5 oxidation aerosol CCN testing flow diagram.

Two issues complicated CCN counter data analysis. First, temperature and flow spikes were observed that were caused by intermittent faults in a sample temperature sensor. This sensor was part of the instrument feedback control loop used to maintain the column thermal gradient, and accordingly these sensor faults upset the column thermal gradient and required some time to settle. Second, for some of the higher ΔT set points, the temperatures were not able to reach the set points but were stable. To correct for these issues, scripts were developed to automatically classify data into stable (used in data analysis) and unstable (excluded) periods. Data were initially binned to 30 s intervals (raw CCN data was at 1 s, CPC data was at 5 s). For each 30 s period, temperature, flow, and pressure stability were calculated and compared to thresholds as described below; periods were then flagged as stable or unstable.

Four temperature tests were used: (i) ΔT varied by no more than 0.16 K from the previous 10 s moving average; (ii) T1 (column low temperature) varied by no more than 0.20 K from the previous 10 s moving average; (iii) T3 (column high temperature) varied by no more than 0.20 K from the previous 10 s moving average; and (iv) that the 1 s values of ΔT varied by no more than 0.37 K during the 30 s period. Pressure and flow were checked individually to make sure the relative percent difference between the current value and the 10 s moving average was lower than 4.5%. These data exclusion thresholds were selected by visual inspection of the data, but final data processing was automated. Failure of a single test in any 30 second period led to exclusion from analysis. For periods compliant with these tests (70%), average CCN and CPC concentration were calculated along with the average ΔT.

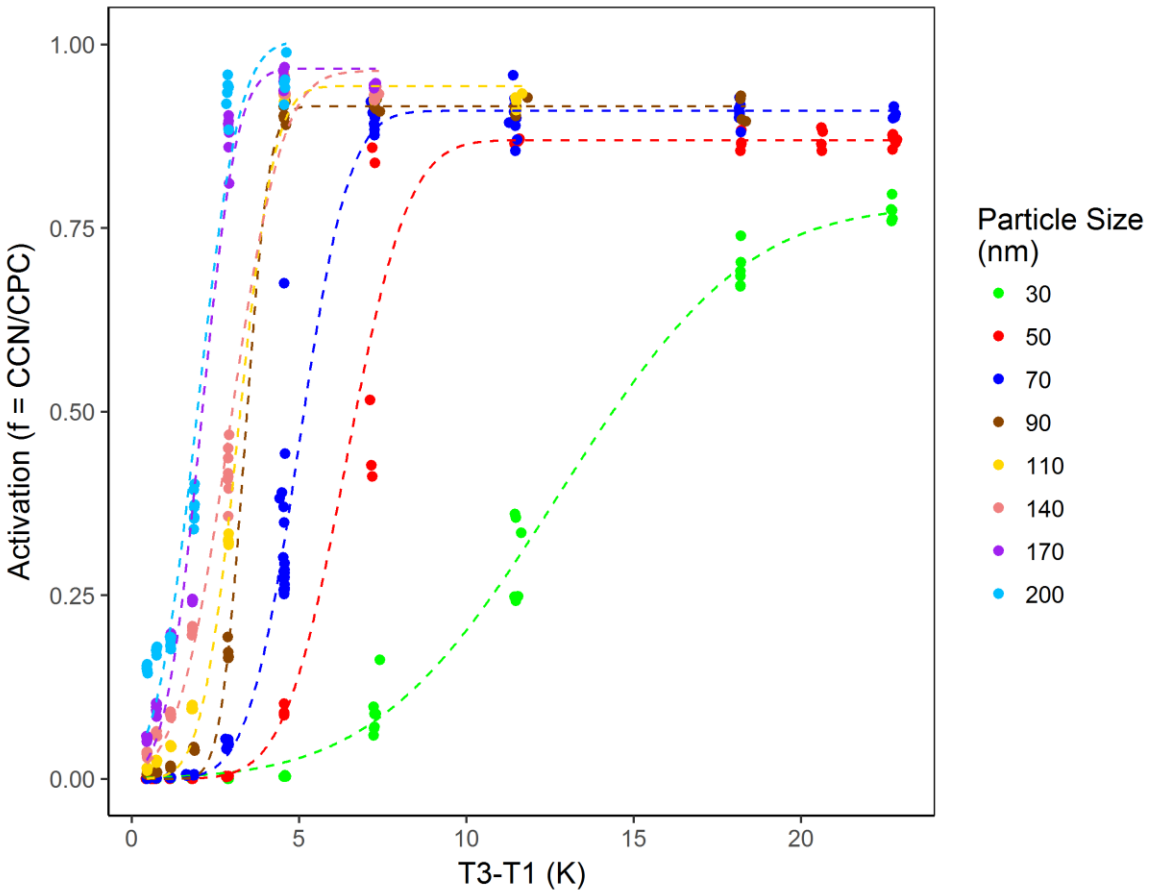

Figure S11: Uncorrected ammonium sulfate aerosol CCN activation curve used for calibration of the ~~DMT CCN~~CCN counter supersaturation. Each point represents an average 30 s ~~DMT~~CCN/CPC measurement.

The AP3 Kohler model was used to relate ammonium sulfate particle diameter to critical supersaturation. The AP3 Kohler model is detailed in Rose et al. (2008). The critical supersaturation is found by writing all equations in terms of the unknown solute mass fraction (x_s) and finding the peak of the resultant Kohler curve.

AP3 Model Parameterization:

1. $\mu_s = \frac{x_s}{M_s(1-x_s)}$
2. a_w is found using a lookup table from the AIM inorganic model of a_w vs μ_s data. The AIM data was run using the web interface for 299.8 K (Clegg et al., 1998; Clegg et al.). The temperature 299.8 K is the average T1 column temperature of the experiments. The T1 temperature was suggested by Rose et al. (2008) since activation is assumed to occur in the first half of the column and the T1 temperature represents the lower bound for the effective column temperature. Linear interpolation was used for the resulting lookup table.
3. $\rho_w = \frac{A_0+A_1*t+A_2*t^2+A_3*t^3+A_4*t^4+A_5*t^5}{1+B_t}$

   t = T – 273.15 K

   Coefficients are found in Rose et al. (2008) Table A.4
4. $\rho_{sol} = \rho_w + \left[[5.92x10^{-3} * (100 * x_s)^1] + [-5.036x10^{-6} * (100 * x_s)^2] + [1.024x10^{-8} * (100 * x_s)^3]\right] * 1000$
5. $g_s = \left(\frac{\rho_s}{x_s*\rho_{sol}}\right)^{1/3}$

   ρ_s = 1770 kg m^{-3} for $(NH_4)_2SO_4$
6. $\sigma_w = 0.0761 - 1.55x10^{-4} * (T - 273\ K)$
7. $\sigma_{sol} = \sigma_w + (2.17x10^{-3} * c_s)$
8. $c_s = \frac{x_s*\rho_{sol}}{M_s*1000}$
9. $s = a_w e^{\left(\frac{4*\sigma_{sol}*M_w}{\rho_w*R*T*g_s*D_s}\right)}$

Defined variables:

μ_s = molality of solute (mol kg^{-1})
x_s = solute mass fraction
M_s = molar mass of solute (0.1321395 kg mol^{-1})
a_w = activity of water
ρ_{sol} = density of solution (kg m^{-3})
ρ_w = density of pure water (kg m^{-3})
g_s = particle growth factor
σ_{sol} = surface tension of solution (N m^{-1})
σ_w = surface tension of pure water (N m^{-1})
c_s = molarity of solute (mol L^{-1})
s = water vapor saturation ratio
M_w = molar mass of water (0.0180153 kg mol^{-1})
R = gas constant (N m k^{-1} mol^{-1})
D_s = dry particle diameter (m)

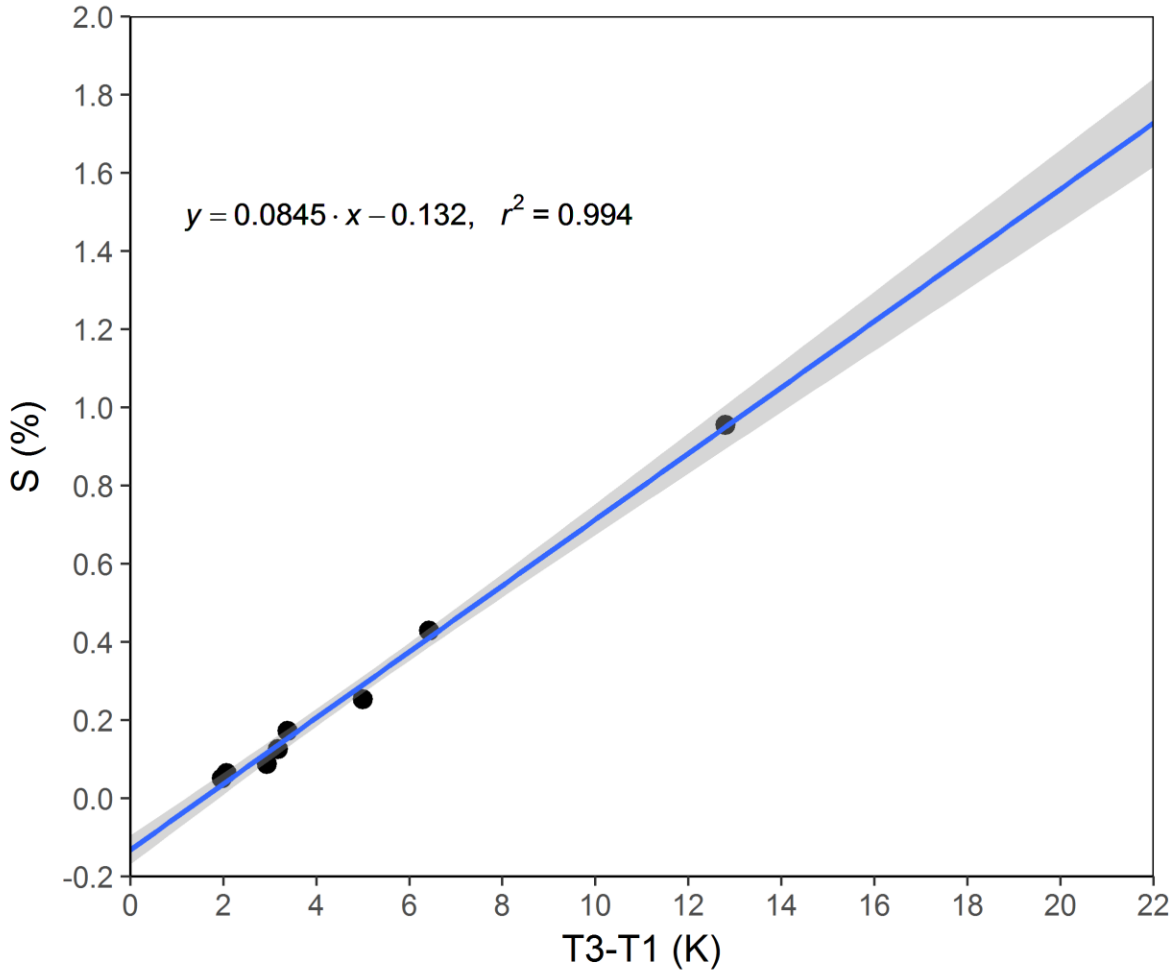

Figure S12: Supersaturation correlation to ~~DMT CCN~~CCN counter ΔT based on ammonium sulfate aerosol calibration. Supersaturation was calculated using the AP3 Kohler model detailed in Rose et al. (2008). The shaded region represents the 95% confidence interval.

Table S6: Calculated size resolved kappa values for ammonium sulfate and D_5 oxidation aerosols.

Diameter (nm)	$(NH_4)_2SO_4$ (polynomial fit)	$(NH_4)_2SO_4$ (linear fit; 95% CI)	o-D_5 κ_a (linear fit; 95% CI)	o-D_5 κ_t (linear fit; 95% CI)
30	0.55	0.56 (0.49 - 0.63)	-	-
50	0.62	0.64 (0.57 - 0.72)	-	-
70	0.52	0.47 (0.40 - 0.54)	0.016 (0.014 - 0.020)	0.0056 (0.0042 - 0.0073)
90	0.97	0.78 (0.59 - 1.09)	0.010 (0.0084 - 0.012)	0.0056 (0.0044 - 0.0071)
110	0.66	0.54 (0.39 - 0.80)	0.012 (0.0099 - 0.014)	0.0060 (0.0049 - 0.0074)
140	0.42	0.36 (0.25 - 0.58)	0.0093 (0.0080 - 0.011)	0.0079 (0.0067 - 0.0093)
170	0.76	1.49 (0.55 - 11.4)	0.010 (0.0085 - 0.011)	0.0078 (0.0067 - 0.0091)
200	0.55	1.45 (0.44 - 43.4)	0.0068 (0.0058 - 0.0079)	0.0063 (0.0054 - 0.0073)
Average	0.63	0.79 (0.46 - 7.40)	0.011 (0.0091 - 0.013)	0.0065 (0.0054 - 0.0079)

Using a third order polynomial fit rather than the linear fit results in improved correlation for low supersaturations and a resulting average ammonium sulfate kappa of 0.63 which is in close agreement with the previously reported value of 0.61 (Petters and Kreidenweis, 2007). We use the linear fit however for the cVMS data due to improved performance at high supersaturations.

Section S8: Volatility

Table S7: Summary of V-TDMA analyzed results. Values represent the average of all trials for the selected particle size and temperature. Dp Bypass (all temps) is the average bypass particle size for all temperature settings of a particular particle size.

T Set (°C)	D_p Set (nm)	T (°C)	D_p Bypass (nm)	D_p Heated (nm)	D_p Bypass (all temps) (nm)	Bypass Number (cm^{-3})	Heated Number (cm^{-3})	Bypass Mass ($\mu g\ m^{-3}$)	Heated Mass ($\mu g\ m^{-3}$)	Heated Trials	Bypass Trials	Diameter Change (%)	Number Change (%)
50	10	50.1	12.76	11.24	12.38	922	1288	0.00130	0.00121	2	2	-9.19	39.7
80	10	80.2	12.59	9.056	12.38	1044	556	0.00132	0.00196	4	2	-26.9	-46.8
110	10	110.4	14.71	10.96	12.38	1703	628	0.00291	0.000960	4	2	-11.5	-63.1
150	10	149.6	10.45	11.36	12.38	1753	544	0.00218	0.000656	3	3	-8.23	-69.0
190	10	191.4	-	9.040	12.38	-	119	-	0.000139	2	0	-27.0	-
50	20	49.8	20.75	20.45	20.68	37848	40177	0.169	0.175	3	1	-1.10	6.15
80	20	80.0	20.64	20.30	20.68	34577	36096	0.153	0.150	4	2	-1.81	4.39
110	20	109.8	20.68	20.18	20.68	35122	35217	0.156	0.141	4	2	-2.39	0.27
150	20	150.9	20.64	19.92	20.68	37235	30917	0.166	0.113	3	2	-3.68	-17.0
190	20	189.4	20.75	19.79	20.68	39831	26877	0.176	0.0911	2	1	-4.29	-32.5
50	30	50.0	30.14	30.05	30.19	70981	81449	1.00	1.14	2	1	-0.47	14.7
80	30	80.3	30.18	29.87	30.19	75440	78321	1.07	1.06	4	2	-1.07	3.82
110	30	110.5	30.19	29.52	30.19	72643	70515	1.02	0.911	4	2	-2.25	-2.93
150	30	149.9	30.19	29.18	30.19	74929	68995	1.06	0.840	4	2	-3.37	-7.92
190	30	189.8	30.30	28.89	30.19	69580	61425	0.994	0.686	2	1	-4.32	-11.7
50	50	50.0	49.85	49.63	49.89	70528	69382	4.54	4.42	2	1	-0.53	-1.63
80	50	80.1	49.96	49.37	49.89	67418	68649	4.36	4.20	4	2	-1.04	1.83
110	50	110.1	49.85	48.94	49.89	69197	66893	4.45	3.96	4	2	-1.91	-3.33
150	50	150.2	49.75	48.84	49.89	63422	65996	4.06	3.72	4	2	-2.10	4.06
190	50	191.1	50.16	48.29	49.89	70161	60349	4.58	3.19	2	1	-3.21	-14.0
50	80	50.1	80.28	79.87	80.14	46485	48112	12.6	12.8	3	1	-0.34	3.50
80	80	80.3	80.08	79.44	80.14	47606	46148	12.9	12.0	4	2	-0.88	-3.06
110	80	110.0	80.16	79.09	80.14	45690	44591	12.4	11.4	4	2	-1.32	-2.41
150	80	150.7	80.07	78.34	80.14	44614	43540	12.0	10.6	3	2	-2.26	-2.41
190	80	189.1	80.25	77.79	80.14	42705	39579	11.5	9.38	2	1	-2.94	-7.32
50	110	50.2	110.2	109.7	110.1	24992	23295	17.7	16.2	3	12	-0.40	-6.79
80	110	80.1	110.1	109.3	110.1	23384	23653	16.5	16.3	4	2	-0.72	1.15
110	110	110.6	110.1	108.6	110.1	25163	22110	17.7	14.9	4	2	-1.39	-12.1
150	110	149.4	110.0	108.1	110.1	23160	22130	16.3	14.7	3	3	-1.83	-4.45
190	110	190.5	109.9	107.9	110.1	20968	19948	14.8	12.9	2	1	-2.00	-4.86

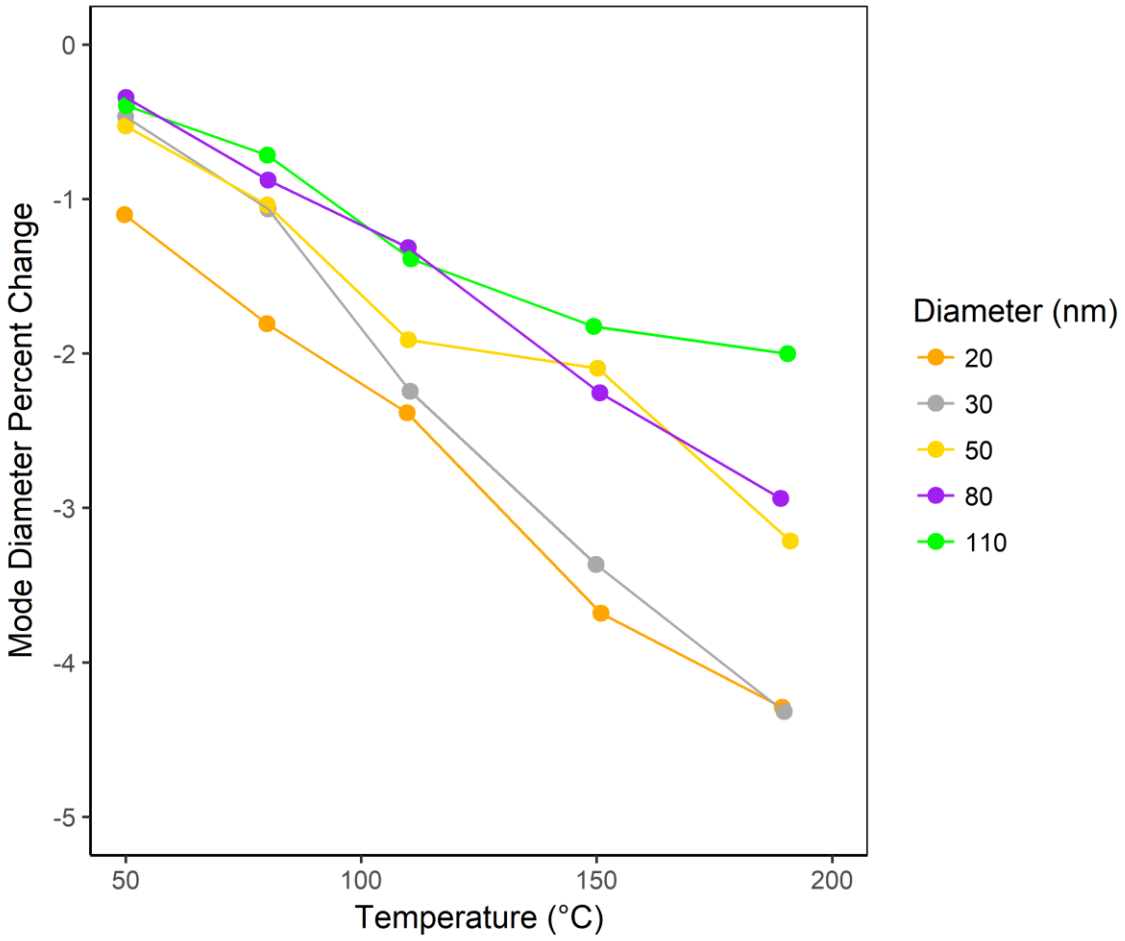

Figure S13: D_5 oxidation aerosol change in mode diameter after exposure to heated conditions in the V-TDMA experiments.

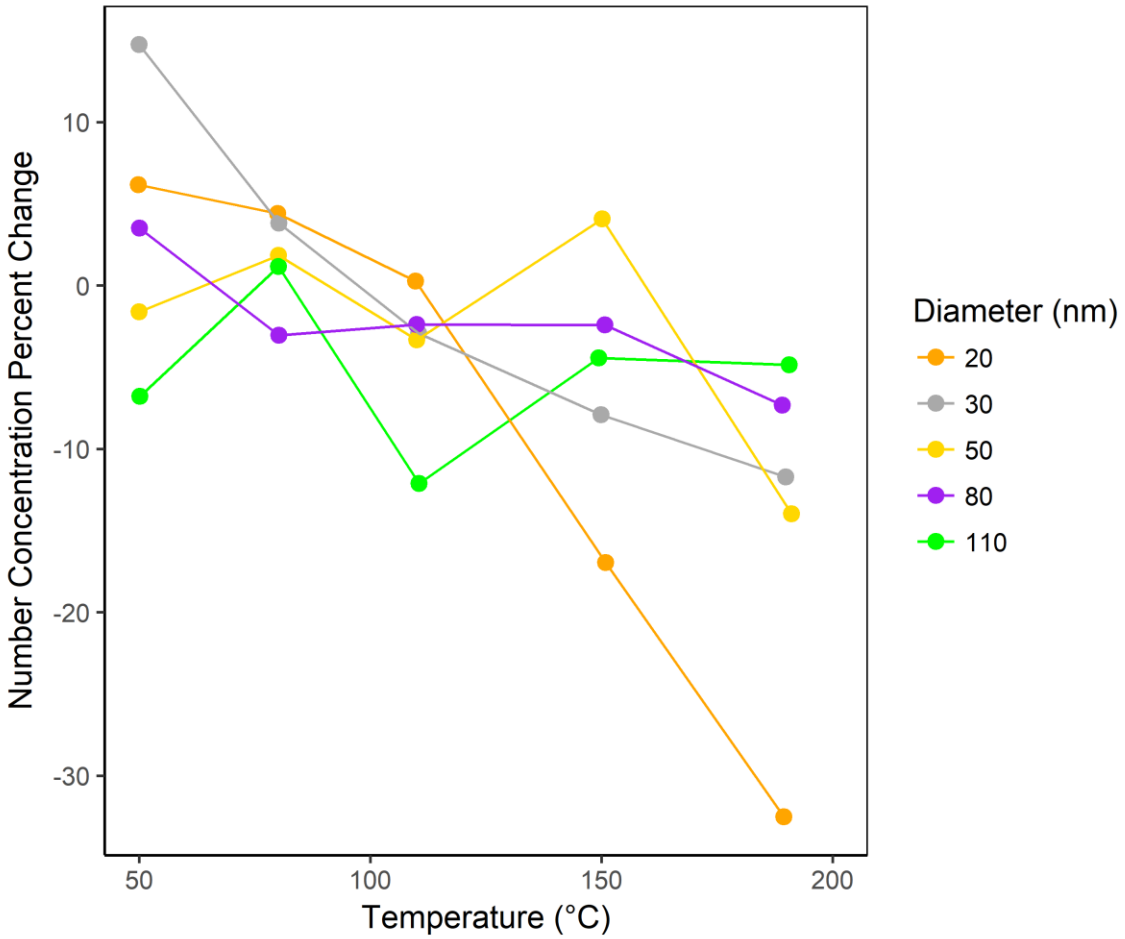

Figure S14: D_5 oxidation aerosol change in number concentration after exposure to heated conditions in the V-TDMA experiments.

References

Extended AIM Aerosol Thermodynamics Model: http://www.aim.env.uea.ac.uk/aim/aim.php, access: November 2017.

Clegg, S. L., Brimblecombe, P., and Wexler, A. S.: Thermodynamic Model of the System H+−NH4+−SO42-−NO3-−H2O at Tropospheric Temperatures, The Journal of Physical Chemistry A, 102, 2137-2154, doi:10.1021/jp973042r, 1998.

Palm, B. B., Campuzano-Jost, P., Ortega, A. M., Day, D. A., Kaser, L., Jud, W., Karl, T., Hansel, A., Hunter, J. F., Cross, E. S., Kroll, J. H., Peng, Z., Brune, W. H., and Jimenez, J. L.: In situ secondary organic aerosol formation from ambient pine forest air using an oxidation flow reactor, Atmos. Chem. Phys., 16, 2943-2970, doi:10.5194/acp-16-2943-2016, 2016.

Petters, M. D., and Kreidenweis, S. M.: A single parameter representation of hygroscopic growth and cloud condensation nucleus activity, Atmos. Chem. Phys., 7, 1961-1971, doi:10.5194/acp-7-1961-2007, 2007.

Rose, D., Gunthe, S. S., Mikhailov, E., Frank, G. P., Dusek, U., Andreae, M. O., and Pöschl, U.: Calibration and measurement uncertainties of a continuous-flow cloud condensation nuclei counter (DMT-CCNC): CCN activation of ammonium sulfate and sodium chloride aerosol particles in theory and experiment, Atmos. Chem. Phys., 8, 1153-1179, doi:10.5194/acp-8-1153-2008, 2008.